Sede Amministrativa: Università degli Studi di Padova
Facoltà di SCIENZE MM. FF. NN.
Dipartimento di Geoscienze

SCUOLA DI DOTTORATO DI RICERCA IN: SCIENZE DELLA TERRA

CICLO XXII

TITOLO TESI:

GEOLOGICAL MAPPING AND ANALYSIS OF DAEDALIA PLANUM LAVA FIELD (MARS)

Direttore della Scuola: Ch.mo Prof. Gilberto Artioli
Supervisore: Dott. Matteo Massironi

Dottoranda: Lorenza Giacomini

Abstract

GEOLOGICAL MAPPING AND ANALYSIS OF DAEDALIA PLANUM LAVA FIELD (MARS)

PhD candidate: Lorenza Giacomini XXII course

Tutor: Dr Matteo Massironi

Abstract

Volcanism is the most important rock-forming processes of the planetary surfaces and represents one of the main clues to investigate the chemical composition of the interior and the thermal history of a planet. Our study has been focused on the Daedalia Planum volcanic region, located to south-west of Arsia Mons, where some of the longest lava flows on Mars were emplaced. THEMIS, MOC and HiRISE images were analyzed in order to perform a stratigraphic and morphological analysis of the area and realize a Daedalia Planum geological map where different flow units are represented.
Several features observed on the flow surface have been interpreted as related to inflation processes on the basis of several similarities with the morfologies of the inflated terrestrial Payen Matru flows (Argentina). This suggests that inflation process is quite common for the Daedalia Planum field, implying that the inflation emplacement mechanism on Martian flows could be more frequent than previously supposed and, consequently, effusion rates and rheological properties of Martian lavas more variable.
In addition, a comparative study performed between the mounds detected on Daedalia Planum and Elysium Planitia regions seems to further confirm the tumuli nature of the Daedalia Planum features and thus the presence of inflated flows in this volcanic field.
The OMEGA data reveal that Daedalia Planum lavas have a spectral response coherent with a basaltic composition. In addition the Spectral Angle Mapper (SAM) classification obtained from the OMEGA data highlights that the flows are characterized by distinctive spectral responses, which should depend on non-compositional factors, like different surface textures of flows but also different mineralogy or rock texture, such as the presence of glass, crystal size or crystal isoorientation.

Introduction

Mars volcanism started very early in its history and it may be still active in very recent time. Consequently different style of volcanism occurred on Mars during this long period producing a great variety of volcanic forms. This thesis is focused on the study of lava flows, in order to establish their origin and their mechanism of emplacement.
Among the various volcanic plains we have chosen the Daedalia Planum one where some of the longest lava flows on Mars were emplaced. We analyzed those lava flows from different points of view: a stratigraphic and morphological study of the flows was performed coupled with a comparison with other terrestrial and Martian volcanic regions. A deeper investigation of the rheological and physical characteristics of flows and a spectral analysis of the region were also taken into account.

Abstract

Inflated flows on Daedalia Planum? A comparison with the Payen volcanic complex (Argentina)

Inflation is an emplacement process of lava flows, where a thin viscoelastic layer, produced at an early stage, is later inflated by an underlying fluid core. The core remains hot and fluid for extended period of time due to the thermal-shield effect of the surface viscoelastic crust. Plentiful and widespread morphological fingerprints of inflation like tumuli and lava rises are found on the Payen volcanic complex (Argentina) where pahoehoe lava flows extend over the relatively flat surface of the Pampean foreland and reach up to180 km in length.
The morphology of the Argentinean Payen flows were compared with lava flows on Daedalia Planum (Mars), using Thermal Emission Imaging System (THEMIS), Mars Orbiter Laser Altimeter (MOLA), Mars Orbiter Camera (MOC), Mars Reconnaissance Orbiter (MRO)/ High Resolution Imaging Science Experiment (HiRISE). THEMIS images were used to map the main geological units of Daedalia Planum and determine their stratigraphic relationships. MOLA data were used to investigate the topographic environment over which the flows propagated and assess the thickness of lava flows. Finally MOC and MRO/HIRISE images were used to identify inflation fingerprints and assess the cratering age of the Daedalia Planum's youngest flow unit which were found to predate the caldera formation on top of Arsia Mons. The identification of similar inflation features between the Daedalia Planum and the Payen lava fields suggests that moderate and long lasting effusion rates coupled with very efficient spreading processes could have cyclically occurred in the Arsia Mons volcano during its eruptive history. Consequently the effusion rates and rheological proprieties of Daedalia lava flows, which do not take into account the inflation process, can be overestimated. These findings raise some doubts about the effusion rates and lava rheological properties calculated on Martian flows and recommends that these should be used with caution if applied on flows not checked with high resolution images and potentially affected by inflation. Further HiRISE data acquisition will permit additional analysis of the flow surfaces and will allow more accurate estimates of effusion rates and rheological properties of the lava flows on Mars particularly if this data is acquired under a favourable illumination.

Tumuli and pingos: a comparative analysis between Daedalia Planum and Elysium Planitia mounds

Tumuli and pingos are important distinctive features for inflated flows and unconsolidated water-rich periglacial terrains respectively. Therefore distinguishing between these two classes of features is useful to understand the origin of the terrain where such features occur; this however could be complex since their morphologies are very similar. We focused our study on the dome-like forms detected on Daedalia Planum and Elysium Planitia regions taking into account a morphological analysis of the features but also of the surrounding terrains, coupled with a density distribution study of mounds and dating of the surfaces where they were observed. Such comparative study revealed that Elysium Planitia features are more compatible with a pingo nature whereas Daedalia Planum features are more likely associable with tumuli. Therefore this would imply that the Elysium Planitia terrain hosting the mounds is likely to be outflow channel deposits and would confirm the presence of inflated flows on Daedalia Planum.

Spectral analysis and mapping of Daedalia Planum

The great variety of morphologies distinguished among the Daedalia Planum lava flows encouraged a more detailed study of their spectral characteristics, both to achieve some information about the lava composition and to detect possible differences in the flows spectra that help us to distinguish the flows inside the lava field. In this work we employed OMEGA data from the Mars Express mission. The spectra collected on the entire lava field appear rather similar to each other with

absorptions between 0.8 and 1.4 μm and 1.8 and 2.5 μm, suggesting the presence of mafic minerals, like pyroxene and olivine. The continuum removal permits us to appreciate the presence of two classes of spectra related to the different content of Ca in the pyroxene. Both these classes are compatible with tholeiitic basalts. Despite these analogies, Daedalia spectra show some differences in reflectance and spectral slope. The SAM classification allows a spectral map to be created revealing that the differences among the spectra are generally in agreement with the lava flows mapped by Giacomini et al. [2009].This suggests that such variability is related to different surface textures of the lava flow. In some cases the spectral map highlights the presence of spectral subunits inside single units on the geological map of Giacomini et al. [2009] due likely to differences in mineralogy or rock texture. Therefore spectral analysis shows itself useful for improving the geological mapping of the Daedalia Planum region.

Abstract

MAPPATURA GEOLOGICA E ANALISI DEL CAMPO VULCANICO DI DAEDALIA PLANUM (MARS)

Dottoranda: Lorenza Giacomini XXII ciclo

Tutore: Dott. Matteo Massironi

Abstract

Il vulcanismo è uno dei più importanti processi che interessano la superficie di un pianeta e rappresenta una delle chiavi per investigare la composizione chimica del suo interno nonché la sua storia termica. Il nostro studio si è focalizzato sul campo vulcanico di Daedalia Planum, a sud ovest di Arsia Mons, dove si trovano alcune delle più lunghe colate conosciute su Marte. Varie immagini di THEMIS, MOC e HiRISE sono state analizzate con l'obiettivo di studiare questa regione sia dal punto di vista stratigrafico che morfologico e di creare una mappa geologica della regione. Da questa analisi sono state individuate varie forme interpretate come collegate al processo di inflation e il confronto con le colate inflate terrestri del Payen (Argentina) sembrano confermare tale ipotesi. Ciò suggerisce che l'inflation è piuttosto comune nel capo lavico di Daedalia Planum e che, in generale, questo processo interessi più colate di Marte di quanto supposto finora. Di conseguenza i tassi di eruzione e le proprietà reologiche delle lave su Marte potrebbero essere molto più variabili.

Uno studio comparativo tra le forme a cupola individuate su Daedalia Planum ed Elysium Planitia confermerebbe ulteriormente che su Daedalia Planum vi è effettivamente la presenza di tumuli e, quindi, di colate laviche inflate.

Infine, prendendo in considerazione i dati OMEGA della regione, si è appurato che le lave presenti su Daedalia Planum hanno una risposta spettrale coerente con una composizione basaltica. Le classificazioni SAM ottenute da dati OMEGA evidenziano, inoltre, come le colate della regione siano effettivamente caratterizzate da distinte risposte spettrali, verosimilmente attribuibili a fattori non composizionali quali la diversa tessitura superficiale o la differente mineralogia e tessitura della roccia, come la presenza di vetro, la dimensione dei cristalli o la loro isoorientazione.

Introduzione

Su Marte il vulcanismo ebbe inizio agli albori della storia del pianeta e alcune evidenze sembrano confermare che possa essere stato attivo in epoca recente. Durante questo lungo periodo di tempo, differenti tipi di vulcanismo si sono succeduti sul Marte, portando alla formazione di una grande varietà di forme vulcaniche. La seguente tesi si è concentrata sullo studio delle colate di lava, allo scopo di stabilire la loro origine e i loro meccanismi di messa in posto.
Tra le varie piane vulcaniche abbiamo scelto di studiare la regione di Daedalia Planum dove si trovano alcune delle più lunghe colate di Marte. Abbiamo analizzato le colate di lava da diversi punti di vista: da quello stratigrafico e morfologico a quello prettamente fisico, per passare successivamente a un'analisi spettrale dell'area.

Inflation sulle colate di lava di Daedalia Planum? Un confronto con il complesso vulcanico del Payen (Argentina)

L'inflation è un processo di emplacement delle colate di lava.. Un sottile strato viscoelastico superficiale della colata, prodotto negli stadi iniziali, si espande successivamente per azione di un nucleo fluido di lava sottostante. Tale nucleo può rimanere caldo e fluido per lunghi periodi di

tempo grazie alla crosta viscoelastica che agisce da scudo termico. Numerosi inflation fingerprints, come tumuli e lava rises, sono stati individuati sulle colate del complesso vulcanico del Payen (Argentina), dove colate di tipo pahoehoe si estendono su una piana a pendenza molto bassa raggiungendo una lunghezza di 180 km. La morfologia di queste colate è stata confrontata con quella delle colate presenti su Daedalia Planum utilizzando i dati di THEMIS (Thermal Emission Imaging System), MOLA (Mars Orbiter Laser Atimeter), MOC (Mars Orbiter Camera) e HiRISE (High Resolution Imaging Science Experiment). Le immagini THEMIS sono state usate per mappare le principali unità geologiche di Daedalia Planum e determinare i loro rapporti stratigrafici. I dati MOLA invece sono stati utilizzati per investigare la topografia dell'area e per stimare la larghezza e lo spessore delle colate presenti. Infine le immagini MOC e HiRISE sono state usate per identificare gli inflation fingerprints e per il conteggio dei crateri allo scopo di determinare l'età delle più giovani colate del campo vulcanico, rivelatisi antecedenti alla formazione della caldera di Arsia Mons. L'identificazione di simili forme di inflation nel campo lavico di Daedalia Planum suggerisce che un effusion rate moderato e duraturo nel tempo possa aver interessato ciclicamente l'Arsia Mons durante la sua storia eruttiva. Di conseguenza gli effusion rate e le proprietà reologiche della lava calcolati utilizzando i modelli tradizionali, che non tengono in considerazione la presenza di inflation, possono essere sovrastimati. Ciò solleva alcuni dubbi riguardo gli effusion rate e le proprietà reologiche calcolati finora per le colate di Marte e evidenzia quanto questi modelli debbano essere usati con cautela se applicati a colate non studiate con immagini ad alta risoluzione, in quanto queste potrebbero essere state interessate da inflation. L'acquisizione di nuovi dati HiRISE permetterà un'ulteriore analisi delle superfici delle colate e quindi una più accurata stima degli effusion rate e delle proprietà reologiche delle colate di Marte.

Tumuli e pingos: un confronto tra le forme di Daedalia Planum e Elysium Planitia

Tumuli e pingos sono forme tipiche rispettivamente di colate di lava interessate da inflation e di terreni periglaciali saturi d'acqua. Riuscire quindi a distinguere questi due tipi di forme è essenziale per conoscere l'origine del terreno su cui si trovano. Tuttavia su Marte tale distinzione può essere piuttosto difficile, dal momento che morfologicamente esse sono molto simili. Abbiamo focalizzato il nostro studio sulle forme a duomo individuate su Daedalia Planum e Elysium Planitia eseguendo un' analisi morfologica non solo delle forme ma anche del terreno circostante. In seguito è stato affrontato uno studio della distribuzione spaziale di tali forme e una datazione delle superfici in cui esse si trovano. I risultati ottenuti rivelano che le forme individuate su Elysium sono associabili ai pingos, mentre quelle individuate su Daedalia sono più compatibili con i tumuli. Ciò rappresenta quindi un' ulteriore prova che le colate di lava presenti su Daedalia Planum sono state interessate da inflation.

Analisi spettrale a mappatura geologica del campo vulcanico di Daedalia Planum

La grande varietà di morfologie che caratterizza le colate di Daedalia Planum ha sollevato la necessità di una più dettagliata analisi delle loro caratteristiche spettrali, sia per acquisire informazioni sulla composizione sia per individuare possibili differenze tra gli spettri che ci possano aiutare nella distinzione delle diverse colate all'interno del capo vulcanico. In questo capitolo abbiamo utilizzato i dati OMEGA della missione Mars Express. Gli spettri, acquisiti su tutta l'area di studio appaiono piuttosto simili fra loro. Le bande di assorbimento osservate in corrispondenza di 1.8 e 2.5 μm suggeriscono la presenza di minerali mafici, come il pirosseno e l'olivina. La rimozione del continuum ha permesso l'individuazione di due classi di spettri

all'interno del campo lavico correlati al diverso contenuto di Ca nel pirosseno. Entrambe queste classi sono compatibili con una composizione basaltica di tipo tholeiitico. Nonostante queste somiglianze, Gli spettri mostrano alcune differenze in riflettanza e spectral slope tra di loro. Grazie all'utilizzo delle SAM è stato possibile creare una mappa spettrale del campo vulcanico, la quale evidenzia che le differenze spettrali tra le colate hanno una buona correlazione con le colate mappate da Giacomini et al. [2009]. Ciò suggerisce che tale variabilità è correlata a una differente tessitura superficiale delle colate. La mappa spettrale ha permesso inoltre di individuare delle subunità spettrali all'interno di una stessa unità della mappa di Giacomini et al.[2009] dovute probabilmente a differenze nella mineralogia o tessitura della roccia. Ciò ha dimostrato il grande potenziale dell' analisi spettrali nel contribuire alla mappatura geologica di Daedalia Planum.

INDEX

Note to the thesis

The chapters of this thesis have been written as scientific papers, except chapter 1, chapter 2 and the conclusions.
The work described in these papers was carried out by me, with the contribution of some professors and researchers with whom I collaborated whenever a very particular expertise was needed.
Dr. Matteo Massironi, as my tutor, followed my PhD activity and reviewed the chapters of this thesis.

The three papers were or will be submitted to international journals. In details:

- chapter 3 was published in Planetary and Space Science (2009), co-authors are M. Massironi, E. Martellato, G. Pasquarè, A. Frigeri, G. Cremonese.
- chapter 4 will be submitted, co-author is M. Massironi
- chapter 5 will be submitted, co-authors are C. Carli, M. Massironi, M. Sgavetti

Some of the results shown in the thesis have been already presented at international workshops.

Introduction

Mars volcanism started very early in its history and it may be still active in very recent time, as suggested by the paucity of impact craters on some volcanic surfaces (Hartmann et al., 1999; Neukum et al., 2004). A different style of volcanism occurred on Mars during this long period, consequently the volcanic expressions are widespread and varied (e.g. Wilson and Head, 1994).
This thesis is devoted to Martian lava flows, in order to establish their origin and their mechanism of emplacement.
Among the numerous volcanic provinces we have chosen Daedalia Planum mainly for its long lava flows. The region has been studied from different points of view: a) stratigraphic analysis of the region was considered to develop a geological mapping of the area; b) morphology and composition of the Daedalia Planum flows were taken into account and compared with terrestrial ones; c) effusion rates and yield strengths of different lava flows were estimated to shed more light on their development; d) dating of some flows were finally performed, both to compare their age with lava flows emplaced in different volcanic fields and to establish how much the erosive agents contributed to the final shape of their features; e) a comparison between Daedalia Planum and Elysium Planitia dome-like features was performed to establish if they are tumuli or pingos and consequently to assess the nature of Daedalia Planum flows, since their general morphologies could be in some cases compatible both with those of mudflows and lava flows.
The thesis is constituted by 5 chapters. The first chapter is dedicated to an overview of volcanism and lava flow morphology on Mars with a final paragraph dedicated to a description of Martian mudflows morphologies. Chapter 2 describes the data used in this work. The subsequent chapters are dedicated specifically to Daedalia Planum. Chapter 3 describes the comparative study between this lava field and the terrestrial Payen Matru (Argentina) volcanic province surface features, performed to find a key of interpretation of Martian lava flows. Chapter 4 is focused on the comparative analysis between the candidate tumuli found on Daedalia field and the mounds detected on Elysium Planitia in order to establish their origin. A more detailed analysis of the compositional and spectral characteristics of Daedalia Planum lava flows is treated in chapter 5.

References

Hartmann W.K., Malin M., McEwen A., Carr M., Soderblom L., Thomas P., Danielson E., James P., Veverka J., 1999. *Evidence for recent volcanism on Mars from crater counts*. Nature,397 (6720), 586-589.

Neukum G., Jaumann R., Hoffmann H., Hauber E., Head J.W., Basilevsky A.T., Ivanov B.A., Werner S.C., Van Gasselt S., Murray J.B., Mccord T., 2004. *Recent and episodic volcanic and glacial activity on Mars revealed by the High Resolution stereo camera*. Nature, 432, 971-979.

Scott D.H. and Tanaka K.L., 1986. *Geologic map of the western equatorial region of Mars, scale 1:15,000,000*. U.S. Geol. Surv. Misc. Invest. Ser., Map I-1802-A.

Wilson L. and Head J.W., 1994. *Mars: Review and analysis of volcanic eruption theory and relationships to observed landforms*. Rev. Geophys., 32, 221– 263.

Zimbelman J.R., 1998. *Emplacement of long lava flows on planetary surfaces*. J. Geophys. Res., 103, 27503 – 27516.

CHAPTER 1- An introduction to Martian volcanism and lava flows

1. Volcanism on Mars

Since up to date there are no clear evidences of the presence of plate tectonics, it is assumed that the volcanism on Mars occurs in correspondence of mantle hot spots (Carr, 2006).
MGS/ Thermal Emission Spectrometer (TES) data reveal that the rock surface composition largely consists on basalt and a more silicic rock, possibly andesite (Bandifield et al., 2000). However a more recent work asserts that the latter can be interpreted also as weathered basalt (Wyatt and McSween, 2002).
Although most Martian volcanism seems to be basaltic, its expression differs from its terrestrial counterpart because of the lower gravity and lower atmospheric pressure. As gravity on Mars is one-third that on the Earth, the buoyant force that permits magma to rise through the crust is correspondingly weaker hence larger conduits and vents are needed (Wilson and Head, 1994). As a result, the eruption rates on Mars are 3 to 5 times higher than on the Earth.
The lower atmospheric pressure on Mars requires far less abundant volatile contents in the magma (i.e. 0.03 wt% on Mars versus 0.1 wt% on the Earth) in order to achieve explosive eruptions (Wilson and Head, 1994); hence explosive volcanism is expected to be more frequent on Mars than on the Earth.
Large shield volcanoes on the Tharsis province and Elysium Mons are the most prominent volcanic edifices in the planet. Olympus Mons, the highest volcano on the Solar System, has a diameter of 540 km and a height of 21 km. Such considerable dimensions could be due to different factors: i) lack of plate tectonics which allows continuous supply of magma in the same place ii) a ticker lithosphere which implies a deep source which in turn implies high edifices.
The shape of these Martian volcanoes resembles the Hawaiian ones; they have the same profile and calderas, lava channels, flow fronts and collapse pits, although the sizes are far larger on Mars due to its lower gravity. Other Martian volcanoes, the "Paterae", have a large base and less vertical relief than the shields, conversely "Tholi" have slopes that are usually steeper than those associated with both Mons and Paterae volcanoes.
Lava plains are the bulk of the Mars' volcanic products. They can be divided into two categories: flow plains and ridged plains. The former are concentrated close to the centre of Tharsis and Elysium volcanic provinces and in Syria Planum; they are characterized by the presence of volcanic features, like lava flows with channels and lava tubes, and absence of wrinkle ridges. These latter can either have tectonic origin and/or form from the contractional strengths occurring during the lava cooling. The ridged plains have been recognized throughout the north polar basin, Chryse and Isidis Planitia, Hesperia Planum and parts of the Hellas basin. They are abundant at about 1000-1500 km beyond the centre of the provinces. In this case wrinkle ridges are common whereas the volcanic features are rare.

1.1 Tharsis region and the volcanic fields of Arsia Mons

The Tharsis plateau hosts most of the volcanic activity on Mars. This region is located on a bulge that rises over 10 km and extends for 5000 km comprehending four large shield volcanoes and seven smaller edifices. They may be the result of a plume of magma that began to erupt at the surface at least from 3.8 Gyr ago and probably still continues, as the crater counting of the more recent flows suggests (Neukum et al., 2004; Hartmann et al., 1999). Apart from Olympus Mons, the main volcanic constructs of the province are Ascraeus Mons, Pavonis Mons and Arsia Mons which, together with the smaller Uranius Paterae and Ceranius Tholus, form a NE-SW trending line, indicating they were originated from the same fault zone. All the major volcanoes are characterized

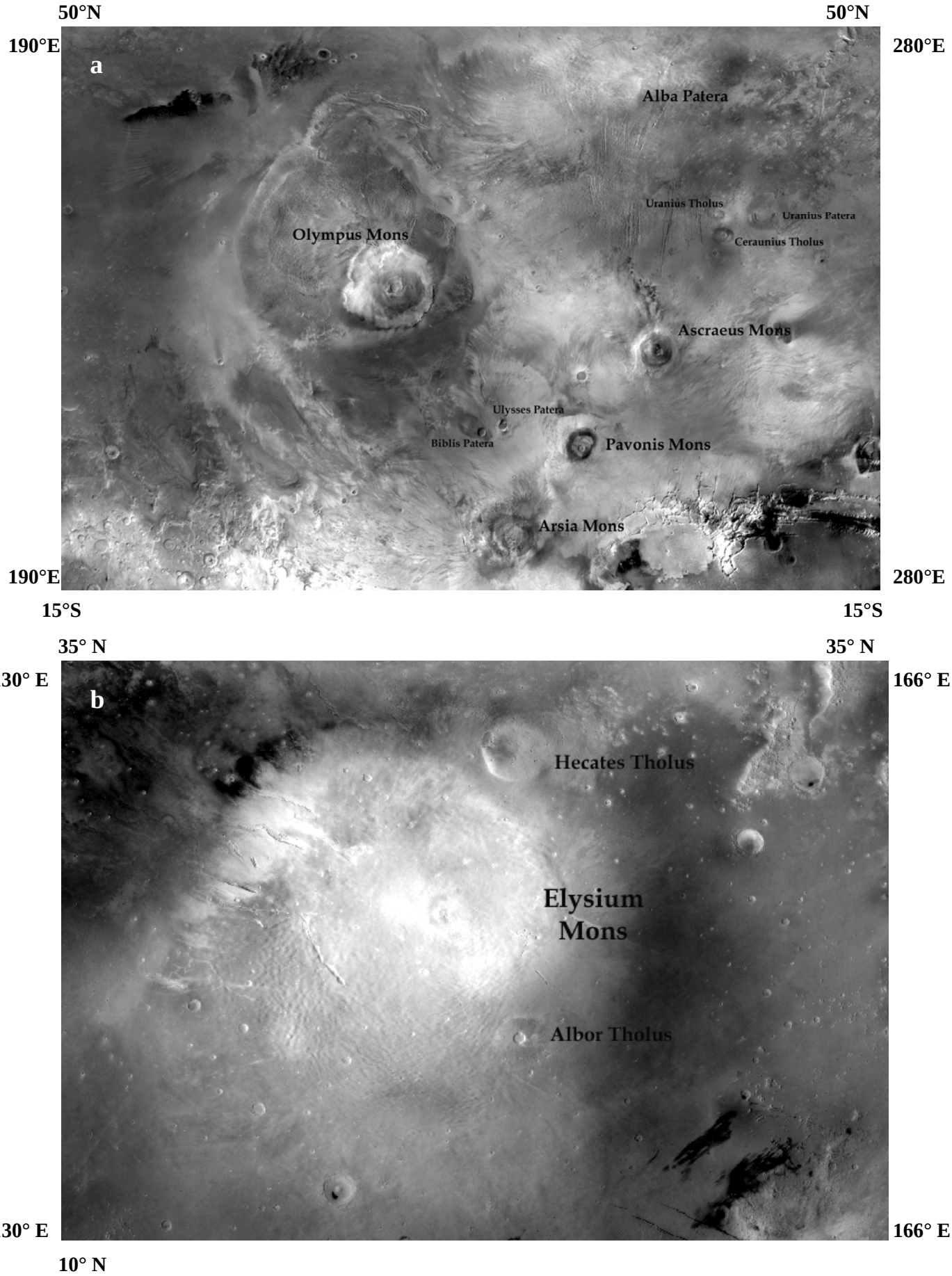

Fig. 1 Main volcanic provinces on Mars a) MOC mosaic of Tharsis region where Olympus Mons, the highest volcano on Mars, is visible. b) MOC mosaic of Elysium province constituted by three volcanoes. The largest and highest one is Elysium Mons, that is the source of the widespread lava field that surrounds the region.

by a central caldera and a gentle flank slope.
Among the volcanoes of Tharsis region, Arsia Mons is distinguished from the others as it is the source of some of the longest lava flows on Mars. Arsia Mons, the southernmost of the three Tharsis Montes, has a basal diameter of 400 km and a summit elevation of 17.7 km (Plescia, 2004). Its flank slope is roughly 5°. The central caldera is bounded by concentric faults and has 130 km of diameter, with a depth of 1.3 km. A line of nine low shields, with a relief of 150m, crosses the floor along a NE-SW trend (Plescia, 2004). Crater dating suggests that the caldera floor is 150 Myr old (Neukum et al., 2004). The western flank of the volcano shows a coarse radial texture, caused partially by irregular pits, whereas the opposing east flank is affected by a fine radial texture. The features located on the northwest part of the shield have been attributed the former presence of glaciers (Head and Marchant, 2003). On the northeast and southwest flanks numerous coalesced pits form rifts from which large volume of lava have erupted. Lava flows from the rift fun form broad aprons on the adjacent plains. Among the others, Daedalia Planum, located to the south-west from Arsia Mons, is characterized by impressive long flows. This plain has an average slope <0.5° and commonly <0.1° (Smith et al., 1999). It is a volcanic field characterized by the presence of a huge number of lava flows, some of them originate from the caldera rim and others from flank pits (Warner and Gregg, 2003). Scott and Tanaka [1986] subdivided the Daedalia Planum lava flows into eight different geological units: the Amazonian At_5 and At_4, the early Amazonian-latest Hesperian AHt_3, and the Hesperian Ht_2, Ht_1, Hsl, Hf, Hpl_3. Older and largest flows extend 1500 km to the south-west, even if establishing their absolute length is difficult because the source vents are covered by subsequent flows. They show the typical pahoehoe and platy-ridged surface textures. The younger and shorter flows reach 600 km of length and extend radially from the Arsia Mons caldera rim; they frequently present a central channel and show a brecciated surface.

In this thesis we have chosen Daedalia Planum field for several reasons: i) lava flows of Daedalia Planum lava field show considerable morphological variations, allowing different mechanisms of emplacement to be studied; ii) Daedalia Planum flows were emplaced during a long time span (about 2.5 Gy), from the middle Hesperian to late Amazonian (Scott and Tanaka, 1986), hence they provide an important key for analyzing the entire evolution of Arsia Mons; iii) Daedalia Planum lava field show very long lava flows, representing some of the longest lava flows on Mars (Zimbelman, 1998); therefore they are important to understand the main factors responsible of the emplacement of long lava flows on Mars.

1.2 The volcanic region of Elysium Planitia

The second largest volcanic province of Mars is Elysium, located on a dome roughly 2000 km across and 5 km height. In this region three large shield volcanoes are located: the greatest Elysium Mons at the centre and the smaller Albor Tholus and Hecates Tholus, on the south and north respectively. Lava flows, radial to the centre of the dome, extend as far as 1000 km to the southeast.
The paucity of large impact craters on the Elysium shields suggests that they have an age between 2 and 1 Gyr, but some flows reveal a more recent age as young as few million years (Hartmann and Berman, 2000; Vaucher et al., 2009).
Elysium Mons is 14 km high and merges gently with the surrounding plains. The basal diameter is of 375 km. Average flank slopes are about 7°. Its caldera is quite shallow, with a diameter of 14 km and a depth of 100m (Plescia, 2004). Extending away from the summit are several lines of pits and fissures. Lava flows are rare on the upper flanks of the volcano, whereas sheet flows and tube-fed flows are common on the gentler slope beyond the main edifice.
Several indications of the presence of water and explosive eruptions in the past occur through the region, like radial channel originated from the volcanoes flanks and smooth ash fields of Hecates Tholus. Moreover on the western part of the region several lahars were observed (Christiansen,

1989), resulting from the interaction between the magma heat and ground ice (see paragraph 3). Water seems to have interested also Cerberus plains, located south-east of Elysium dome. They contain some of the youngest lava flows on the planet (Berman and Hartmann, 2002), probably originate from Cerberus Fossae and several low shields (Plescia, 2003). However Cerberus Fossae is indicated also as the source of water that feed at least two outflow channels, Athabasca Vallis and Grjota Vallis (Carr, 2006). Water from some of the outflow channels probably pooled in the Cerberus Plain and exited to the west, cutting Marte Vallis (Burr, 2002). Most of the Cerberus lava flows outpoured after the outflow channel formation and were confined inside these pre-existing depressions.

2. Lava flows on Mars

Lava flows are spread in the Martian volcanic provinces, like in Tharsis and Elysium region, and originate generally from the central crater of the volcanic edifice or from its flank fractures or pits. A wide variety of morphologies have been observed among the flows. Their shape depends on several factors: 1) planetary variables, like atmospheric conditions and surface temperatures, controlling the cooling rate, and gravity, that controls the effusion rate (2) rheological proprieties of lavas 3) size and shape of the vent and 4) terrain slope.
On Mars narrow lava flows with leveed channels, expression of relatively high effusion rates (25-840 m^3/s, Glaze et al., 2009), have been detected as well as long sheetlike flows which can be compared to terrestrial flood basalts and are the result of large volume and high effusion rates (up to 10^6 m^3/s, Keszthelyi and McEwen., 2000). Long tube-fed flows are common; a lava tube formed by channels which have been roofed over and it requires a constant effusion rate, viscosity and thermal conductivity.
Lava flows show extremely varied surface textures. Wrinkly, ropy surfaces are typical of pahoehoe flows; very smooth or platy-ridged surfaces are instead characteristics of flood lava flows. More rough-surfaced flows are instead typical of aa type lavas.
Probably the more distinguishing aspect of the Martian lava flows is their huge length. The lower gravity of Mars favours the emplacement of long lava flows. A flow has to reach a critical thickness (t) in order to move. This is expressed by the following equation by Hulme [1974]:

$$t = \tau / \rho g \tan\alpha \qquad (1.1)$$

where τ is the yield strength, ρ is the density, g is the gravity acceleration and α is the topographic slope. A greater thickness causes a greater velocity (V):

$$V = \rho g t^2 / B\eta \sin\alpha \qquad (1.2)$$

where η is the viscosity and B is a constant. Therefore, as the cooling rates on the two planets are similar, assuming the same terrain slope and a comparable effusion rate flows on Mars can be cover longer distances than on the Earth.
In addition the lower gravity is responsible of effusion rates from 3 to 5 times higher on Mars than on Earth (Wilson and Head, 1994). As result the Martian lava flows can be up to six times longer than the terrestrial ones. Several example of long flows have been recognized on Mars volcanic areas like Tharsis region (Zimbelman, 1998), Alba Patera (Schneeberger and Pieri, 1991) and Elysium Planitia (Mouginis-Mark and Yoshioka, 1998).
An efficient transport system can contribute to the emplacement of a flow: lava channels and lava tubes allow the lava to cover long distances as they insulate the flowing lava and delay its cooling.

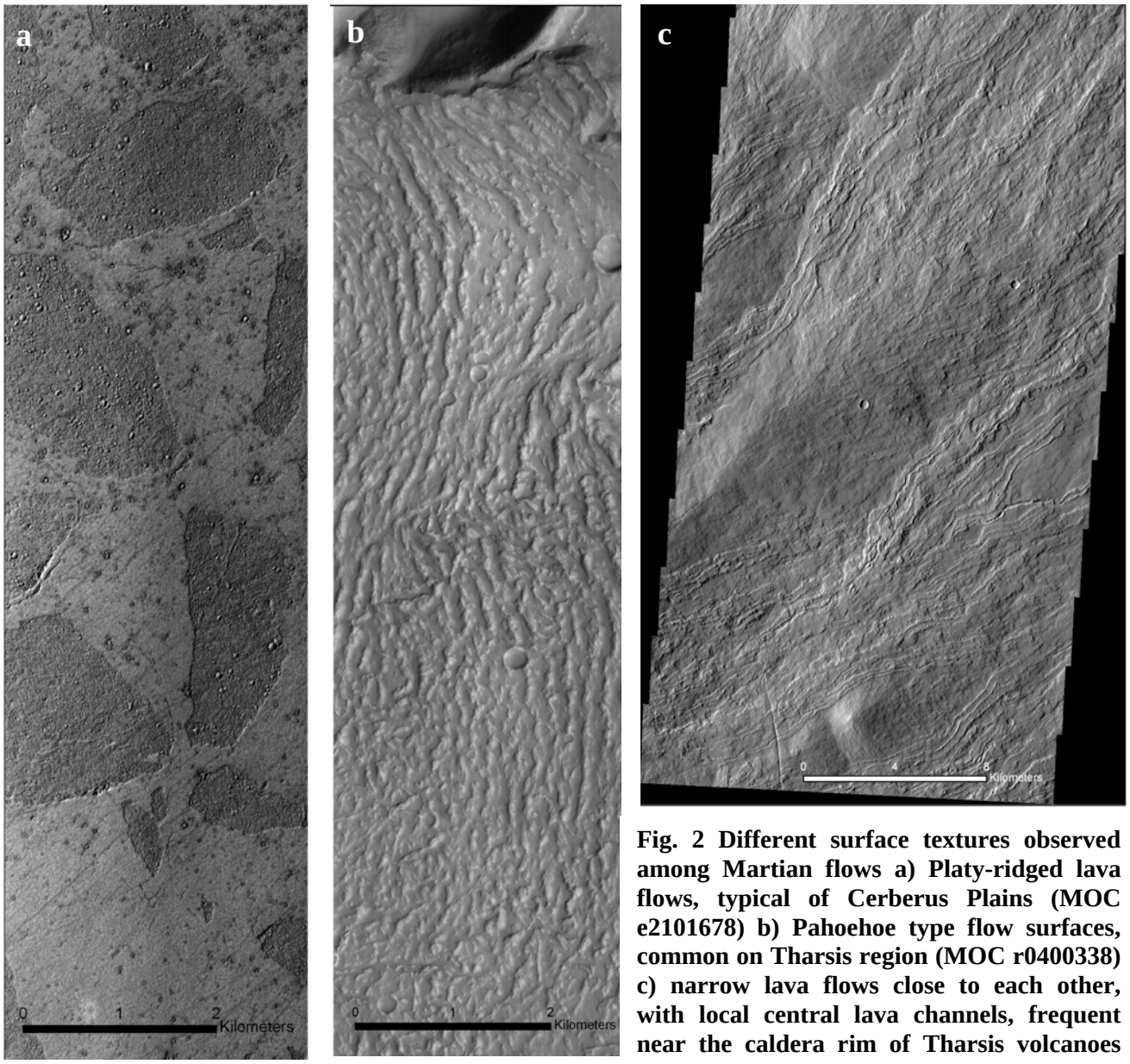

Fig. 2 Different surface textures observed among Martian flows a) Platy-ridged lava flows, typical of Cerberus Plains (MOC e2101678) b) Pahoehoe type flow surfaces, common on Tharsis region (MOC r0400338) c) narrow lava flows close to each other, with local central lava channels, frequent near the caldera rim of Tharsis volcanoes (THEMIS V11251006).

However some flows show so high lengths that can not be explained considering only the above factors described, consequently there should be other agents that favour their emplacement. The inflation process has been proposed (e.g. Cashman et al., 1998; Keszthelyi et al., 2008). The inflation allows lava to flow beneath a colder crust, which acts as a thermal shield. In this way the lava remain hot and fluid for long time and in this way can reach great distances from its source. An inflated flow can be recognized thanks to some morphological fingerprints, like tumuli, lava rises and lava ridges.
One of the main objectives of the present thesis is establishing which factors contribute to the emplacement of the Daedalia Planum lava flows.

3. Martian mud flows

Mud flows are the rapid movement of fine-grained sediments which have been mobilized by water. When a mud flow is linked with volcanism it is called “lahars”. In this latter case sediments are

generally represented by pyroclastic deposits and the water is produced by melting of the ground ice due to magmatic heat.
Lahars consist commonly in a multiply digitate lobes, their surface are smooth with gentle undulations. Where the slopes are steep, flows are thin and become thicker on more gentle slopes. On the Earth, water infiltration, upward expulsion and evaporation causes surface water ponding, branching sapping valleys and collapse pits that represent important geomorphic clues to distinguish a lahars (Lawson, 1982). Moreover, after the emplacement of many lahars, underloaded flood waters erode earlier deposits forming runoff valleys.
On Mars possible lahars in the Elysium region were described by Mouginis-Mark et al.[1984] and Christiansen [1989]. They extended 1000 km from the margin of the Elysium volcanic field, covering 1 000 000 km^2, and seem to be originated from the fracture system on the northwester flanks of the Elysium volcano. Near the source the deposit is thin and smooth and have channeled surfaces .The channels form a anastomose system of tributaries that become shallower and less distinct to the northwest. Several works (Malin, 1976, Mouginis-Mark et al., 1984) asserted that the channels were caused by fluvial erosion, their intimate association with the flow suggests a genetic correlation with the deposits. The interchannels areas with frequent collapse depressions have more hummocky surfaces than the proximal part. These morphologic changes are consistent with an increase of viscosity due to freeze or evaporation of liquid water.

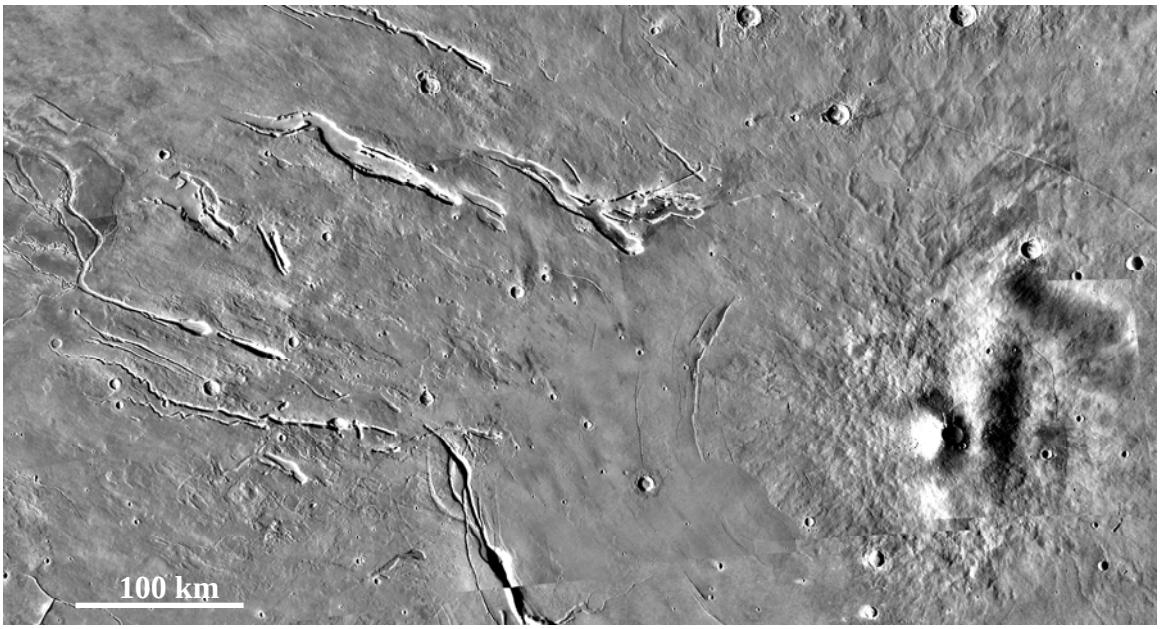

Fig. 3 Probable lahars located north-west to Elysium Mons. Several large channels have their origin from the flank of the volcano, perhaps carved by flowing mud and water released by the heat associated with the Elysium volcanism. (VIKING mosaic).

Several lines of evidence suggest that lahars occur also in Tharsis region: a) Ascraeus Mons is surrounded by some long lobate flows that seem to be the result of more fluid flows than the shield lavas which are more viscous and have produced a much steeper volcanic edifice b) the emplacement time is different as these apron flows overlap the shield lavas c) the apron flows appear smooth while the shield lavas have leveed channels topographically higher than the surrounding lavas d) in the apron flows several channels emerge from fractures that appear to be water carved (Murray et al., 2009).
The presence of fine sediments and water associated with lahars is the suitable condition for the formation of pingos, which are mounds of mud with an ice core that form in periglacial environments (Page and Murray, 2006; de Pablo and Komatsu, 2009; Burr et al., 2009) When the temperatures begin to decrease, pore water concentrates due to the hydrostatic pressure and freezes

progressively forming the ice core. The growth of ice core causes the doming of the overlying terrain and cracks may appear on the summit of the dome.
In plan view mud flows generally appear with lobate boundaries with elevated margins and often with a central channel. Such morphologies are common to gravity-driven flow of all viscous, non-Newtonian fluids that have significant yield strength, like lava flows. Moreover on the morphologically point of view pingos may have similar characteristic of the tumuli on inflated lava flows. Therefore in some cases distinguishing mudflows from lava flows is rather complex. In chapter 5 of the thesis we used the comparison between the Daedalia Planum candidate tumuli and the features on Elysium Planitia as key to establish which of these two different processes is the responsible of Daedalia Planum flows.

References

Bandfield J.L., Hamilton V.E., Christensen P.R., 2000. *A Global View of Martian Surface Compositions from MGS-TES*. Science, 287, 1626-1629. DOI: 10.1126/science.287.5458.1626.

Berman D. C., Hartmann W.K., 2002. *Recent Fluvial, Volcanic, and Tectonic Activity on the Cerberus Plains of Mars*. Icarus,159(1), 1-17.

Burr D. M., Grier J. A., McEwen A. S., Keszthelyi L. P., 2002. *Repeated Aqueous Flooding from the Cerberus Fossae: Evidence for Very Recently Extant, Deep Groundwater on Mars*. Icarus, 159(1), 53-73.Burr, D. M., Tanaka, K. L., Yoshikawa, K., 2009. *Pingos on Earth and Mars*. Planetary and Space Science,57(5-6), 541-555.

Cashman K., Pinkerton H. and Stephenson J., 1998. *Introduction to special section: Long lava flows*. J. Geophys. Res., 103, 27281– 27289.

Carr M., 2006. *The Surface of Mars*. Cambridge University Press, New York.

Christiansen E.H., 1989. *Lahars in the Elysium region of Mars*. Geology, 17(3), 203-206.

de Pablo, M. Ángel, Komatsu, G., 2009. *Possible pingo fields in the Utopia basin, Mars: Geological and climatical implications.* Icarus, 199(1), 49-74.

Hartmann W.K., Malin M., McEwen A., Carr M., Soderblom L., Thomas P., Danielson E., James P., Veverka J., 1999. *Evidence for recent volcanism on Mars from crater counts*. Nature,397 (6720), 586-589.

Hartmann, W.K., Berman, D.C., 2000. *Elysium Planitia lava flows: Crater count chronology and geological implications*. J. Geophys Res., 105(E6), 15011-15026.

Glaze L.S., Baloga S.M., Garry W. B., Fagents S. A., Parcheta C., 2009. *A hybrid model for leveed lava flows: Implications for eruption styles on Mars*. JGR,114(E7), CiteID E07001.

Head J.W. and Marchant D.R., 2003. *Cold-based mountain glaciers on Mars: Western Arsia Mons.* Geology, 31, 641-644.

Hulme G., 1974. *The interpretation of lava flow morphology*. Geophys. J. R. Astron. Soc., 39361–39383.

Keszthelyi L., McEwen A.S. and Thordarson T., 2000. *Terrestrial analogs and thermal models for Martian flood lavas*. J. Geophys. Res., 105, 15027-15050.

Keszthelyi L., Jaeger W., McEwen A., Tornabene L., Beyer R.A., Dundas C. and Milazzo M., 2008. *High Resolution Imaging Science Experiment (HiRISE) images of volcanic terrains from the first 6 months of the Mars Reconnaissance Orbiter Primary Science Phase*. J. Geophys. Res., 113, CiteID E04005.

Lawson D.E., 1982. *Mobilization, Movement and Deposition of Active Subaerial Sediment Flows, Matanuska Glacier, Alaska*. Journal of Geology, 90, 279-300.

Malin, M. C. (1976). *Age of Martian channels*. J. Geophys. Res., 81(26), 1976, pp. 4825-4845.

Mouginis-Mark P. J., Wilson L., Head J. W., Brown S. H., Hall J. L., Sullivan K. D., 1984. *Elysium Planitia, Mars - Regional geology, volcanology, and evidence for volcano-ground ice interactions*. Earth, Moon, and Planets, 30, 149-173.

Mouginis-Mark P., Tatsumura Yoshioka M., 1998. *The long lava flows of Elysium Planita, Mars*. JGR, 103(E8), 19389-19400.

Murray, J.B., van Wyk de Vries B., Marquez A., Williams D. A., Byrne P., Muller J., Kim J., 2009. *Late-stage water eruptions from Ascraeus Mons volcano, Mars: Implications for its structure and history*. Earth and Placet. Sci. Lett., In Press.

Neukum G., Jaumann R., Hoffmann H., Hauber E., Head J.W., Basilevsky A.T., Ivanov B.A., Werner S.C., Van Gasselt S., Murray J.B. and Mccord T., 2004. *Recent and episodic volcanic and glacial activity on Mars revealed by the High Resolution stereo camera*. Nature, 432, 971-979.

Page, D. P., Murray, J. B., 2006. *Stratigraphical and morphological evidence for pingo genesis in the Cerberus plains*. Icarus, 183(1), 46-54.

Plescia, J. B., 2003. Cerberus Fossae, Elysium, Mars: a source for lava and water. Icarus,164(1), 79-95.

Plescia J. B., 2004. *Morphometric properties of Martian volcanoes*. JGR, 109(E3), CiteID E03003.

Schneeberger D.M., Pieri D. C., 2001. Geomorphology and stratigraphy of Alba Patera, Mars. JGR, 96, 1991, 1907-1930.

Scott D.H. and Tanaka K.L., 1986. *Geologic map of the western equatorial region of Mars, scale 1:15,000,000*. U.S. Geol. Surv. Misc. Invest. Ser., Map I-1802-A.

Smith D.E. et al., 1999. *The global topography of Mars and implications for surface evolution*. Science, 284, 1495-1503.

Vaucher J., Baratoux D., Toplis M. J., Pinet P., Mangold N., Kurita K., 2009. *The morphologies of volcanic landforms at Central Elysium Planitia: Evidence for recent and fluid lavas on Mars*. Icarus, 200(1), 39-51.

Warner N.H., Gregg T.K.P., 2003. *Evolved lavas on Mars? Observations from southwest Arsia Mons and Sabancaya volcano*. J. Geophys. Res., 108, 5112-5127.

Wilson L. and Head J.W., 1994. *Mars: Review and analysis of volcanic eruption theory and relationships to observed landforms*. Rev. Geophys., 32, 221– 263.

Wyatt, M.B., McSween Jr., H.Y., 2002. *Spectral evidence for weathered basalt as an alternative to andesite in the northern lowlands of Mars*. Nature, 417, 263–266.

Zimbelman J.R., 1998. *Emplacement of long lava flows on planetary surfaces*. J. Geophys. Res., 103, 27503 – 27516.

CHAPTER 2 - Methods

To answer the several questions about Daedalia Planum flow field, several different aspects have to be analyzed:

a) morphological characteristics of flows, such as surface textures and features, and their morphometric proprieties, such as length, width and thickness. These characteristics permit to perform a geomorphologic mapping of the region and to gain some information about the flow development.
b) comparative study between Daedalia Planum and other Martian or terrestrial fields in order to find similarities or differences. This helps to understand the genesis and history of Daedalia field;
c) estimation of composition and rheological proprieties of lavas, coupled with the estimate effusion rates. This is necessary to shed more light on the emplacement mechanism of flows;
d) comparative study between spectral characteristics of flows (absorption bands, spectral slope, albedo) inside the field, which highlights different spectral behaviors among the flows. This permits to create a spectral map using the Spectral Angle Mapper (SAM) classification;
e) dating the flows which is important to compare their age with the flows of other Martian fields.

In order to study all these aspects the employment of a wide range of data is required (Table 1). Mars Odyssey/ Thermal Emission Imaging System (THEMIS) Infrared (IR) and visible (VIS) images were used to outline the boundary of the flows, as well as to infer their emissivity and reflectivity proprieties. MGS/Mars Orbiter Camera (MOC) and MRO/High Resolution Imaging Science Experiment (HiRISE) images, having a spatial resolution of some meter and decimetres per pixel respectively, allowed the detection of the smallest surface features.
In order to obtained morphometric parameters of flows and slope of underlying terrain, MGS/Mars Orbiter Laser Altimeter (MOLA) data were employed. In this thesis we used the MOLA Mission Experiment Gridded Data Records (MEGDRs), which have a grid size of 463 m/pixel. They are global topographic maps of Mars created by binning altimetry values products acquired over the entire MGS mission. We choose these data essentially because they do not require further processing.
The compositional characteristics of lavas were achieved by MEX/Visible and Infrared Mineralogical Mapping Spectrometer (OMEGA) data, having a spectral range from 0.5 to 5.2 microns.
All these data were managed and processed using several softwares: i) ISIS, for image geo- of THEMIS VIS-IR data; ii) ENVI, to geo-reference HiRISE images, obtain OMEGA spectra of any region and perform SAM classifications; iii) ArcGis, to collect the images of all the instruments and create the geological map of Daedalia Planum; iv) Gridview, to obtain sections of lava flows from MOLA data in order to establish their width and thickness. Since Daedalia Planum is located near the equator we used the equirectangular projection has been used the geo-reference processing.

The geological mapping of Daedalia Planum was realized integrating the geomorphologic and spectral maps of the region. The geomorphologic map was performed on the basis of the flow surface textures similarities (e.g. ropy surfaces, presence of platy-ridged morphologies or brecciated texture) and stratigraphic relationships. The spectral map was through the SAM classification. This technique is an automated method for directly comparing image spectra to known end member spectra (usually determined in the laboratory). This method treats both the spectra as vectors and calculates the spectral angle between them. In our work the endmember spectra used by SAM are the mean spectra of the Daedalia Planum geological units calculated for each OMEGA orbit. This

technique, when used on calibrated reflectance data, is relatively insensitive to illumination and albedo effects. Smaller angles represent closer matches to the reference spectrum. If the spectral angle is greater than the specified maximum angle, the pixel is not classified (Kruse et al., 1993).

The dating of the region of interest was performed by crater counting. In order to determine the age of a surface three procedures have to be carried out: 1) measurement of the surface area, 2) counts of the primary craters present in the surface, 3) fit of the obtained crater size-frequency distribution (CSD) with a specific Production Function. The cumulative size-frequency distribution plot relates the cumulative number and the crater diameters. The error bars represent the confidence interval $\pm \sigma$, which for the *n*th crater is given by $\log = [(n \pm \sqrt{n}) / Area]$ (Arvidson et al., 1979).

We used a semi-automatic program running on IDL software both to count and fit the CSD with the Neukum Production Function (NPF) (Neukum, 1983; Neukum and Ivanov, 1994; Neukum et al., 2001). This function represents the size–frequency distribution of a crater population recorded in a geological unit at a specific time. The production function is given by an eleventh-degree polynomial:

$$\log_{10}(\mathrm{N}) = a_0 + \sum_{n=1}^{11} a_n \left[\log_{10}(D)\right]^n \qquad (2.0)$$

where N is the cumulative number of craters (number of craters per km^2 per Gyr), a_0 represents the amount of time during which the unit has been exposed to the meteorite bombardment, D is the crater diameter expressed in km. Coefficient a_n for Mars is described by Ivanov [2001].

The extrapolated cumulative number for D≥1 km is used with the chronology model of Neukum et al. [2001] to estimate surface age. The model is well established for the lunar surface and is inferred for Mars, by applying some scaling laws relative to the projectile flux, and by taking into account the presence of an atmosphere and a different gravity (e.g., Neukum et al., 2001; Ivanov, 2001; Hartmann and Neukum, 2001; Ivanov et al., 2002).

The dating by crater counts assumes that all the craters considered are primary and does not take into account the presence of secondaries. To avoid the influence of the latters, we do not consider the craters related to rays and clusters or showing an elliptical rim.

Tab.1 List of the instruments whose data have been used in this thesis.

Mission/ Instrument	Spectral bands	Spatial resolution (m/pixel)	Employment	References
Mars Odissey/ THEMIS	**10 IR bands**: 6.78 μm (used twice), 7.93 μm, 8.56 μm, 9.35 μm, 10.21 μm, 11.04 μm, 11.79 μm, 12.57 μm, 14.88 μm **5 VIS bands:** 0.425 μm, 0.540 μm, 0.654 μm, 0.749 μm, 0.860 μm	IR : 100 VIS : 18	Used to detect the flows boundaries and surface textures.	Saunders et al., 2004; Christensen et al., 2004;
Mars Global Surveyor/ MOC (narrow angle camera)	**Panchromatic**: 0.500-0.900 μm	1.5 to 12	Used to study the smallest features of the flow surfaces.	Albee et al., 1992; Malin et al., 1992;
Mars Reconnaissance Orbiter/ HiRISE	**3 bands** : 0.400 to 0.600 μm 0.550 to 0.850 μm 0.800 to 1.000 μm	0.25	Used to study the smallest features of the flow surfaces and for the crater counting.	McEwen et al., 2007; Zurek and Smrekar., 2007;
Mars Express/ OMEGA	**96 VNIR bands**: from 0.36 to 1.07 μm **128 SWIR(2) bands**: from 0.93 to 2.7 μm from 2.6 to 5.2 μm	300 to 4000	Used to the compositional and spectral analysis of lava flows.	Chicarro et al., 2004; Bibring et al., 2004;
Mars Global Surveyor/ MOLA	-	Surface spot size: 130 m Along-track shot spacing: 330 m Absolute vertical accuracy: <10m	Used to calculate the terrain slope and the thickness of flows.	Zuber et al., 1992; Smith et al., 2001;

References

Albee A. L., Arvidson R. E., Palluconi F. D., 1992. *Mars Observer Mission*. JGR, 97(E5), 7665-7680.

Arvidson R. E., Boyce, J., Chapman, C., Cintala M., Fulchignoni M., Moore H., Neukum G., Schultz P., Soderblom L., Strom R., Woronow A., Young R., 1979. *Standard techniques for presentation and analysis of crater size-frequency data*. Icarus, 37, 467-474.

Bibring, J.-P., Soufflot A., Berthé M., Langevin Y., Gondet B., Drossart P., Bouyé M., Combes M., Puget P., Semery A. et al., 2004. *OMEGA: Observatoire pour le Mineralogie, l'Eau, les Glaces et l'Activite´, Eur*. Space Agency Spec. Publ., ESA SP 1240, 37–49.

Chicarro A., Martin P., Trautner R., 2004. *The Mars Express mission: an overview*. In: Mars Express: the scientific payload. Ed. by Andrew Wilson, scientific coordination: Agustin Chicarro. ESA SP-1240, Noordwijk, Netherlands: ESA Publications Division, ISBN 92-9092-556-6, 3 – 13.

Christensen P.R., Jakosky B.M., Kieffer H.H., Malin M.C., McSween Jr. H.Y., Nealson K., Mehall G.L., Silverman S.H., Ferry S., Caplinger M., Ravine M., 2004. *The Thermal Emission Imaging System (THEMIS) for the Mars 2001 Odyssey Mission*. Space Science Reviews, 110, 85-130.

Hartmann W.k., Neukum G., 2001. *Cratering Chronology and the Evolution of Mars*. Space Science Reviews, 96(1-4), 165-194.

Ivanov B.A., 2001. *Mars/Moon Cratering Rate Ratio Estimates*. Space Science Reviews, 96(1-4), 87-104.

Ivanov B. A., Neukum G., Bottke W. F.Jr., Hartmann W. K., 2002. *The Comparison of Size-Frequency Distributions of Impact Craters and Asteroids and the Planetary Cratering Rate*. Asteroids III, W. F. Bottke Jr., A. Cellino, P. Paolicchi, and R. P. Binzel (eds), University of Arizona Press, Tucson, 89-101.

Kruse, F.A., Lefkoff, A.B., Boardman, J.B., Heidebrecht, K.B., Shapiro, A.T., Barloon, P.J., Goetz, A.F.H., 1993. *The Spectral Image Processing System (SIPS) - Interactive Visualization and Analysis of Imaging spectrometer Data*. Remote Sensing of the Environment, 44,. 145-163.

Malin M.C., Danielson G.E., Ingersoll A.P., Masursky H., Veverka J., Ravine M.A., Soulanille T.A., 1992. *The Mars Observer Camera*. JGR, 97(E5), 7699-7718.

McEwen A. S., Eliason E.M., Bergstrom J.W., Bridges N.T., Hansen C.J., Delamere W.A., Grant J.A., Gulick V.C., Herkenhoff K.E., Keszthelyi L. et al., 2007. *Mars Reconnaissance Orbiter's High Resolution Imaging Science Experiment (HiRISE)*. JGR, 112(E5), CiteID E05S02.

Neukum, G., PhD Thesis, 1983. *Meteoriten bombardement und Datierung Planetarer Oberflaechen*. Munich, 1-186.

Neukum G., Ivanov B. A., 1994. *Crater size distributions and impact probabilities on Earth from lunar, terrestrial-planet, and asteroid cratering data*. In Hazards Due to Comets and Asteroids (T. Gehrels, ed.), pp. 359-416. Univ. of Arizona, Tucson. 1300 pp.

Neukum G., Ivanov B.A. and Hartmann W.K., 2001. *Cratering Records in the Inner Solar System in Relation to the Lunar Reference System*. Space Science Reviews, 96, p. 55-86.

Saunders R. S., Arvidson R. E., Badhwar G. D., Boynton W. V., Christensen P. R., Cucinotta F. A., Feldman W. C., Gibbs R. G., Kloss C.Jr., Landano M. R. et al., 2004. *2001 Mars Odyssey Mission Summary*. Space Sci. Rev., 110(1), 1-36.

Smith D.E., Zuber M. T., Frey H.V., Garvin J.B., Head J.W., Muhleman D.O., Pettengill G.H., Phillips R.J., Solomon S. C., Zwally H. J., et al., 2001. *Mars Orbiter Laser Altimeter: Experiment summary after the first year of global mapping of Mars*. JGR, 106(E10), 23689-23722.

Zuber M. T., Smith D. E., Solomon S. C., Muhleman D. O., Head J. W., Garvin J. B., Abshire J. B., Bufton J. L., 1992. *The Mars Observer laser altimeter investigation*. JGR, 97(E5), 7781-7797.

Zurek R. W., Smrekar S. E., 2007. *An overview of the Mars Reconnaissance Orbiter (MRO) science mission*. JGR,112, E05S01,:10.1029/2006JE002701.

CHAPTER 3- Inflated flows on Daedalia Planum (Mars)? Clues from a comparative analysis with the Payen volcanic complex (Argentina)

Abstract

Inflation is an emplacement process of lava flows, where a thin viscoelastic layer, produced at an early stage, is later inflated by an underlying fluid core. The core remains hot and fluid for extended period of time due to the thermal-shield effect of the surface viscoelastic crust. Plentiful and widespread morphological fingerprints of inflation like tumuli and lava rises are found on the Payen volcanic complex (Argentina) where pahoehoe lava flows extend over the relatively flat surface of the Pampean foreland and reach up to180 km in length.
The morphology of the Argentinean Payen flows were compared with lava flows on Daedalia Planum (Mars), using Thermal Emission Imaging System (THEMIS), Mars Orbiter Laser Altimeter (MOLA), Mars Orbiter Camera (MOC), Mars Reconnaissance Orbiter (MRO)/ High Resolution Imaging Science Experiment (HiRISE). THEMIS images were used to map the main geological units of Daedalia Planum and determine their stratigraphic relationships. MOLA data were used to investigate the topographic environment over which the flows propagated and assess the thickness of lava flows. Finally MOC and MRO/HIRISE images were used to identify inflation fingerprints and assess the cratering age of the Daedalia Planum's youngest flow unit which were found to predate the caldera formation on top of Arsia Mons. The identification of similar inflation features between the Daedalia Planum and the Payen lava fields suggests that moderate and long lasting effusion rates coupled with very efficient spreading processes could have cyclically occurred in the Arsia Mons volcano during its eruptive history. Consequently the effusion rates and rheological proprieties of Daedalia lava flows, which do not take into account the inflation process, can be overestimated. These findings raise some doubts about the effusion rates and lava rheological properties calculated on Martian flows and recommends that these should be used with caution if applied on flows not checked with high resolution images and potentially affected by inflation. Further HiRISE data acquisition will permit additional analysis of the flow surfaces and will allow more accurate estimates of effusion rates and rheological properties of the lava flows on Mars particularly if this data is acquired under a favourable illumination.

1. Introduction

Lava flows in the order of 2000 km have been identified on the Mars surface (Keszthely et al., 2000; Fuller et al., 2002) and the mechanisms which have facilitated this length are still matter of debate. On Earth long lava flows (greater than 100 km in length) are the result of combined mechanisms such as high effusion rates, steep slopes, low viscosity lavas, high temperature lavas, and efficient transport systems (channels or tubes) (Kilburn and Lopes, 1991; Pinkerton and Wilson, 1994; Keszthelyi, 1995; Keszthelyi and Self, 1998; Cashman et al., 1998; Sakimoto and Zuber, 1998; Zimbelman, 1998). Concerning Martian flows, several authors have suggested that the extremely high effusion rates (10^4-10^6 m^3/s) are the dominant cause of long flows (Walker, 1973; Warner and Gregg, 2003) whereas other authors have also invoked particular emplacement mechanisms dominated by lava tube networks (Keszthelyi, 1995; Dragoni et al., 1995; Sakimoto et., 1997). To shed more light over lava flows on Mars, new Earth analogues, beyond the classical ones from Hawaii and Iceland, are needed.
The lava field of Payen volcanic complex, belonging to the back-arc extensional area of the Andes (Argentina), represents an outstanding model for several Martian lava fields, since it shows a multiplicity of flow surface morphologies linked to different lava types and related emplacement mechanisms. The most striking features of the Payen lava field are pahoehoe flows advancing more than 100 km from their feeding vents. These flows represent some of the longest lava flows in the world. Among them the Pampas Onduladas flow is the longest sub-aerial individual lava flow currently known on the surface of Earth (Pasquaré et al., 2008) and its considerable dimensions (180 km of length) is comparable with several long individual flows on Mars (see for example Peitersen and Crown, 1999).

In this work the very long lava flows of the Payen lava field are described and compared with the flows covering Daedalia Planum which are some of the longest flows on Mars (Zimbelman et al., 1998).
The main reason of the Payen lava flows' length is the very low viscosity of the olivine basalt lavas, coupled with the inflation process (Pasquarè et al., 2005; 2008). We have dedicated the first section to this particular mechanism of lava emplacement. The Payen Matru volcanic complex and the Pampas Onduladas and Los Carrizales flows are described in section 3. The stratigraphic and geomorphological analysis on Daedalia Planum flows, realized using MOLA, THEMIS, MOC and MRO/HIRISE, are illustrated in section 4. The absolute model age has been determined from the cratering record of one of the youngest flows and explained in section 5. Section 6 discuss the effusion rates and physical properties of Daedalia flows highlighting how apparent incongruence between Martian and terrestrial long flows can rise if the presence of inflation process is neglected.

2. The Inflation process

The inflation process is typical of many long lava flows among which the best investigated are the Hawaiian ones (Walker, 1991 and Hon et al., 1994). Lava, still hot and fluid, flows beneath a thin colder crust, which behaves as a thermal shield. This crust develops a sufficient strength to retain the incoming lava producing an increase in hydrostatic head at the flow front. By the continuous injection of lava the tensile stress increases until the inflated front breaks and a new lava lobe forms. The repetition of this phenomenon creates a series of inflated lobes linked together to form a unique sheet inflated lava flow (Fig.1). Anderson et al. [1999] hypothesized that inflation process occurs as a sequence of pulses. Their studies about the dilational fractures on Hawaiian pahoehoe flows suggest that these latter have been subject to different magma injections affecting localized portions of the flow. This implies the presence of an interior plumbing system capable of injecting small batches of magma beneath a cooled crust.
Commonly the inflation process takes place in smooth areas with a slope lower than 1-2° and requires long lasting and moderate effusion rates (Self et al., 1996, 1997). On Kilauea volcano Hon et al. [1994] observed pahoehoe flows that initially propagated as a thin sheet of 20-30 cm of thickness uplifted up to 1-5 metres after the inflation process. The same authors calculated the effusion rate responsible of inflated flows on Kilauea using their area and average thickness and knowing their emplacement lapse time. A supply rate of the order of 1-2 m^3/s was obtained, which is similar to that calculated by Rowland and Walker [1990] during 7 years of direct monitoring of the Kilauea volcano activity (effusion rate of ~5 m^3/s). Icelandic inflated pahoehoe flows, originating from monogenetic shield volcanoes, are the result of low supply rate, with a range between 3-10 m^3/s (Thorarinsson, 1966; Rossi and Gudmundsson, 1996).
These effusion rates for pahoehoe lavas are, however, strictly related to lava flows characterized by narrow fronts (< 100 m). For some inflated continental basalt flows whose fronts can reach several tens kilometres, effusion rates up to ~4000 m^3/s were estimated (e.g. Roza in the Columbia River Province, Thordason and Self, 1998; Keszthelyi and McEwen, 2007).

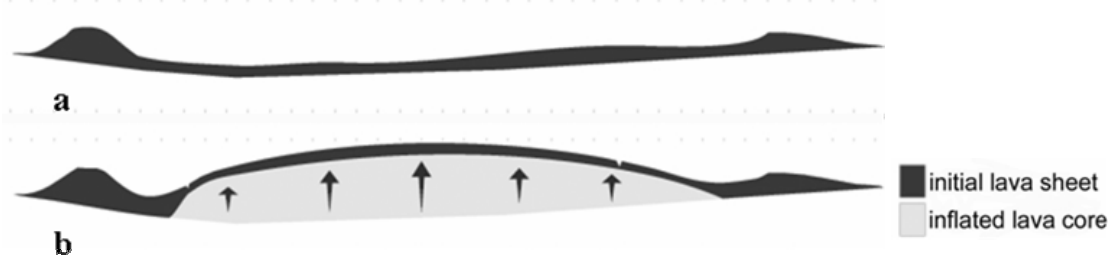

Fig.1. Effects of the Inflation process: an original thin lava flow (a) is subsequently inflated by injection of lava hot and fluid beneath the colder surface crust (b).

Inflated lava flow surfaces show some characteristic features. At small scale tumuli, lava rises and lava ridges could be present (Walker, 1991), whereas at large scale the inflation may create flat-topped pahoehoe sheet flows, hummocky pahoehoe flows and tumuli-dominated flows (Hon et al., 1994). Although not limited to inflated flows, squeeze-ups are particularly frequent since they are generated by vertical growth and fracturing of the sealing crust followed by effusion of hot lava continuously injected beneath the flow surface.
Tumuli are positive topographic features created by magmatic overpressure which can locally induce uplift and tensile stress of the sealing crust. They have typical circular or elliptical map-shapes and are characterized by joints radially distributed on their top. The axial cracks, called clefts, are usually wider than the others and along them squeeze-ups occur locally (Rossi and Gudmundsson, 1996). Studying Icelandic pahoehoe lava flows, Rossi and Gudmundsson [1996] recognized three morphotypes of tumuli: (1) lava-coated tumuli, (2) upper-slope tumuli and (3) flow-lobe tumuli. The first type is typical of the upper, steep flanks of the Icelandic shield volcanoes and they are covered by lava squeezing out from the inflation cracks. Upper-slope tumuli form on shallower slopes at greater distances from the vent, they are not buried by lava although axial cracks are still used as outflow channels by lava. Finally the flow-lobe tumuli occur on the middle and lower flanks of the volcanoes and they do not show out-flows from their cracks.
Lava rises are flat-topped lava reliefs characterized by very steep flanks and bounded by marginal clefts and squeeze-ups. Often they assume distinctive irregular and lobate shapes.
Finally, lava ridges form by lateral compression deforming the visco-elastic lava crust when an inflated lava flow comes across pre-existing positive topographic obstacles, like small cones or dikes.
Hon et al. [1994] hypothesized that tumuli and other inflation features require the formation of preferential pathways under the insulating crust. Initially the movement of lava under the sheet inflated flow is distributed uniformly throughout the liquid core, but after the emplacement the flow begins to chill from the sides as well as the top and bottom. This focuses lava flux toward the centre of the flow where preferred pathways develop. On steeper slopes (>1-2°) these pathways form a network of narrow capillary tubes and when obstacles are encountered a localized inflation may create tumuli and other inflation features.
Inflated lava flows were also recognized on Mars. In particular, Keszthelyi et al. [2008] detected at Cerberus Fossae some inflated sheet flows associated with several lava rises, whereas at the southern margin of Elysium Planitia some still debated forms (Murray et al., 2005) have been interpreted by Keszthelyi et al. [2008] as the result of two phases of inflation, one responsible for several tumuli like features and the other for kilometre-scale uplifts.

3. The Payen volcanic complex: an outstanding source of inflated morphologies

3.1 *Geological framework of the Payen volcanic complex*

Payen is a fissural volcanic complex located in the back-arc volcanic province of Payenia in Argentina. It developed from a 70 km long alignment of eruptive centres related to the W-E Carbonilla fault system. The activity of the Payen volcanic complex began during the Early Quaternary when pahoehoe basaltic lava shield and related scoria and spatter cones developed over the eastern end of Carbonilla fault system (Germa et al., 2007). A large volume of olivine basaltic lavas covered the shield with large fields of compound and single pahoehoe inflated lava flows, among them the longest ones are the Pampas Onduladas flow (POF) and Los Carrizales lava field flows (Pasquarè et al., 2005, 2008). One sample collected from one of the flows of Los Carrizales lava field yields a K/Ar age of 0.40 ± 0.1 Ma (Melchor and Casadio, 1999).
After the formation of the Payen eastern shield new volcanic activity developed in the central part of the Carbonilla creating two great trachytic and trachyandesitic stratovolcanoes, called

respectively Payen Liso and Payen Matru. While the first was not involved in other volcanic activity, the latter was partially destroyed by an 8 km wide caldera, which collapsed at around 168 ka (Germa et al., 2007) and was followed by highly viscous trachytic and trachyandesitic lavas eruptions (Llamblias, 1966). Finally a Holocene phase of basaltic volcanism developed on both extremities of the Carbonilla fault system. In the eastern one both aa and pahoehoe young olivine-basaltic lavas outpoured, partly covering POF and Los Carrizales lava field (Inbar and Risso, 2001). The magmatism of the Payen Volcanic Complex belongs to the Na-alkaline series and is constituted mainly by basaltic rocks ranging from hawaiites to slightly sub-alkaline basalts, but a significant component of more evolved magmas, up to trachytic composition, are however abundant, especially in the volcanism after POF (Gonzalez Diaz, 1972).

3.2 Pampas Onduladas and Los Carrizales lava flows

The POF is an individual basaltic pahoehoe flow clearly visible in satellite images and aerial photos thanks to its black and unvegetated surface. The flow moving over the nearly flat Pampean foreland (slope of 0.3°) reached a length of 180 km (Pasquarè et al; 2005, 2008) (Fig.2).
The morphological and textural characteristics of POF allow four main sectors to be distinguished in its longitudinal development (Fig.3) (Pasquarè et al., 2008). In the first sector (A in Fig.2), located near the vent area, POF is constituted by uninflated pahoehoe units, sometimes channelized into levees. When the slope decreases from 2° to around 1° these units become progressively inflated lobes and toes which cooled together, forming a unique very large front. Beyond the front begins the second sector (B in Fig.2) where POF presents a very large sheet flow with tumuli, lava rises, and other inflation features. Locally some open arcuate tension gashes develop between lobes and sheet flow and several kilometre long fractures occur, some of which are partly filled by squeeze-ups.

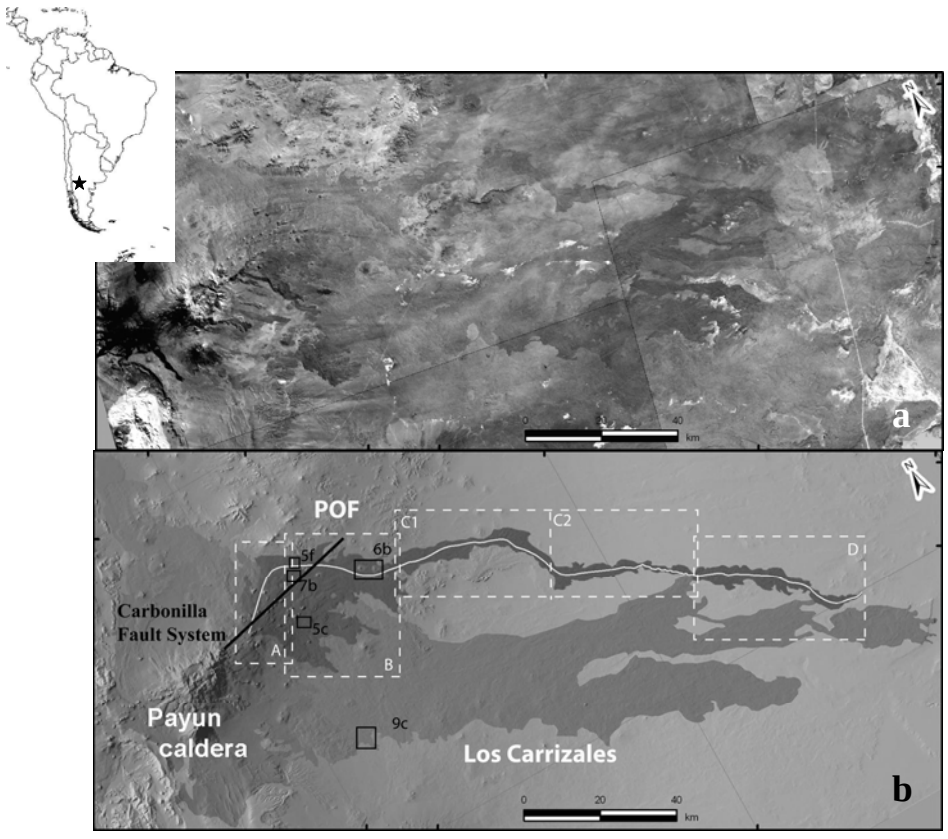

Fig.2. Landsat 7ETM image mosaic (grey scale representation of a RGB = 742 false color composite image) (a) and sketch map (b) of the Payen Matru Volcanic Complex. POF: Pampas Onduladas lava flow. Black boxes indicate the location of the inflation features shown in Fig.5, 6, 7, 9.

In this sector the POF main branch flowing eastward has a minimum thickness of 20 m. When the flow reaches a gradient of 30 m over one kilometre the flow morphology changes significantly: lava rises disappear and tumuli tend to be associated in clusters with a very discontinuous distribution. The tumuli seem to be concentrated in more depressed portions of the flow and locally placed along the axis of long marginal ridges. In this section the flow thickness has been derived by the topography and it is around 10-15 m. After the fall of 30 m over one kilometre, there is the third sector of POF (C1 in Fig.2) which is confined by a Tertiary volcanic tabular relief on the south and a river channel on the north. Here POF width is reduced from 10 km to 3 km and thickness to around 5 meters. From here onward POF can be classified as a constant flow sensu Peitersen and Crown [1999, 2000]. In fact the topographic confinement disappears when POF reaches the Pampean alluvial piedmont plain but the flow maintains its tongue-like shape because it is self-confined by lateral ridges (C2 in Fig.2). On the other hand its flat internal portions became depressed and characterized by a slightly hummocky surface. Further downstream the fourth sector begins (D in Fig.2) with a flow width of 500 m. This is morphology characterized by a central longitudinal tabular ridge showing a deep axial cleft partially filled with squeeze-ups. Many short lobes and toes form by lateral breakouts from the central ridge. The final part of POF begins after a new bottle neck-like narrowing of the flow. The previous tabular ridges disappear giving way to a interconnected, wide, long and billowy braided lobes. After reaching an alluvial terrace the lava flow spills over a 25 m scarp and ends in piles of chaotic blocks.

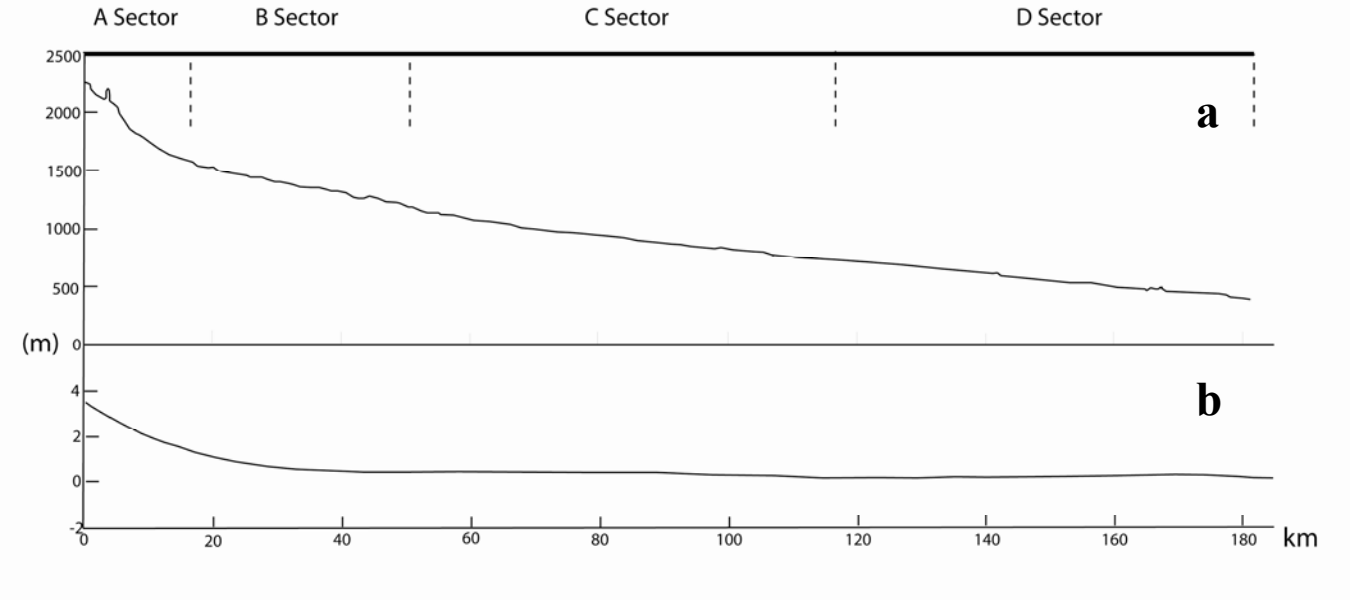

	A sector	B sector	C sector	D sector
Length (km)	16.9	33.6	66.0	65.0
Width (km)	20	10	3 to 0.5	5
Thickness (m)	-	20 to 15	5	4
Slope	2°	1°	0.25°	0.25°
Morphologies	Uninflated pahoehoe units	Sheet flows with tumuli, lava rises and other inflation features (lava ridges and squeeze-ups)	Topographic to self confined flows with a flat internal portion characterized by hummocky surface.	Billowy braided lobes

Fig.3. (a) Longitudinal and slope profiles of POF along the white line crossing the flow in Fig. 2b (After Pasquarè et al., 2008).The underneath table indicates the main characteristics of the four different sectors of POF.

Located to the south of POF, the Los Carrizales lava field (Fig.2) is composed of four individual lava flows one of which reaches 172 km from the source vent. Even though field observations of the lava field are limited, remote sensing studies reveal that the surface of these lava flows are similar to POF, with the upper part characterized by hummocky sheet flow (Pasquarè, 2005). The morphology of these initial sectors suggests the presence of an efficient system of capillary tubes, whose occasional obstruction causes the formation of tumuli and other inflation features like lava rises, ridges and squeeze-ups. The morphologies of the lower part of the Los Carrizales lava field instead reveal a transition to a narrower, irregular and channelized system where are present large tubes, open-channel flows and terraced lava tongues with long and narrow pressure ridges

The POF and Los Carrizales rocks are holocrystalline with low phenocryst contents of olivine (ca. 5 vol.%) and minor plagioclase. The Rare Earth Element (REE) content suggests that parental magma of POF is generated from the partial melting of a mantle probably affected by slab-derived metasomatism (Pasquarè et al., 2008). The POF magma temperature has been calculated on the basis of mineral/liquid geothermometers giving a range of 1130-1160° C, whereas assuming a 0.5-2% of volatile elements and the absence of phenocryst and voids, the viscosity in the magma ranges between 3-73 Pa-s (Pasquarè et al., 2008).

4. The Daedalia Planum lava flows compared with the Pampas Onduladas and Los Carrizales flows: looking for morphological evidence of inflation

Daedalia Planum is one of the Tharsis volcanic plains and is located southwest of the Arsia Mons, (Fig. 4). Arsia Mons is a shield volcano with a basal diameter of 350 km and a height of about 20 km. According to MOLA data, the flanks of Arsia have an average slope <5°, while the surrounding regions, including Daedalia Planum, have slopes <0.5° and commonly <0.1° (Smith et al., 1999). Daedalia Planum is covered by a huge number of lava flows. Some of these originate from the central caldera rim of Arsia Mons but others seem to originate from its flank pits (Warner and Gregg, 2003). If the first origin is assumed, the older and larger lava flows have a calculated length greater than ~1500 km (Carr et al., 1977; Moore et al., 1978; Shaber et al., 1978; Scott and Tanaka, 1981), however determining their absolute length is difficult as subsequent lava flows have buried the source vents. Scott and Tanaka [1986] subdivided the Daedalia Planum lava flows into eight units: the Amazonian At_5 and At_4, the early Amazonian-latest Hesperian AHt_3, and the Hesperian Ht_2, Ht_1, Hsl, Hf, Hpl_3. The older units (Ht_2, Ht_1, Hsl) are composed of long lava flows which extend towards west-southwest of Arsia Mons. The youngest flows (At_5, At_4) are shorter and were emplaced radially around the caldera. MOLA and THEMIS image mosaics were used to develop a Daedalia Planum geological map (Fig.4) where different flow units were represented. THEMIS images, in particular, facilitate the detection of flow edges and therefore were particularly useful for determining stratigraphic relationships. High resolution images of MOC and HiRISE were used to identify several new units and their relationships with the Scott and Tanaka [1986] geological map (Tab.1).

Table 1
Comparison between the Daedalia Planum units shown in Fig.4 and the geological units from Scott and Tanaka [1986].

Fig.4	Scott and Tanaka (1986)
D13	At_5
D12	At_4 AHt_3
D11	AHt_3
D10	AHt_3
D9	Ht_2
D8	AHt_3
D7	Ht_2 AHt_3
D6	Ht_1
D5	Ht_1 Ht_2 Hsl
D4	Ht_2
D3	Ht_2
D2	Ht_2
D1	Ht_1
t	Hf

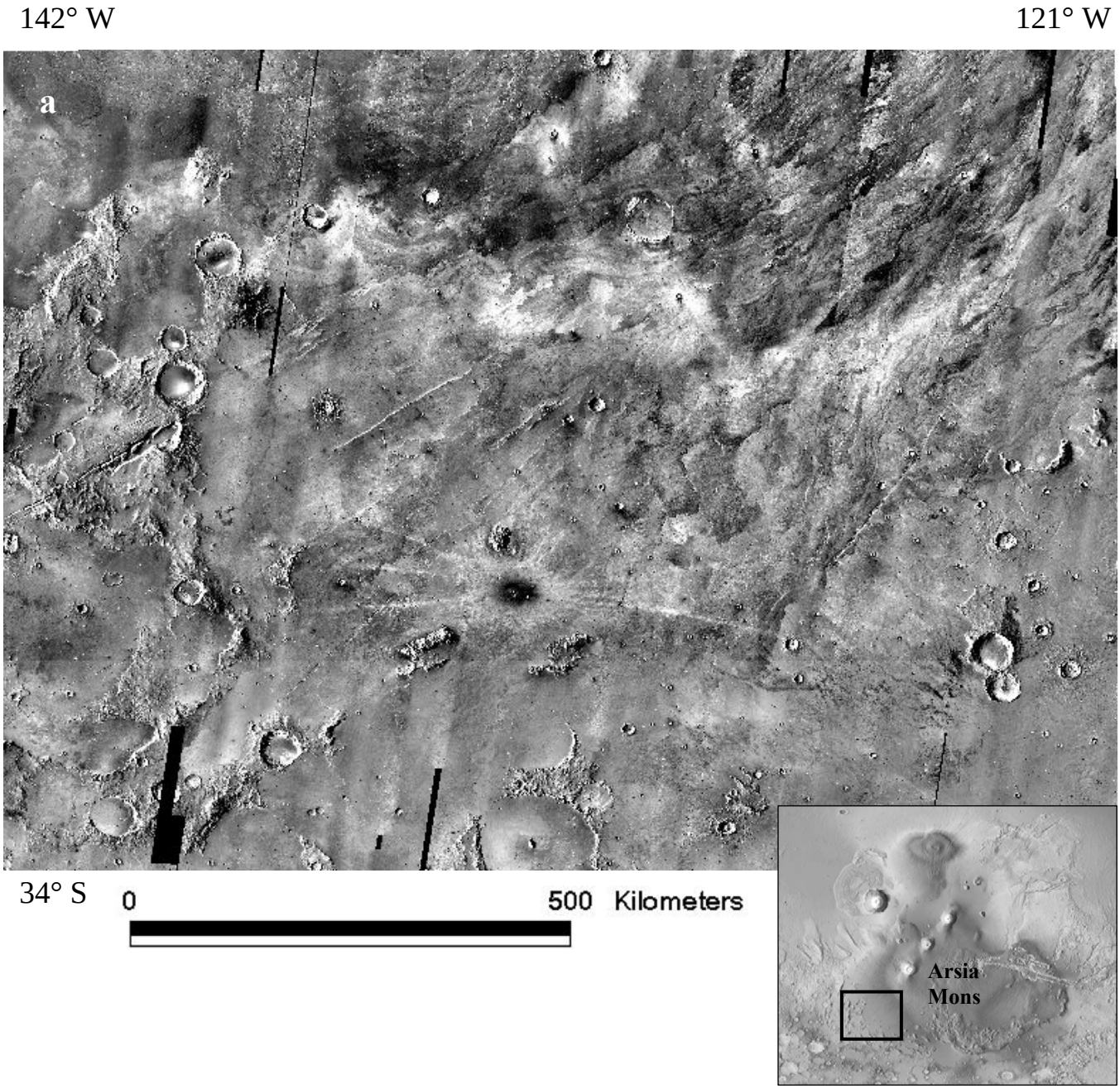

Fig.4. **Daedalia Planum lava field (a) THEMIS image mosaic (daytime thermal infrared 12.57µm) (b) our geological map of the Daedalia Planum lava field. The legend indicates geological units from the youngest to the oldest. No-volcanic materials are indicated by "t"; "nd" indicates the regions not considered in this work. Lower-case letters distinguish the single lava flows. The smaller and numerous flows belonging to D13 and D10 were not isolated (except for D13a and D10a), as well as the D3, D5 flows whose boundaries are often not clearly detectable. The locations of possible inflation features have been marked: black box in D3 indicates the position of possible tumuli, lava rises and lava lobes (Fig. 5b;5e;7d). Black circle and the star in D3 localizes lava ridges (Fig.6a) and squeeze-ups (Fig.7a) respectively. Black box in D12 marks the location of possible lava ridges (Fig.12) and the one in D10 defines the area of HiRISE image PSP_002711_1550 of Fig. 9a. The three flows bordered by black line have been chosen to calculate effusion rates, yield strengths and viscosities (see text for details).**

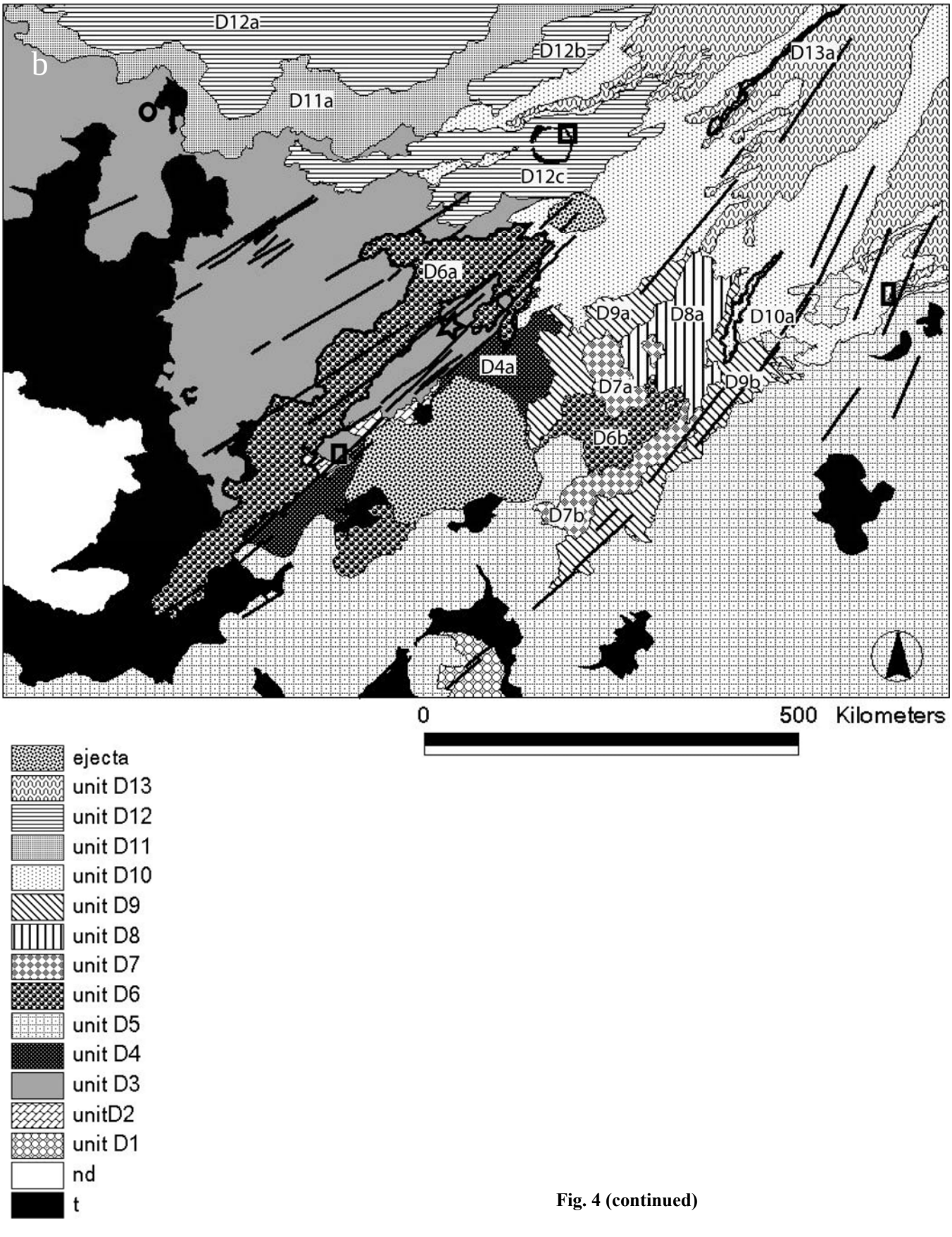

Fig. 4 (continued)

The flows were finally classified into thirteen different units on the basis of their surface textures similarities and stratigraphic relationships. The overlapping relationships are straightforward for all units except for D1 that, although constituted by lavas infilling a 100 km crater at the base of D5, does not show any outcropping contact with D2, D3 and D4.
Among all the units exposed on the study region, some are of particular interest because of the length and surface morphology of their flows and/or the availability of high resolution acquisitions.
In particular the Hesperian D3 and D5 units, respectively cropping out at the north-western and south-eastern part of the studied area, are composed by extremely widespread and long lava flows (up to 2000 km from the Arsia caldera rim) that are characterized by irregular and discontinuous margins and a bright smooth texture on the daytime thermal infrared THEMIS images (Fig.4a). Considering the low slope of the plain (generally < 1°) the inflation process is expected for these flows, however the high and very high resolution images (MOC and HiRISE) suggest variable mechanisms of emplacement for each unit.
On the D3 flows, several forms with a dome-shaped cupola, have been detected. They appear isolated or clustered and show generally an elliptical shape with a wide range of dimensions: from 30 metres up to 100 metres in length and from 20 to 80 metres in width (Fig. 5b). Since all the Daedalia Planum lack evidence of glacial action, it is improbable that these morphological forms can be attributed to cold-based mountain glaciers like those described by Head and Marchant [2003] on the Western Arsia Mons. In addition, unlike glacial and eolian forms that are widespread, contiguous and numerous, these positive topographic features are less abundant and concentrated in limited zones. They moreover suggest a direct interaction with the substratum rather than an embayment relationship. For all these reasons these features can be interpreted as tumuli and, more precisely as flow-lobe tumuli (see Rossi and Gudmundsson, 1996) since they are emplaced in the lower flank of Arsia Mons. Unfortunately, the MOC images where they appear do not have a spatial resolution sufficient for detecting possible axial clefts. In some cases these flow-lobe tumuli appear aligned to possible interior flux pathways, like lava tubes, and their longitudinal axis are oriented accordingly (Fig.5b). In the same area and strictly associated with tumuli, there are some features showing morphological characteristics typical of lava rises with flat surfaces reaching few square kilometres (5 to 10 km^2) and low-relief margins that recall localized and small squeeze-ups (Fig.5e).
All these forms show important similarities with positive inflation morphologies on POF. On POF the tumuli are either isolated or associated in small groups. They show longitudinal axis and central extensional fissures parallel to the flow direction. Their heights do not exceed 10 metres and their shapes, usually elliptical with around 20 metres in width and not over 50 metres in length, are comparable with the D3 tumuli like morphologies (Fig.5c-d) (Pasquarè et al., 2008). Lava rises of POF are scattered over the sheet flow and have different sizes and forms, from few thousands of square metres up to square kilometres; their elevation reaches 10 metres (Pasquarè et al., 2008). The larger lava rises are flat-topped, with their surface bounded by marginal cleft along which vertical squeeze-ups can occur. Clefts separate the lava rise flat surfaces from their flanks whose slopes are of 20° - 40°. However the POF lava rises partly differ from the D3 ones, since they are often associated with irregular and undulated edges (Fig.5f) that contrast with the more rectilinear borders of the flat topped reliefs associated to the D3 (later rectification by erosive processes?).
Other inflation derived morphologies on top of D3 lava flows are lava ridges surrounding pre-existing topographic irregularities (Fig.6a), squeeze-ups cutting the lava flow surface for several kilometres (Fig.7a), and several lava lobes showing lengths from few hundred metres to kilometres (Fig.7d.). Like tumuli and lava rises also these features find their straightforward analogues on the POF counterparts.

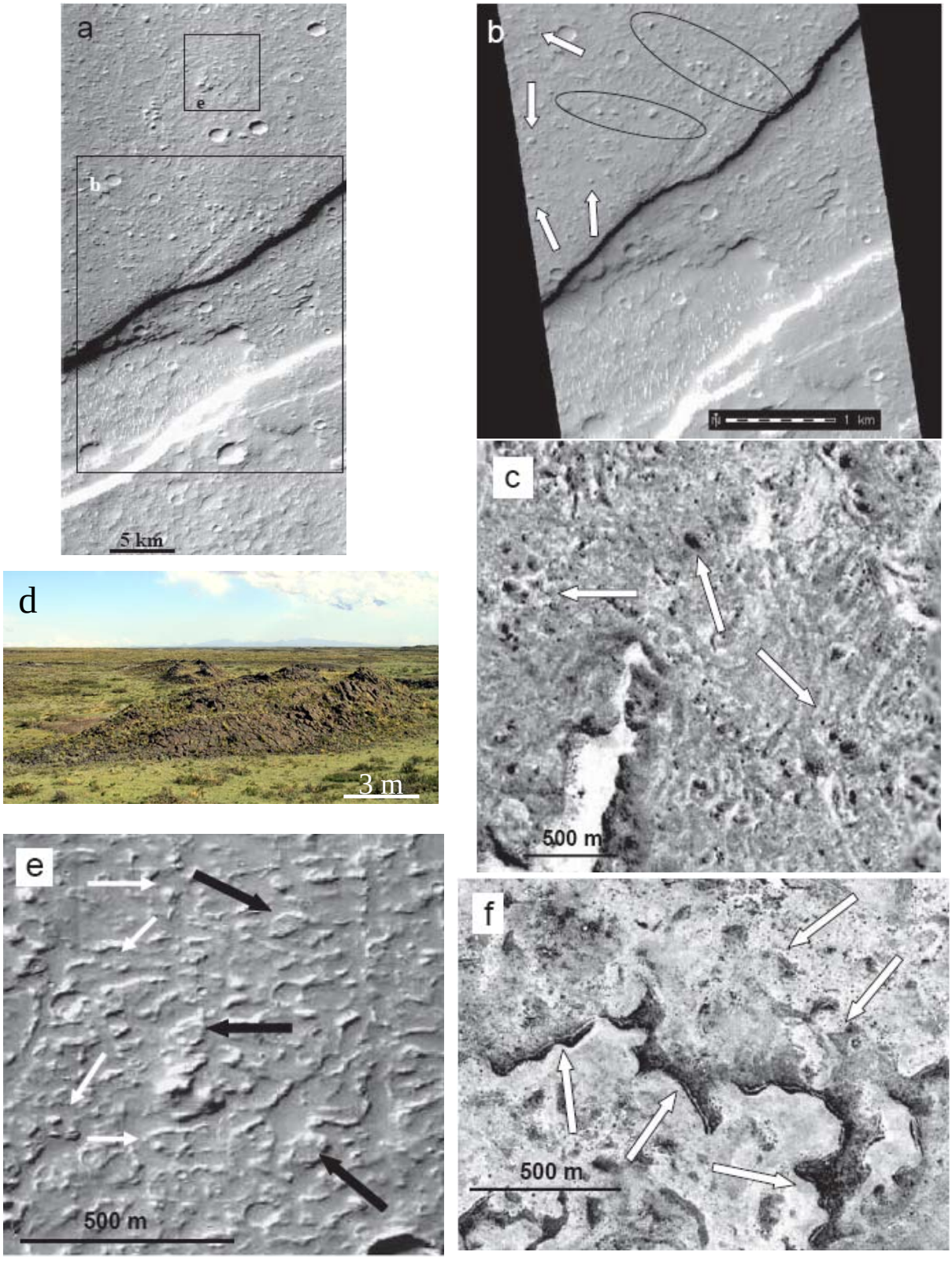

Fig.5. Surface features of D3 flows compared with POF ones (a) MOC image (m2200686) of a D3 lava flows in which possible tumuli and lava rises have been recognized. A graben is shown in the lower part of the image (b) a close-up view of the MOC image where possible tumuli have been discovered. The encircled features show a clear NW-SE orientation, which could represent the local direction of the endogen inflated flux. Other tumuli (white arrows) are scattered on the flow surface (c) Satellite IKONOS image of POF showing small groups of tumuli scattered over the flow (white arrows). (d) POF tumulus with wide axial clefts (length: 15m; height: 3m) (e) a close-up view of the MOC image where features similar to lava rises (black arrows) and tumuli (white arrows) are indicated (f) Satellite IKONOS image of a POF lava rise showing its lobate apophysis (indicated by white arrows) (after Pasquarè et al., 2008).

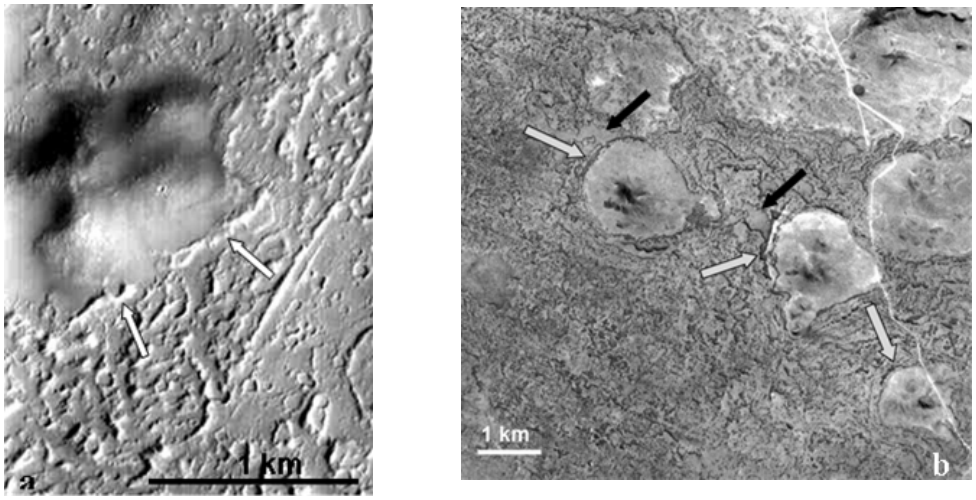

Fig.6. Surface features of D3 flows compared with POF ones (a) MOC image (r0401560) showing a lava ridge (indicated by white arrows) formed at the border of a pre-existing topographic high (b) Satellite image of POF showing some annular lava ridges that surround pre-existing cinder or lava cones (white arrows). Black arrows indicate some lava rises. Grey scale representation of ASTER false colour composite image (RGB=321).

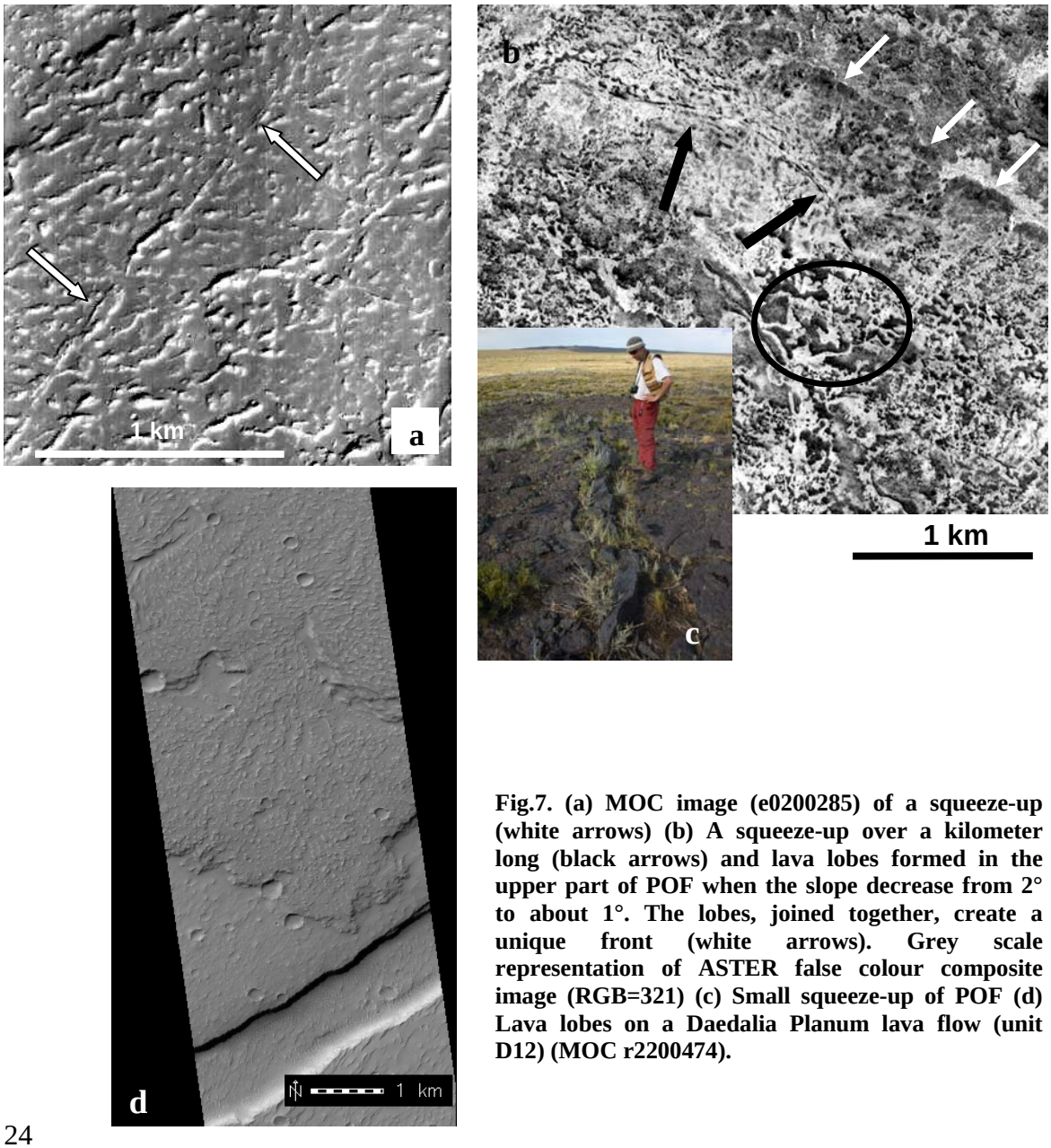

Fig.7. (a) MOC image (e0200285) of a squeeze-up (white arrows) (b) A squeeze-up over a kilometer long (black arrows) and lava lobes formed in the upper part of POF when the slope decrease from 2° to about 1°. The lobes, joined together, create a unique front (white arrows). Grey scale representation of ASTER false colour composite image (RGB=321) (c) Small squeeze-up of POF (d) Lava lobes on a Daedalia Planum lava flow (unit D12) (MOC r2200474).

In particular on POF narrow and sinuous lava ridges surround pre-existing dikes, cinder and lava cones, forming sharp annular rims (Fig.6b), squeeze-ups are frequently, even if not uniquely, located on lava rises and ridges and can reach over than 1.5 kilometres in length (Fig.7b-c) and lava lobes are frequently joined together forming unique very large fronts (Fig.7b). All this evidence strongly suggests that D3 flows were dominated by inflation processes.
By contrast the high resolution HiRISE images of D5 flows reveal a quite different morphological pattern where ropy and ridged plates several kilometres wide raft over smooth flows with channel levees (Fig.8). These flows, quite common on Mars (e.g. at Cerberus Palus, Keszthelyi et al., 2008), are supposed to be the results of two stages of emplacement in which a dominant inflation is followed by disruption of the insulating crust due to sustained lava surges (Keszthelyi et al., 2000; Keszthelyi and McEwen, 2007). There are no similar flows on the Payen volcanic complex, however the Icelandic rubbly pahoehoe flows could represent their nearest terrestrial analogues (Keszthelyi et al. 2004, 2007).
Another possible candidate for inflation among Hesperian units is the D6a flow which is the best defined lava flow of the considered area and extends for at least 700 km over the plain (Fig.4). Like POF and many other flows on Mars (Peitersen and Crown, 1999) this flow can be also classified as a constant individual flow since it is characterized by a width varying about a mean along its length. Unfortunately no high resolution images are available for this flow and its emplacement process must await further data acquisition to be accurately defined. Among the units at an intermediate stratigraphic position the early Amazonian-latest Hesperian D10 contains a huge number of narrow and ~1000 km long lava flows, some of them possibly emplaced through inflation. For example, on the HiRISE image of Fig.9a a lava flow show, at its margins, several tumuli and kilometric squeeze-ups that in some cases bound irregular lava rises (Fig 9b; Fig.11c). Such features were created by the pressure of the lava fluid underneath, whose flow was impeded by the progressive cooling and consequent obstruction of the internal conduits. This mechanism contributes to creating a terraced flow with several irregular squeeze-ups generating these particular morphologies remarkably similar to those present on Los Carrizales lava field (Fig.9c). In addition, in the upper part of the

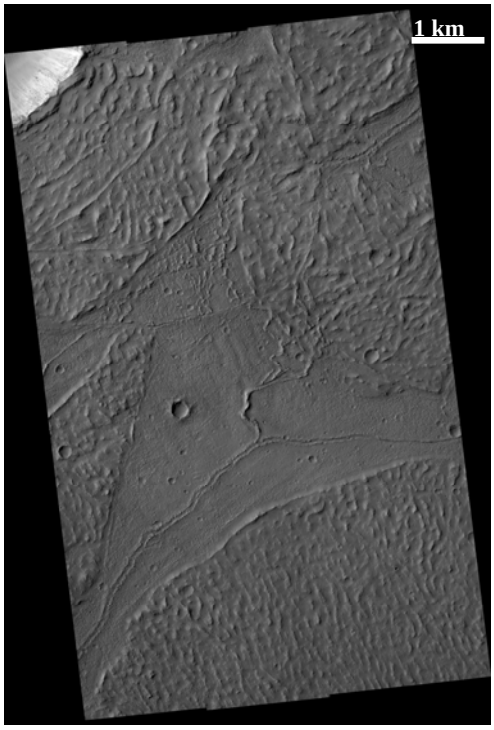

Fig.8. Platy ridged lava morphology in a D5 lava flow, interpreted as the results of the inflation process followed by disruption of the insulating crust due to sustained lava surges (PSP_001960_1450 HiRISE image).

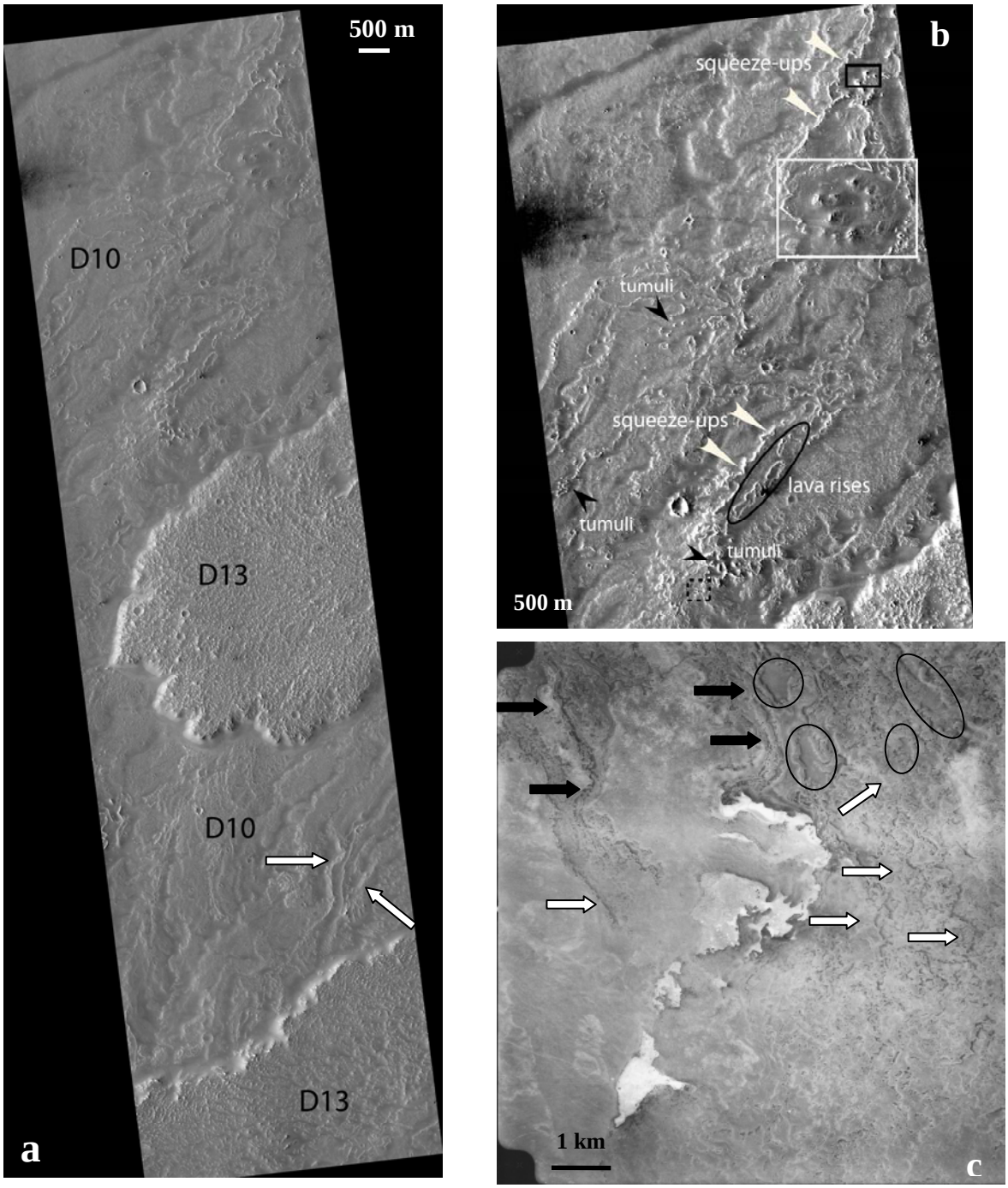

Fig.9. Surface features of Daedalia Planum D10 lava flows and comparison with Los Carrizales lava field morphologies. (a) HiRISE image (PSP_002711_1550) of a Daedalia Planum lava flows belonging to D10 and D13 units. A lava channel, indicated by white arrows, is visible on a D10 flow (b) a close-up view of the same image in which are highlighted different expressions of inflation interesting a D10 lava flow. Some tumuli are indicated with black arrows, whereas NE-SW squeeze-ups are highlighted by white arrows. Lava rises bounded by squeeze -ups are encircled. Inside the white box: a circular lava rise is bounded by squeeze-ups and associated to large tumuli. A close up-view of black and dashed squares are shown in Fig10b and Fig.10c respectively (c) Aerial image of some Los Carrizales lava flows showing numerous ridges (black arrows) and squeeze-ups (white arrows) similar to those seen on D10 flow.

HiRISE image a particular circular lava rise have been detected (white box on Fig.9b) at the centre of which the pressure of underlying lava was able to create several tumuli with length and width up to 190 and 150 metres respectively. Some of these tumuli have clear clefts on their top (Fig.10a and 10d), and do not apparently show evidence of outflows. This, coupled with their distances from the

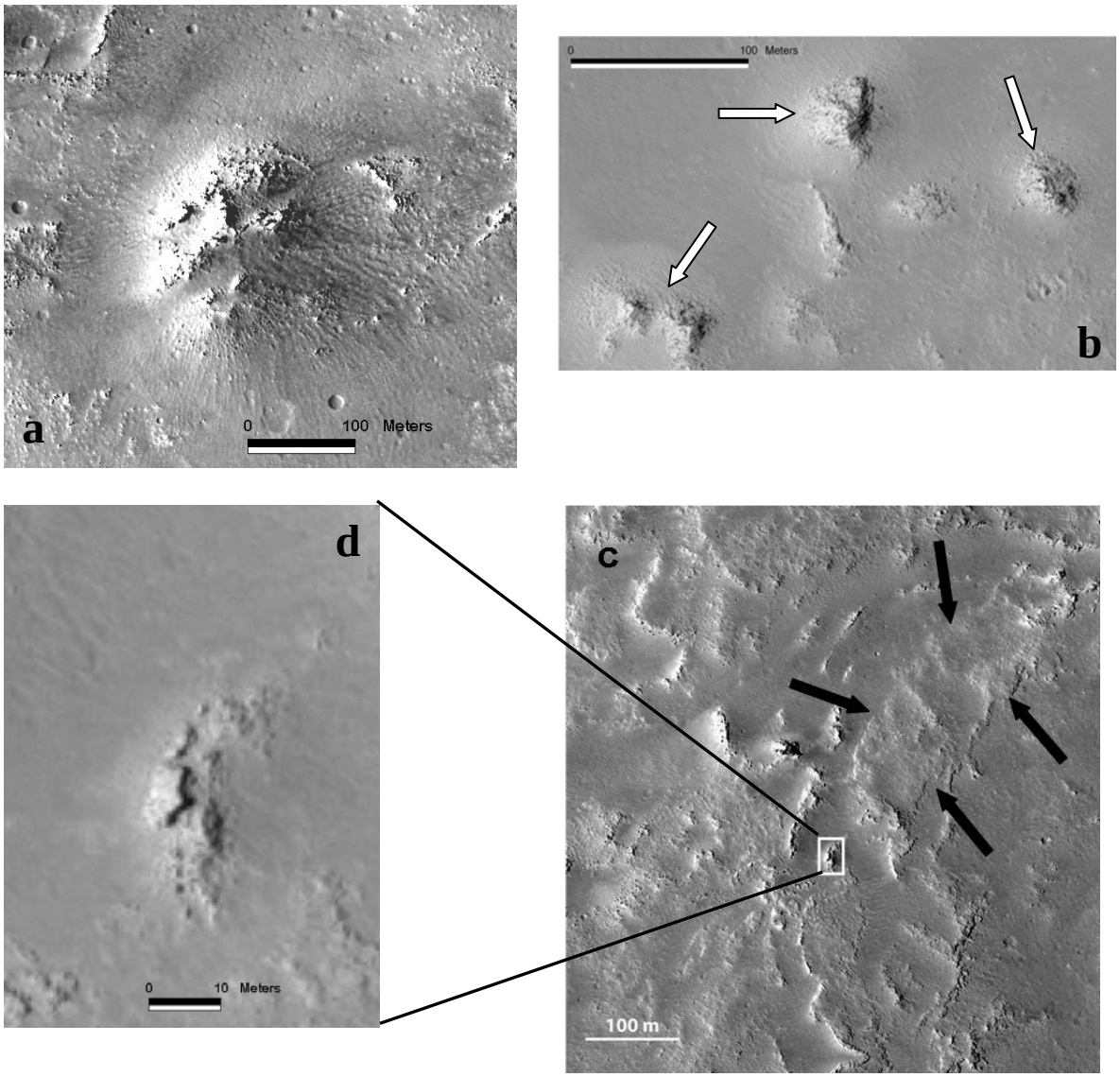

Fig.10. Surface features of Daedalia Planum D10 lava flows. (a) a close-up view of a tumulus on the middle of the lava rises underlined by the white box in Fig.9b. Radial clefts cut its summit (b) a close-up view of the area highlighted by the black square on Fig.9b. Group of possible tumuli showing a rough surface and lacking of clefts (c) close-up view of the area underlined by the dashed square in Fig.9b. A possible lava rise is indicated by black arrows whereas a tumulus with an axial cleft is shown in close-up view in (d).

Arsia Mons summit, suggests that they are flow-lobe tumuli (Rossi and Gudmundsson, 1996), like those recognized on D3 flows. However most of tumuli do not preserve extensional clefts and simply appear as positive elliptical reliefs with a rough surface covered by blocks (Fig.10b). The lack of the axial fractures could be due to an insufficient pressure of the inflated lava which was capable of plastically deforming the upper crust but which not reach the strain rate necessary to cause an elastic failure of it. Alternatively the clefts could have been obliterated by later erosion.

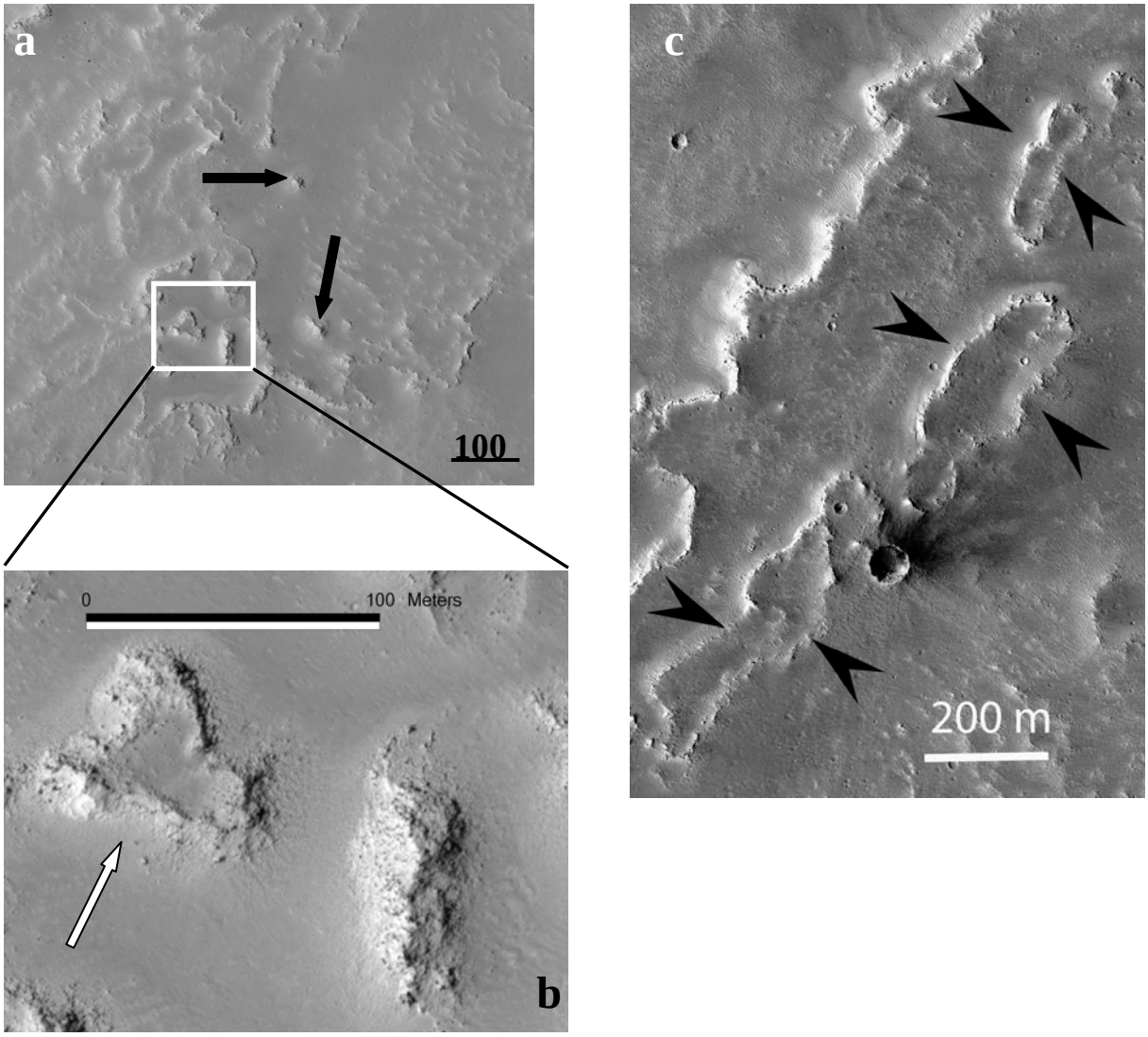

Fig.11. Surface features of Daedalia Planum D10 lava flows (PSP_002711_1550 HiRISE image) (a) area where possible tumuli (black arrows) and candidate lava rise (b, white arrow) are detected (c) several irregular lava rises bounded by squeeze-ups. Their tops appear slightly deflated and the eastern flanks are covered by dust.

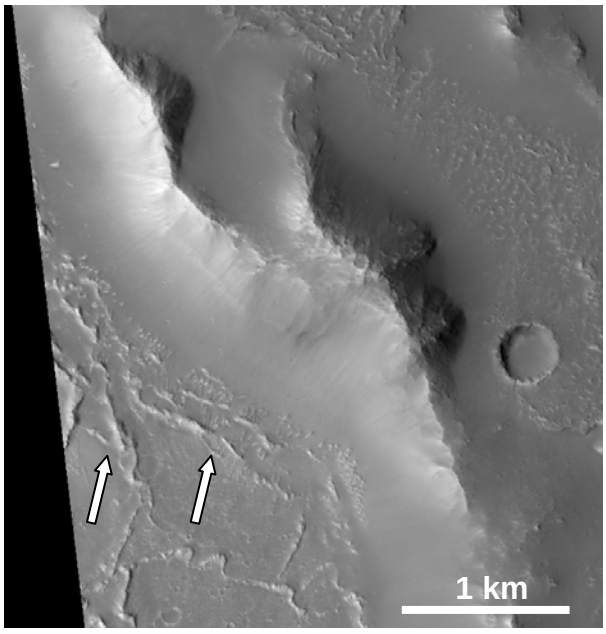

Fig.12. HiRISE image of Daedalia Planum D12 lava flow showing several lava ridges (white arrows) formed close to crater walls (PSP_003331_1580 HiRISE image).

In order to confirm this deduction, we determined the density of D10a features within an area of 38.89 km^2, obtaining a value of 6.9 ±0.4 (Poisson error) tumuli per km^2. This result is similar to that obtained for tumuli of the sector B of POF (6.1±0.3 tumuli per km^2) and point to an effective inflation origin of the D10 forms (Tab.2).

Table 2
Spatial distribution of tumuli on POF and D10 flow compared with distribution of knobs on D13 flow.

	POF (a)	**Daedalia D10 Flow (b)**	**Daedalia D13 Flow (c)**
N° of features	460	269	677
Considered area (km^2)	75.76	38.89	23.5
Spatial frequency per km^2	6.1 ± 0.3	6.9 ± 0.4	28.8 ± 1.1

The considered area for POF is located in the upper part of the flow (sector b). For D10 and D13 flow we considered the area visible on PSP_002711_1550 and PSP_003621_1585 HiRISE images respectively. Spatial distributions of POF and D10 flow are comparable, validating the hypothesis that the features on D10 are tumuli. On the other hand the features on D13 flow have a spatial distribution about 5 times higher, suggesting that the features are simply knobs of the surface. The errors of spatial distribution are Poisson errors.

In the same area where tumuli were emplaced cuesta like morphologies, surrounded by talus slope and detritus have been detected. Although these features do not appear to be lava rises, the presence in the surrounding areas of long squeeze-ups and lava ropes, typical of pahoehoe flows, suggest that they could have an inflation genesis and have afterward been modified by erosion (Fig.11a-b).
Beside the D10 inflated flow there are other flows that apparently lack inflation and are characterized by channel levees (Fig.9a). This suggests that inflation is not common to all the flows of D10 and/or could have not been maintained along their full length.
Among the Amazonian units the inflation features are rare and associated to platy ridges flows. The D12 flows, outcropping in the upper part of the studied area, are characterized by numerous lobes and tongues and an irregular surface texture. Indeed they can locally show a series of lava ridges surrounding pre-existing topographic reliefs like the crater walls of Fig.12, but their overall morphology recalls the platy-ridged flows as defined by Keszthelyi et al. 2008 in Marte Vallis.
Similarly the youngest D13 flows, which are closely spaced and marked by lobate flow fronts, show irregular and rough surfaces with numerous small topographic features that may suggest the presence of tumuli. Actually at higher resolutions it is possible to see that these features are eroded knobs (Fig.13).

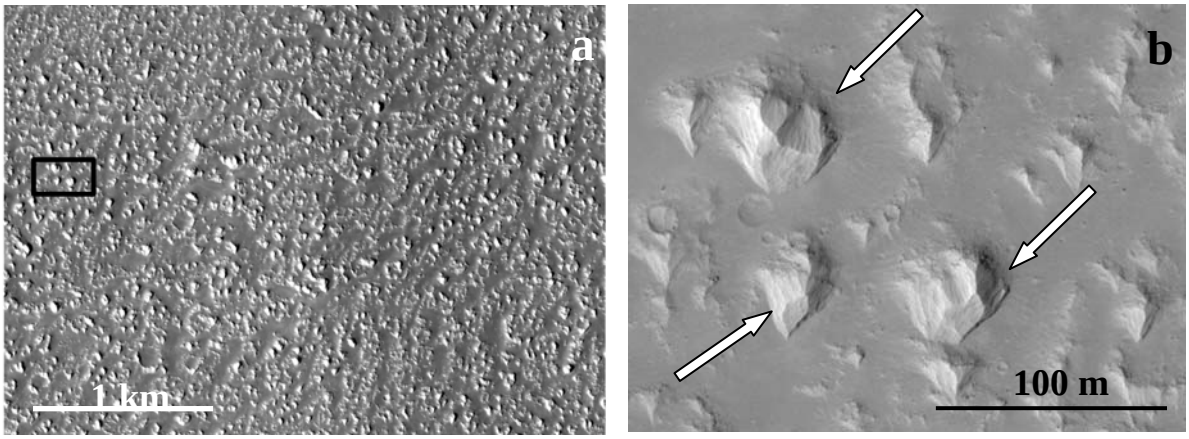

Fig.13. (a) several knobs recognized on the D13 unit flow shown on PSP_003621_1585 HiRISE image. (b) a close-up view of the knobs (indicated by white arrows). The asymmetric shape of such features reveals heavy erosion likely due to the wind.

Calculating the density of these features, within a total area of 23.5 km^2, we obtained a value of 28.8 ± 1.1 per km^2 which is nearly five times higher than the density of D10a and Payen tumuli (Tab.2). This result definitively rules out any possible correlation with tumuli and supports the hypothesis of Keszthelyi et al. [2008] that these knobs are simply a morphological expression of a brecciated flow top comparable to that of the Icelandic rubbly pahoehoes.
In conclusion the inflation fingerprints concentrate on the Hesperian D3 unit and on some flows of the latest Hesperian-early Amazonian D10 unit (Fig.4). On the contrary, the morphological expressions of inflation are ambiguous or completely lacking on D5 and the analyzed Amazonian flows, both instead characterized by platy ridged or brecciated tops. However, several inflation morphologies have been only identified thanks to the recently acquired high resolution HiRISE images, therefore the presence of inflation cannot be totally excluded on flows for which very high resolution data are not yet available (e.g. D6 flows). All these observations suggest a cyclical manifestation of the inflation process during the eruptive history of Arsia Mons that, consequently, may have experienced important fluctuations in its effusion rates.

5 Youngest lava flows' age constraints

Hartmann et al. [1999] and Neukum et al. [2004] found particularly young model ages for the flow inside the caldera of Arsia Mons proving its recent activity (40-200 My, Hartmann et al., 1999; 130 My, Neukum et al., 2004). To assess the time span between emplacement of the unit at the top of the analyzed stratigraphic sequence and the main structuring of Arsia Mons caldera, an age analysis by crater counting on one of the youngest D13 flows has been completed using HiRISE image (PSP PSP_003621_1585).

Age determination by crater statistics is based on counting impact craters in a geological unit, displaying results as a cumulative plot and fitting data by the Neukum crater production function (NPF; e.g. Neukum, 1983; Neukum and Ivanov, 1994; Neukum et al., 2001), which represents the size–frequency distribution of a crater population recorded in a geological unit at a specific time. The extrapolated cumulative number for $D \geq 1$ km is used with the chronology model to estimate surface age. The model is well established for the lunar surface and is inferred for Mars, by applying some scaling laws relative to the projectile flux, and by taking into account the presence of an atmosphere and a different gravity (e.g., Neukum et al., 2001; Ivanov, 2001; Hartmann and Neukum, 2001; Ivanov et al., 2002).

The inferred meteoroid flux, obtained from the lunar crater size−frequency distribution in the diameter range D<1Km and then used to determine the Martian crater distribution, may be affected by secondary craters not obviously related to rays and clusters (distant secondaries) (Hartmann, 2005; McEwen et al. 2005). However, other authors (e.g. Neukum and Ivanov, 1994; Hartmann, 1999; Werner et al., 2002; Neukum et al., 2004) assert that the small cratering records (D<1 km) is not contaminated by secondaries and the typical steepening of the distribution toward smaller crater diameters is simply the expression of debris falling from space. In particular Neukum et al., 2004 state that the secondary field is negligible (<10%) and Hartmann, 2005 and Quantin et al., 2007, although admitting the influence of distant secondaries on the cratering distribution curve, do not see major drawbacks on age determinations based on small craters on Mars.

In the study area (23.53 km^2), which is 200 km from the nearest crater with visible ejecta, craters with diameter less of 200 m have been taken into account.

The crater counting was completed using a self developed semi–automatic program running on IDL software. According to this program, the crater parameters (i.e. co–ordinates centre and radius), are derived by the best fitting circle approximating each crater; the diameters obtained in pixel are converted in kilometers by using the spatial resolution of the analyzed image (3.70 m/pixel); the error on the diameter calculation is evaluated by considering that the rim of each crater has a thickness of 0.6 Radii (Melosh, 1989). According to Sawabe et al. [2006] and Oberst et al. [2008], only craters with diameter greater than or equal to 4 pixels were selected. Our counting results consist of 917 craters with diameters ranging from 15 m to 196 m. These are represented as a cumulative plot (Arvidson et al., 1979), reported in Fig. 14a. By using the chronological model of Neukum (e.g. Hartmann and Neukum, 2001; Ivanov, 2001), an age of 260±30Myr was obtained for the D13 flow. This means that the youngest flows of the studied sequence occurred before the complete formation of the Arsia Mons caldera and were coeval with the volcanic activity associated with the first caldera collapses determined for the top of Ascraeus and Olympus Mons (Neukum et al., 2004).

This result may also be used to assess the minimum period separating the Daedalia Planum and Elysium Planitia inflated flows. This period can account for the more degraded aspect of the inflated features of D10 flows with respect to the Elysium Planitia ones. According to Hartmann et al. [2000] the inflated flows of the southern Elysium Planitia have an age ranging between 100 and 10 Myr. However the Hartmann cratering chronology model differs from the Neukum one used for the age determination of Daedalia Planum lava flow.

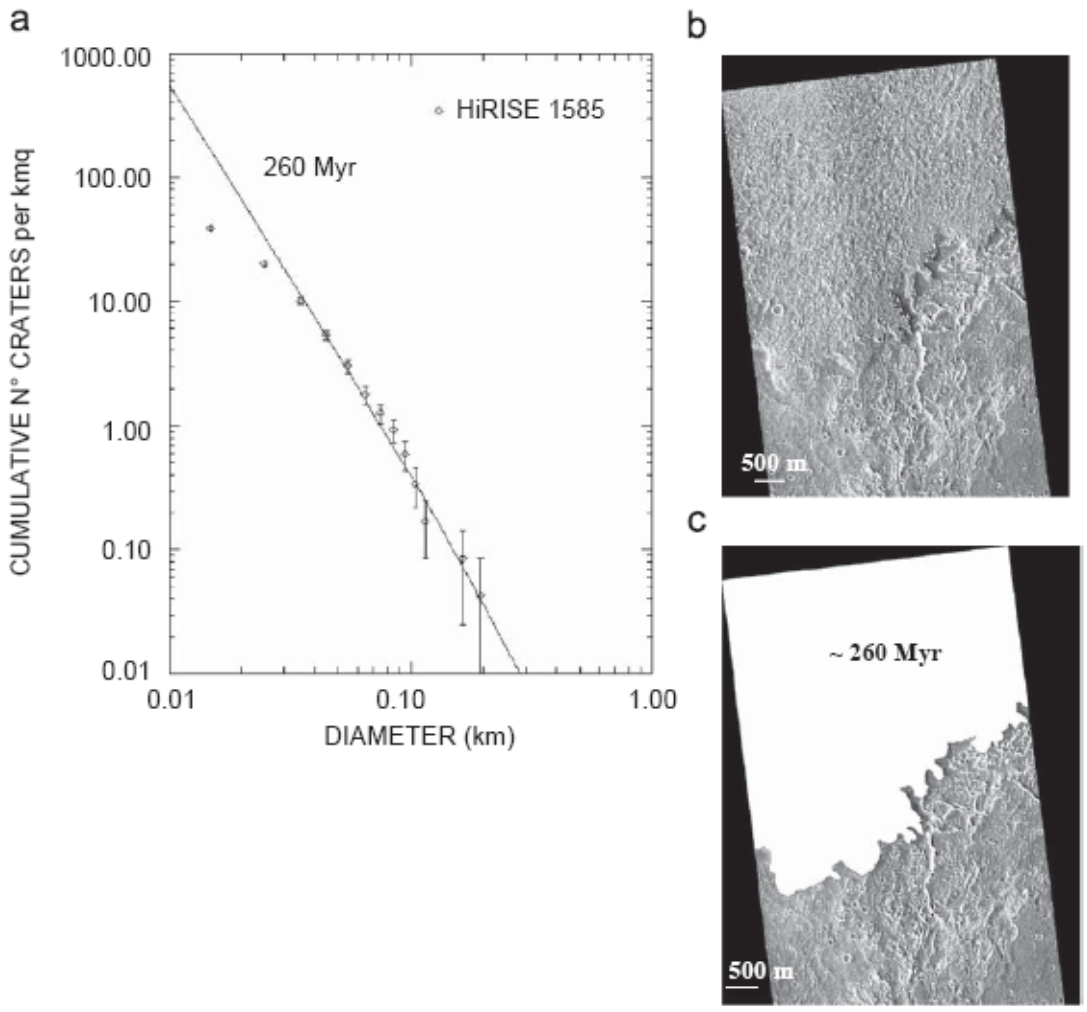

Fig.14. (a) Cumulative plot of the D13 flow located in HiRISE 003621_1585 image. The size frequency distribution of D13 has been plotted against the NPF isochrone of the derived model age. Error bars represent statistical error. (b) HiRISE image and (c) counting area of the investigated D13 flow (PSP_003621_1585).

In Hartmann [1999], a comparison of the two Martian production functions was performed, revealing that the two models differ progressively and reach a maximum gap of a factor of two during the Amazonian. Reinterpretation of observations according to this methodology determines the age of the D13 flow to be 130 Ma and the age gap between this flow and the emplacement of the Elysium inflated lavas would be in the order of 30 to 120 Myr. The Daedalia inflated flows are older than the D13 lavas, and this result suggests that the period, calculated using the methodology, between the emplacement of the Daedalia end Elysium inflated flows would be insufficient to account for the observed differences in the degree of erosion.

Determinations of age have been based on the assumption that the flux remained constant over the last 3 Gyr, whereas Quantin et al. [2007] on the basis of geological considerations have recently proposed a reduction rate of a factor of 3 in the last 3 Gyr. The declining cratering rate generates a variation of absolute crater chronology of Mars that causes an increase of the ages by a non linear factor which depends on the surface age (younger ages = greater corrections). According to this new model the considered D13 flow would yield an age of 546 Ma and predate the Elysium Planitia inflated flows by between 111 to 503 Myr. This result appears more consistent with the level of degradation observed on some Daedalia inflated flows with respect to the Elysium counterparts. Morphological observations support the Quantin et al . [2007] model.

6. Estimates of effusion rates and physical properties of the Daedalia Planum flows: implications of the inflation process

As already noted by Warner and Gregg [2003], the length of the Daedalia Planum flows cannot be explained with emplacement on steep slopes because the MOLA data indicates a rather flat topography (slope <0.5°) (Smith et al, 1999). According to these authors most of the longest flows do not show channels or collapsed lava tubes that could have suggested an efficient transport system responsible for long lava flows. The comparative study completed found that several Daedalia Planum lava flows show occasional features such as tumuli, lava rises, lava lobes and lava ridges similar to those present on POF and Los Carizales lava field. This suggests that also several Daedalia Planum flows were emplaced thanks to the inflation process which, indeed, is an efficient transport mechanism. To estimate the influence of this spreading process on Daedalia Planum, effusion rates, yield strength and viscosity have been calculated assuming non inflated flows, inconsistencies with theoretical considerations and the properties of pahoehoe basaltic lavas on the Earth have also been evaluated. It is shown that the internal consistency among all the Martian lavas and at the same time their discrepancy with what is known on pahoehoe lavas on the Earth (including POF) can be explained assuming that the inflation process on Martian flows emplacement is much more prevalent than previously theorized.

6.1. Effusion rates

Generally, for non inflated flows the effusion rate Q (m^3/s) can be calculated as

$$Q = G_z \ \kappa L W_F / h \qquad (1)$$

where G_z is the Graetz number, κ is the thermal diffusivity (m^2/s), L is the flow length (m), W_F is the flow width (m) and h is the flow height (m) (e.g. Wilson and Head, 1983; Zimbelman, 1985a,b; Pinkerton and Wilson, 1994; Hiesinger et al., 2007). The Graetz number (given by e.g. Knudsen and Kantz, 1979) is a dimensionless parameter which relates the rate of heat loss from a flow to the rate of advection within a flow along its length (Gregg and Fink, 1996). Consistently with other authors a value of 300 for the Graetz number has been chosen (Pinkerton and Wilson, 1994; Warner and Gregg, 2003; Hiesinger et al., 2007), as there are theoretical and observational evidences that terrestrial lavas cease to flow when the Graetz number decreases to about that value (e.g. Wilson and Head, 1983). The thermal diffusivity for Daedalia Planum lava flows used by Warner and Gregg [2003] is 3.0×10^{-7} m^2/s, which is generally representative of andesites (Gregg and Fink, 1996) and Gregg and Zimbelman, 2000), but, unlike these authors, we preferred a value of 5.0×10^{-7} m^2/s more in keep with the known thermal diffusivity of basalts (Gregg and Zimbelman, 2000).

The effusion rates calculations were made for three of the best exposed flows of Daedalia Planum belonging to different units and characterized by a nearly uniform width (Tab.3). The length and width of lava flows were measured on THEMIS images while the average height was derived from numerous MOLA profiles, particularly suited for flow thickness estimates (Glaze et al., 2003; Hiesinger et al., 2007).

The first two flows considered are D6a and D10a (see geological sketch of Fig.4) whose feed vents are not detectable as they covered by subsequent effusions. As a result of the feed vents being obscured a minimum and a maximum flow length were considered for both events. The minimum length is determined as being the length of the exposed flow and the maximum length is one corresponding to the distance between the lava front and the caldera rim. In all cases applying equation (1) effusion rates on the order of 10^4 - 10^5 m^3/s were obtained (Tab.3).

Our results are clearly in the range with those calculated for Arsia Mons by Warner and Gregg [2003] which estimated a minimum value of 7.69×10^2 m^3/s and a maximum value of 2.17 x

10^5 m^3/s. On the Earth the effusion rates of basaltic lavas range from a few to thousands m^3/s, being the highest values related to aa and the lowest to pahoehoe flows (Tab. 4). On the other hand for these latter great effusions rate, up to 2000-4000 m^3/s, can be acceptable, if large flow fronts (up to 100 km) are considered (Thordanson and Self, 1998). Wilson and Head [1994] demonstrated that the lower Mars gravity induces effusion rates 5 times higher than those of the Earth when the magma motion is laminar and 3 times higher when it is turbulent. Therefore, our results and similar calculations for other Martian effusions (Warner and Gregg, 2003) can be supported on the basis of these theoretical concerns only considering very large lava fronts or assuming that most of the studied flows on Mars are of aa type. Even with such assumptions several calculation are out of the boundary limits suggested by Wilson and Head (1994), hence it is very likely that several effusion rates were overestimated. The inflation record on the Daedalia Planum lava field may represent a solution to this apparent inconsistency. The presence of inflation invalidates equation (1), as this equation permits lava to cover long distances beneath an insulating crust over long period of time and increases the overall thickness of lava flows. Therefore the effusion rate could be lower than those previously estimated. If the effusion rate of Payen Matru is calculated with equation (1) a value of 1.4×10^4 m^3/s is determined, which is too high for any inflated pahoehoe flow on the Earth (Rowland and Walker, 1990; Hon et al., 1994; Thordanson and Self, 1998). Another solution can be represented by the spreading mechanism proposed by Keszthelyi et al. [2000] for the Martian platy ridged lava flows. The effusion rates calculated by thermal modelling are of the order of 10^4 m^3/s, however these rates can be attributed only to lava flows, where platy ridged or

Table 3
Calculated effusion rates, yield strengths and viscosities of Daedalia Planum flows and POF

		Flow			
		D6a	**D10a**	**D13a**	**POF**
Average thickness (m)		70.1 ± 18.4	38.6 ± 7.5	38.2 ± 9.9	8.8
Average width (km)		59.1 ± 13.8	12.24 ± 3.9	8.6 ± 4.0	10.0
Length (km)		minimum 687.45 maximum 1656.78	minimum 241.90 maximum 1179.43	761.68	181
Effusion rate (m^3/s)		min $1.0\times10^5 \pm 2.0\times10^4$ max $2.2\times10^5 \pm 4.9\times10^4$	min $1.6\times10^4 \pm 2.5\times10^3$ max $7.9\times10^4 \pm 1.2\times10^4$	$2.5\times10^4 \pm 7.3\times10^3$	1.5×10^4
Yield Strength (Pa) 1	**ρ = 2500 kg/ m^3**	$3.4\times10^3 \pm 9.2\times10^2$	$1.6\times10^3 \pm 4.6\times10^2$	$1.8\times10^3 \pm 4.8\times10^2$	2.7×10^3
	ρ = 3000 kg/ m^3	$4.0\times10^3 \pm 1.1\times10^3$	$2.0\times10^3 \pm 5.5\times10^2$	$2.2\times10^3 \pm 5.7\times10^2$	3.3×10^3
Yield Strength (Pa) 2	**ρ = 2500 kg/ m^3**	$8.0\times10^2 \pm 3.4\times10^2$	$7.4\times10^2 \pm 2.6\times10^2$	$1.7\times10^3 \pm 4.8\times10^2$	2.9×10^2
	ρ = 3000 kg/ m^3	$9.7\times10^3 \pm 4.0\times10^3$	$8.9\times10^2 \pm 3.1\times10^2$	$2.0\times10^3 \pm 5.7\times10^2$	3.5×10^2
Viscosity (Pa-s)	**ρ = 2500 kg/ m^3**	min $1.7\times10^6 \pm 9.0\times10^5$ max $4.0\times10^6 \pm 3.3\times10^6$	min $2.4\times10^5 \pm 2.0\times10^5$ max $1.2\times10^6 \pm 9.7\times10^5$	$1.0\times10^6 \pm 9.4\times10^5$	2.7×10^5
	ρ = 3000 kg/ m^3	min $2.0\times10^6 \pm 1.6\times10^6$ max $4.8\times10^6 \pm 4.0\times10^6$	min $2.9\times10^5 \pm 2.4\times10^5$ max $1.4\times10^6 \pm 1.2\times10^6$	$1.3\times10^6 \pm 1.1\times10^6$	3.2×10^5

Both Daedalia Planum and POF effusion rates, yield strengths and viscosities have been calculated assuming not inflated flows. Yield strength 1 was calculated using equation (2), yield strength 2 was calculated applying equation (3). For the D6a flow 24 profiles have been taken into account, whereas for D10a and for D13a have been considered 18 and 13 profiles respectively.

Table 4.
Comparison of rheological properties and effusion rates of basaltic lava flows on Earth.

Location	Yield Strength (Pa)	Viscosity (Pa-s)	Effusion rate (m^3/s)	Lava type	Source
Mauna Loa (Hawaii)		$6.0x\ 10^2$ -$6.0x\ 10^3$	4-19	pahoehoe	Rowland and Walker (1988) Rowland and Walker (1990)
	$3.5x\ 10^2$ - $7.2x\ 10^3$	$1.4x\ 10^2$ - $5.6x\ 10^6$	417-556 32-1044	aa	Moore (1987) Rowland and Walker (1990)
Kilauea (Hawaii)		$6.0x\ 10^2$ -$6.0x\ 10^3$	2-5	pahoehoe	Rowland and Walker (1988) Rowland and Walker (1990)
	$1.5x\ 10^3$ - $5x\ 10^4$	$0.2\text{-}8.2x\ 10^6$	28-300	aa	Fink and Zimbelman (1986) Rowland and Walker (1990)
Columbia River Basalt Group	$< 7x\ 10^3$	$5.0\text{-}4.0x\ 10^3$	~4000	pahoehoe	Thordarson, 1998; Self et al. (1996) Murase and McBirney (1973) McBirney and Murase (1984)
Pampas Onduladas Lava Flow (Argentina)		3-73		pahoehoe	Pasquarè et al. (2008)

brecciated tops have been detected (e.g. D13 Fig.13, D12 Fig.12 , D5 Fig. 8), although cannot be totally excluded for long flows for which high resolution images are not yet available (e.g. D6a).
In order to activate the inflation process the confined magma overpressure, which is directly related to effusion rate (Hon et al., 2004), must be at least equal to the lithostatic load caused by the flow thickness (magmatic overpressure $\geq \rho gh$, where ρ is density, g is gravity and h is thickness). Therefore as effusion rate depends on gravity also the magma overpressure is influenced by it. Moreover the lithostatic load is proportional to the gravity, then on Mars the uplift of the flow is more favoured than on the Earth. The rate of effusion for inflated lavas can be derived from height and basal diameter of tumuli which are related to the magmatic overpressure (Rossi and Gudmundsson, 1996). Daedalia Planum tumuli are on average two times larger than the terrestrial ones, but their height, which is of paramount importance for these calculations, is still unknown as MOLA data has insufficient resolution to establish their height and shadow measurements on HIRISE are not possible as the sun inclination does not facilitate such calculations.

6.2. Yield strength and viscosity

Assuming non inflated flows the yield strength and the viscosity of Daedalia Planum lavas can be determined by dimensions derived by remotely sensed data (Wilson and Head, 1983). These values have also been compared with other calculations on Martian flows and the rheological properties of terrestrial basaltic lavas (POF included).
Yield strength (Pa) is the stress at which lava exceeds its elastic limit and starts to deform permanently. According to Hulme [1974] its physical expression is:

$$Y = \rho g h \sin\theta \qquad (2)$$

where ρ is the fluid density, g the gravitational acceleration, h the flow thickness and θ the flow surface slope.
A second model (Orowan, 1949) expresses the yield strength as:

$$Y = \rho g h^2 / w \qquad (3)$$

in which also the flow width (w) is taken into account.
Both models consider lava flow as a Bingham fluid. Warner and Gregg [2003] assumed an average density of Martian volcanic rock ranging from 2000 to 3000 kg/m^3 while Hiesinger et al. [2007] considered a range from 1250 to 3750 kg/m^3. A density ranging between 2500-3000 kg/m^3, which

is considered more reliable for basaltic lavas (Murase and McBirney, 1973), was selected. An average slope of 0.3° for Daedalia Planum has been obtained from MOLA data. On the basis of these values the yield strengths for the same three flows considered in paragraph 6.1 have been calculated. Applying the equation (2) and (3) we obtained a value ranging from 10^2 to 10^3 Pa (Tab.3).
According to other works (Warner and Gregg, 2003; Hiesinger et al., 2007) lava viscosity η (Pa-s) has been derived from the expression of Fink and Griffiths [1990] (4) that approximates lavas as Newtonian flows.

$$h = (Q\eta / \rho g)^{1/4} \quad (4)$$

Viscosity values have been obtained for each effusion rate calculated in paragraph 6.1 assuming different densities (Tab.3). The results obtained, although affected by large error bars, range from 10^5 to 10^6 Pa-s.
Both the obtained yield strength and viscosity are in agreement with those calculated for Arsia Mons and Tharsis Montes (Hulme, 1976; Moore, 1978; Zimbelman, 1985a,b; Warner and Gregg, 2003; Hiesinger et al., 2007). The results determined by the study do not fit the properties of pahoehoe lavas on the Earth which are characterized by lower yield strengths and much lower viscosity (Tab.4). The viscosity values are however comparable to those estimated for Mauna Loa aa basaltic lavas (Moore, 1987). As several Daedalia Planum lava flows may be inflated, pahoehoe lavas should be frequent in this region, consequently the obtained yield strengths and viscosity are inconsistent with the observations. It is probable that the values calculated are overestimated as inflation may have increased the flow thickness invalidating the result from equations (2), (3) and (4). To verify this theory equation (4) has been applied to POF, with a density range from 2500 to 3000 kg/ m^3, and a viscosity of 2.7-3.2 x 10^5 Pa-s has been obtained. The result is approximately four orders of magnitude greater than those calculated using mineral and whole rock chemistry (3-73 Pa-s, Pasquarè et al., 2008). Accordingly the lava viscosity calculated for Daedalia Planum inflated flows may be lowered by the same order of magnitude thus obtaining values which are closer to terrestrial pahoehoe lavas (10^2 - 10^3 Pa-s, Shaw et al., 1968; Rowland and Walker, 1988).

7. Conclusion

The basalt lava flows of the Payen Volcanic Complex (Argentina) represent the longest Quaternary individual flows emplaced in sub-aerial condition on the Earth. More precisely the Pampas Onduladas lava flow (POF) and the flows of Los Carizales lava field extend for 170-180 km over the nearly flat surface of the Pampean foreland and are characterized by striking inflation features that suggest inflation as the main factor responsible for their length.
POF and Los Carizales lava flows were compared to the Daedalia Planum lava field that, located southwest of Arsia Mons, includes some of the longest flows on Mars extending over an almost flat topography and consequently likely emplaced also through inflation mechanisms. These lava flows belong to at least 13 different geological units covering a time span from the Late Hesperian to the Late Amazonian and predating the formation of the Arsia Mons caldera. Some of the flows are characterized by smooth or platy-ridged surfaces, whereas the others are associated with wrinkly and ropy surfaces, typical of pahoehoe lavas of basaltic composition. As expected, numerous inflation features, having a surface density comparable to POF's ones, were discovered on the latter flows. However several tumuli and lava rises appear degraded if compared to the POF and Los Carizales ones and to the recently detected inflated morphologies of Cerberus Fossae. Subsequent alteration and erosion may account for these differences but a significant time span between the emplacement of Elysium Planitia and Daedalia Planum inflated flows is required. This can be

concluded if the model by Quantin et al. [2007] of a declining cratering rate in the last 3Ga is considered during cratering age assessment. In this case the youngest Daedalia Planum flow yields an age of about 546 Ma and predates the Elysium Planitia lavas by 111 to 503 Myr.
The variability of flows morphologies in Daedalia Planum suggests that Arsia Mons experienced important fluctuations in effusion rates during its evolution. However the detection of pahoehoe flows with inflation features similar to the ones encountered on POF and Los Carrizales lava field suggest that inflation played an important cyclical role on the emplacement of the Daedalia Planum flow succession. Since the detection of many inflation fingerprints was only possible on very high resolution HiRISE images, it is likely that the inflation process on Martian flows could be more frequent than previously supposed. This finding has an important consequence on the estimation of effusion rates and rheological properties of lavas on Mars as they are normally derived assuming non inflated flows. The calculations can be affected by overestimations if applied to flows dominated by inflations. In the case of some Daedalia Planum flows the calculations indicated effusion rates, yield strength and viscosity which can be reasonable for aa or platy ridge flows but are improbable for the pahoehoe lavas found in the region.

References

Anderson S.W., Stofan E.R., Smrekar S.E., Guest J.E. and Wood, B., 1999. *Pulsed inflation of pahoehoe lava flows: implications for flood basalt emplacement*. Earth and Planetary Science Letters, 168, 7-18.

Arvidson R., Boyce J., Chapman M., Cintala M., Fulchignoni M., Moore H., Neukum G., Schulz P., Soderblom L., Strom R., Woronow A. and Young R., 1979. *Standard Techniques for Presentation and Analysis of Crater Size–frequency Data*. Icarus, 37, 467-474.

Carr M.H., Greeley R., Blasius K.R., Guest J.E. and Murray J.B., 1977. *Some Martian volcanic features as viewed from the Viking orbiters*. J. Geophys. Res., 82, 3985-4015.

Cashman K., Pinkerton H. and Stephenson J., 1998. *Introduction to special section: Long lava flows*. J. Geophys. Res., 103, 27281– 27289.

Dragoni M., Piombo A. and Tallarico A., 1995. *A model for the formation of lava tubes by roofing over a channel*. J. Geophys. Res., 100, 8435-8447.

Fink J.H. and J.R. Zimbelman, 1986. *Rheology of the 1983 Royal Garden basalt flows, Kilauea volcano, Hawaii*. Bull. Volcanol., 48, 87–96.

Fink J.H. and Griffiths R.W., 1990. *Radial spreading of viscous-gravity currents with solidifying crust*. J. Fluid Mech., 221, 485– 500.

Fuller E.R. and Head J.W., 2002. *Evidence from MOC and MOLA for Pre-aureole Olympus Mons Volcanism.* American Geophysical Union. Abstract P32A-07.

Garry W.B., Zimbelman J.R. and Gregg T.K.P., 2007. *Morphology and emplacement of a long channeled lava flow near Ascraeus Mons Volcano, Mars*. J. Geophys. Res., 112, E08007.

Germa A., Quidelleur X., Gillot P.Y. and Tchilinguirian P., 2007. *Volcanic evolution of the back-arc complex of Payun Matru (Argentina) and its geodynamic implications for caldera-forming eruption in a complex slab geometry setting*. IUGG 2007, Perugia, Italy. Abstract 10028.

Glaze L.S., Baloga S. and Stofan E.R., 2003. *A methodology for constraining lava flow rheologies with MOLA*. Icarus, 165, 26– 33.

Gonzáles Díaz E.F., 1972. *Descripción Geológica de la Hoja 30 d (Payún-Matru), Provincia de Mendoza*. Dirección Nacional de Geología y Minería. Bol. 130. Buenos Aires.

Gregg T.K.P. and Fink J.H., 1996. *Quantification of extraterrestrial lava flow effusion rates through laboratory simulations*, J. Geophys. Res., 101, 16891– 16900.

Gregg T.K.P. and. Zimbelman J.P, 2000. *Volcanic vestiges: Pulling it together, in Environmental Effects on Volcanic Eruptions: From Deep Oceans to Deep Space*, edited by J.R. Zimbelman and T.K.P. Gregg, pp. 243–251, Springer, New York.

Hartmann W.K., Malin M., McEwen A., Carr M., Soderblomk L., Thomas P., Danielson E., James P.and Veverka J., 1999. *Evidence for recent volcanism on Mars from crater counts.* Nature, 397, 586-589.

Hartmann W.K., 1999. *Martian cratering VI: Crater count isochrones and evidence for recent volcanism from Mars Global Surveyor*. Meteoritics & Planetary Science, 34, 167−177.

Hartmann, W.K., 2005. *Martian cratering. 8. Isochron refinement and the chronology of Mars*. Icarus, 174, 294–320.

Head J.W. and Marchant D.R., 2003. *Cold-based mountain glaciers on Mars: Western Arsia Mons.* Geology, 31, 641-644.

Hiesinger H., Head J.W. and Neukum G., 2007. *Young lava flows on the eastern flank of Ascraeus Mons: Rheological properties derived from High Resolution Stereo Camera (HRSC) images and Mars Orbiter Laser Altimeter (MOLA) data*. J. Geophys. Res., 112, CiteID E05011.

Hon K., Kauahikaua J., Denlinger R. and Mackay K., 1994. *Emplacement and inflation of pahoehoe sheet flows; observations and measurements of active lava flows on Kilauea Volcano, Hawaii*. GSA Bulletin, 106, 351-370.

Hulme G., 1974. *The interpretation of lava flow morphology*. Geophys. J. R. Astron. Soc., 39361–39383.

Hulme G., 1976. *The determination of the rheological properties and effusion rate of an Olympus Mons lava*. Icarus, 27, 207–213.

Inbar M. and Risso C., 2001. *A morphological and morphometric analysis of a high density cinder cone volcanic field-Payun Matru, south-central Andes, Argentina*. Z. Geomorph. N.F., 45, 321-343.

Ivanov B.A., 2001. *Mars/Moon Cratering Rate Ratio Estimates*. Space Science Reviews, 96(1-4), 87-104.

Ivanov B. A., Neukum G., Bottke W. F.Jr., Hartmann W. K., 2002. *The Comparison of Size-Frequency Distributions of Impact Craters and Asteroids and the Planetary Cratering Rate*. Asteroids III, W. F. Bottke Jr., A. Cellino, P. Paolicchi, and R. P. Binzel (eds), University of Arizona Press, Tucson, 89-101.

Keszthelyi, L.P., 1995. *A preliminary thermal budget for lava tubes on the Earth and planets*. J. Geophys. Res., 100, 20411 – 20420.

Keszthelyi L.P. and Self S., 1998. *Some physical requirements for the emplacement of long basaltic lava flows*. J. Geophys. Res., 103, 27447–27464.

Keszthelyi L., McEwen A.S. and Thordarson T., 2000. *Terrestrial analogs and thermal models for Martian flood lavas*. J. Geophys. Res., 105, 15027-15050.

Keszthelyi L., Thordarson T., McEwen A., Haack H., Guibaud N., Self S., Rossi M.J., 2004. Icelandic analogs to Martian flood lavas. Geochem. Geophys. Geosyst, 5, Q11014, doi:10.1029/2004GC00758.

Keszthelyi L.P and McEwen A., 2007. *Comparison of flood lavas on Earth and Mars. In: "The Geology of Mars: evidence from earth based analogues"*. M. Chapman (Ed.), 126-150.

Keszthelyi L., Jaeger W., McEwen A., Tornabene L., Beyer R.A., Dundas C. and Milazzo M., 2008. *High Resolution Imaging Science Experiment (HiRISE) images of volcanic terrains from the first 6 months of the Mars Reconnaissance Orbiter Primary Science Phase*. J. Geophys. Res., 113, CiteID E04005.

Kilburn C.J. and Lopes R.M.C., 1991.*General patterns of flow field growth: Aa and blocky lavas*. J. Geophys. Res., 96, 19721– 19732.

Knudsen J.G. and Katz D.L., 1958. *Fluid Dynamics: Heat Transfer*, McGraw-Hill, New York, 81–82.

Llambías E.J., 1966. *Geología y petrografía del volcán Payún Matrú*. Acta Geológica Lilloana, 8, 265-310.

McBirney A.R. and Mursae T., 1984. *Rheologic properties of magmas*. Annu. Rev. Earth Planet. Sci., 12337–12357.

McEwen A.S., Preblich B.S., Turtle E.P., Artemieva N.A., Golombek M.P., Hurst M., Kirk R.L., Burr D.M. and Christensen P.R., 2005. *The rayed Crater Zunil and interpretations of small impact craters on Mars*. Icarus, 176, 351–381.

Melchor R. and Casadío S., 1999. *Hoja Geológica 3766-III La Reforma, provincia de La Pampa*. Secretaría de Minería de la Nación, SEGEMAR, Boletín Nº 295, 63p. Buenos Aires.

Melosh H.J., 1989. *Impact Cratering: A Geologic Process*. Oxford Univ. Press.

Moore H.J., Arthur D.W.G. and Schaber G.G., 1978. *Yield Strengths of Flows on the Earth, Moon, and Mars*. Proc. Lunar Planet. Sci. Conf., 9th, 3351-3378.

Moore H.J., 1987. *Preliminary estimates of the rheological properties of 1984 Mauna Loa lava, in Volcanism in Hawaii*. Edited by R.W. Decker, T.L. Wright, and P.H. Stauffer, U.S. Geol. Surv. Prof. Pap., 2, 1569– 1588.

Murase T. and McBirney A.R., 1973. *Properties of Some Common Igneous Rocks and Their Melts at High Temperatures*. Geol. Soc. Amer. Bull, 84, 3563-3592.

Murray J.B., Muller J., Neukum G.,Werner S.C., van Gasselt S., Hauber E., Markiewicz W.J.,Head III J.W., Foing B.H., Page D, Mitchell K.L., Portyankina G. and The HRSC Co-Investigator Team, 2005. *Evidence from the Mars Express High Resolution Stereo Camera for a frozen sea close to Mars' equator.* Nature, 434, 352 – 356.

Neukum, G., PhD Thesis, 1983. *Meteoriten bombardement und Datierung Planetarer Oberflaechen*. Munich, 1-186.

Neukum G., Ivanov B. A., 1994. *Crater size distributions and impact probabilities on Earth from lunar, terrestrial-planet, and asteroid cratering data*. In Hazards Due to Comets and Asteroids (T. Gehrels, ed.), pp. 359-416. Univ. of Arizona, Tucson. 1300 pp.

Neukum G., Ivanov B.A. and Hartmann W.K., 2001. *Cratering Records in the Inner Solar System in Relation to the Lunar Reference System*. Space Science Reviews, 96, p. 55-86.

Neukum G., Jaumann R., Hoffmann H., Hauber E., Head J.W., Basilevsky A.T., Ivanov B.A., Werner S.C., Van Gasselt S., Murray J.B. and Mccord T., 2004. *Recent and episodic volcanic and glacial activity on Mars revealed by the High Resolution stereo camera*. Nature, 432, 971-979.

Oberst J., Schwarz G., Behnke T., Hoffmann H., Matz K.–D., Flohrer J., Hirsch H., Roatsch T., Scholten F., Hauber E., Brinkmann B., Jaumann R., Williams D., Kirk R., Duxbury T., Leu C. and Neukum G., 2008. *The imaging performance of the SRC on Mars Express*. Planetary and Space Science, 56, 473–491.

Orowan E., 1949. *Remark from joint meeting of British Glaciological Society*, British Rheologists' Club, and Institute of Metals, J. Glaciol., 1, 231.

Pasquarè G., Bistacchi A. and Mottana A., 2005. *Gigantic individual lava flows in the Andean foothills near Malargüe (Mendoza, Argentina).* Rendiconti dell'Accademia dei Lincei, 9, 127-135.

Pasquarè G., Bistacchi A., Francalanci L. Bertotto G.W., Boari E., Massironi M. and Rossetti A., 2008. *A very long pahoehoe inflated basaltic lava flow in the Payenia volcanic province (Mendoza, Argentina).* Revistas de la Asociaciòn Geologica Argentina, 63, 131-149.

Peitersen M.N., Crown D.A., 1999. *Downflow width behaviour of Martian and terrestrial lava flows.* Journal of Geophysical Research, 104, 8473-8488.

Peitersen M.N., Crown D.A., 2000. *Correlation between topography and intraflow width in Martian and terrestrial lava flows.* Journal of Geophysical Research, 105 (E2), 4123-4134.

Pinkerton H. and Wilson L., 1994. *Factors controlling the lengths of channel-fed lava flows*. Bull. Volcanol., 56, 108– 120.

Quantin C., Mangold N., Hartmann W., Allemand P., 2007. *Possible long-term decline in impact rates: 1. Martian geological data.* Icarus, 186, 1-10.

Rossi M.J. and Gudmundsson A., 1996. *The morphology and formation of flow-lobe tumuli on Icelandic shield volcanoes*. J. Volc. Geotherm. Res., 72, 291-308.

Rowland S.K. and Walker, G.P.L. 1988. *Mafic-crystal distributions, viscosities and lava structures of some Hawaiian lava flows*. J. Volc. Geotherm. Res., 35, 55-66.

Rowland, S.K., and Walker G.P.L., 1990. *Pahoehoe and aa in Hawaii: Volumetric flow rate controls the lava structure*. Bull. Volcanol., 52, 615–628.

Sakimoto S.E.H., Crisp J. and Baloga S.M., 1997. *Eruption constraints on tube-fed planetary lava flows*, J. Geophys. Res., 102, 6597– 6613.

Sakimoto S.E.H. and Zuber M.T., 1998. *Flow and convection cooling in lava tubes*. J. Geophys. Res., 103, 27465–27487.

Sawabe Y., Matsunaga T. and Rokugawa S., 2006. *Automated detection and classification of lunar craters using multiple approaches.* Advances in Space Research, 37, 21–27.

Schaber G.G., Horstman K.C. and Dial A.L., 1978. *Lava flow materials in the Tharsis region of Mars*. Lunar Planet. Sci. Conf., 9th, 3433-3458.

Scott D.H. and Tanaka K.L., 1981. *Mars: Paleostratigraphic restoration of buried surfaces in the Tharsis Montes area, Mars*. Icarus, 45, 304-319.

Scott D.H. and Tanaka K.L., 1986. *Geologic map of the western equatorial region of Mars, scale 1:15,000,000*. U.S. Geol. Surv. Misc. Invest. Ser., Map I-1802-A.

Self S., Thordarson Th., Keszthelyi L., Walker G.P.L., Hon K., Murphy M.T., Long P. and Finnemore S., 1996. *A new model for the emplacement of Columbia River basalts as large, inflated pahoehoe lava flow fields*. Geophys. Res. Lett., 23, 2689-2692.

Self S., Thordarson T. and Keszthelyi L., 1997. *Emplacement of continental flood Basalt lava flows. In Large igneous provinces: continental, oceanic, and planetary flood volcanism*. Geophysical monograph, 100, 381-410.

Shaw H.R., Wright T.L., Pech D.L. and Okamura R., 1968. *The viscosity of basaltic magma: an analysis of field measurements in Makaopuhi lava lake, Hawaii*. American Journal of Science, 266, 225-264.

Smith D.E. et al., 1999. *The global topography of Mars and implications for surface evolution*. Science, 284, 1495-1503.

Thorarinsson S., 1966. *The Surtsey Eruption, Course of Events and the Development of Surtsey and other New Islands*. Surtsey Res. Prog. Rep. 2. The Surtsey Research Society, Reykjavík, 117–125.

Thordarson T. and Self S., 1998. *The Roza Member, Columbia River Basalt Group: A gigantic pahoehoe lava flow field formed by endogenous processes?*. J. Geophys. Res., 103, 27411–27445.

Walker G.P.L., 1973. *Lengths of lava flows*. Phil. Trans. R. Soc. London, Ser. A, 274, 107– 118.

Walker G.P.L., 1991. *Structure and origin by injection of lava under surface crust, of tumuli, "lava rises", "lava-rise pits", and "lava-inflation clefts" in Hawaii*. Bull. Volcanol., 53, 546-558.

Warner N.H. and Gregg T.K.P., 2003. *Evolved lavas on Mars? Observations from southwest Arsia Mons and Sabancaya volcano*. J. Geophys. Res., 108, 5112-5127.

Werner S.C., Harris A.W., Neukum G. and Ivanov B.A., 2002. *The Near−Earth Asteroid Size−Frequency Distribution*. Icarus, 156, 287−290.

Wilson, L., and Head J.W., 1983. *A comparison of volcanic eruption processes on Earth, Moon, Mars, Io, and Venus*. Nature, 302, 663– 669.

Wilson L. and Head J.W., 1994. *Mars: Review and analysis of volcanic eruption theory and relationships to observed landforms*. Rev. Geophys., 32, 221– 263.

Zimbelman J.R., 1985a. *Estimates of rheological properties for flows on the Martian volcano Ascraeus Mons*. Proc. Lunar Planet. Sci. Conf. 16th, Part 1, J. Geophys. Res., 90(suppl.), D157–D162.

Zimbelman J.R., 1985b. *Estimates of Rheologic Properties for Six Martian Lava Flows*. Lunar and Planetary Science, 16, 932-933. Abstract.

Zimbelman J.R., 1998. *Emplacement of long lava flows on planetary surfaces*. J. Geophys. Res., 103, 27503 – 27516.

CHAPTER 4- Tumuli and pingos: a comparative analysis between Daedalia Planum and Elysium Planitia mounds

Abstract

Tumuli and pingos are important distinctive features for inflated flows and unconsolidated water-rich periglacial terrains respectively. Therefore distinguishing between these two classes of features is useful to understand the origin of the terrain where such features occur; this however could be complex since their morphologies are very similar. We focused our study on the dome-like forms detected on Daedalia Planum and Elysium Planitia regions taking into account a morphological analysis of the features but also of the surrounding terrains, coupled with a density distribution study of mounds and dating of the surfaces where they were observed. Such comparative study revealed that Elysium Planitia features are more compatible with a pingo nature whereas Daedalia Planum features are more likely associable with tumuli. Therefore this would imply that the Elysium Planitia terrain hosting the mounds is likely to be outflow channel deposits and would confirm the presence of inflated flows on Daedalia Planum.

1. Introduction

The distinction between pingos and tumuli on Mars is an aspect still debated among the planetary geologists since has important implications about the nature of the hosting terrain. Tumuli are the most prominent fingerprints of inflated lava flows (Walker, 1991; Hon et al., 1994) whereas pingos can form in periglacial environments under various condition, like on mudflows (de Pablo and Komatsu, 2009) or outflow channel deposits (e.g. Burr et al., 2005). For these reason distinguishing one from the other become crucial.
Indeed both lava flows and outflow channels or mudflows frequently occur in the same region and are superimposed upon each other (see for example Marte Valles; Burr et al., 2002a); moreover their morphologies are rather similar and distinguishing them can be rather complex.
In this work we intend to analyze and compare the mounds present on Daedalia Planum with the most discussed dome-like forms on Elysium Planitia, in order to shed more light on their respective origin. We choose a morphological approach, with attention also for the context in which these features were emplaced as well as spatial distribution of the forms and dating of the surface.

2. Tumuli and pingos: a description

Tumuli and pingos are important features as they can be used as indicators of a specific environment. They appear like domed morphologies, usually with clefts on their top, with a wide range of dimensions. They both can have diameters varying from few meters up to a hundred of meters (Walker, 1991; Burr et al., 2009).
Tumuli are positive topographic features occurring on the surface of inflated lava flows. They form by the injection of hot lava which induces a local uplift and tensile stress in the colder but still visco-elastic crust (Fig.1). A tumulus has generally a circular or elliptical dome shape with clefts radially distributed on their top or with an axial crack. On the Earth Rossi and Gudmundsson [1996] classified three different types of tumuli on the basis of their morphologies and position with respect to the volcano flanks: i) lava-coated tumuli, observed on the upper and steeper flanks of volcanoes and covered by lavas that squeezed up from the cracks ii) upper-slope tumuli, detected on shallower slopes; they aren't buried by lava but it still flows through the cracks and iii) flow-lobe tumuli detected in the middle and lower flanks and not showing lava squeezed-up from their cracks.
Pingos are instead ice-cored mounds that form in periglacial terrain resulting of pressurized groundwater flow and progressive freezing. On the Earth pingos are divided into two classes according to their different way of formation. Open-system (or hydraulic) pingos (Fig.2) form through artesian pressure in correspondence of "taliks" (sites of unfrozen ground) which are connected with the unfrozen layer below the permafrost. Water flowing beneath the low-permeability layer is supplied under hydraulic pressure and is injected via taliks toward the surface.

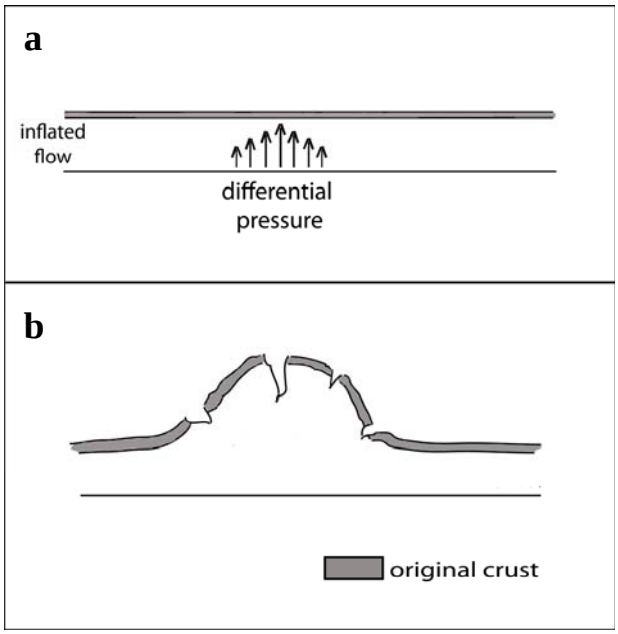

Fig1. Schematic sketch showing the formation mechanism of a tumulus the lava flowing beneath a colder crust is affected by differential pressure due to different causes, as terrain irregularities (a). This causes a vertical injection of lava and the progressively uplift of the crust up to form a real dome-like feature (b). The original crust breaks forming radial, axial or concentric clefts on the tumulus surface.

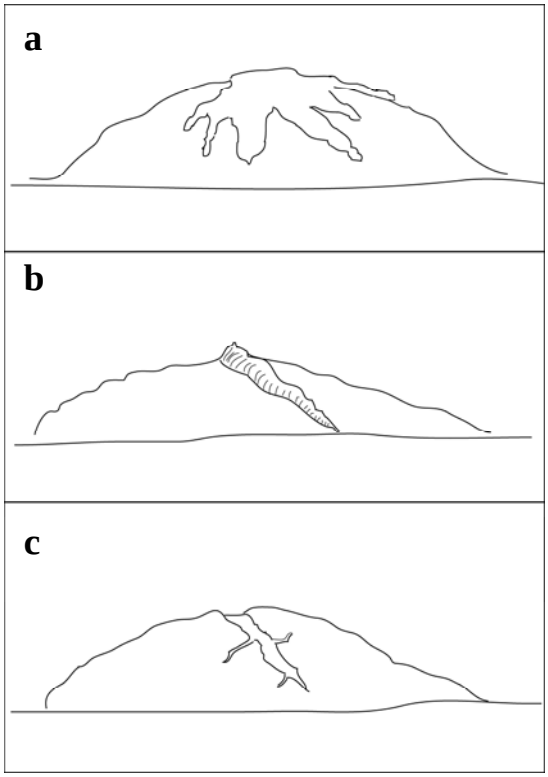

Fig. 2 Sketch of the three different types of tumulus, as described by Rossi and Gudmundsson [1996]. a) lava coated tumulus. Lava squeezes up from the clefts and covers the tumulus; b) upper slope tumulus with squeeze-up lava filling the cleft; c) flow lobe tumulus. The squeeze-up lava is absent.

The subsequent freezing of water causes the formation of the ice core that forces the ground up and the growing of pingo. The second class is represented by closed-system (or hydrostatic) pingos (Fig.3). In this case the permafrost layer is continuous and the pingos form in correspondence of drained lake or channel where taliks are isolated from the unfrozen ground layer. Saturated sediments are exposed to the atmosphere and this causes their progressive freezing and the accretion of permafrost. The water is expelled from the sediment pores and begins to concentrate to form a massive body of ground ice that deforms the overlying permafrost forming the pingo. Pingos show a variety of morphologies according to their stages of growth (Burr et al., 2009 and references therein). In the first stages a pingo is a low mound with a smooth surface. During the gradual growth of the ice-core, pingo assumes a convex, domical shape. Dilatational cracks are present on their top; they are commonly radial and more rarely semi-concentrical from the top. If during accretion the ice core is exposed through the fractures, the ice melts or sublimes causing the

collapse of the pingo summit. The result is a formation of a summit crater. In final growth stage the collapsed pingo form a raise-rimmed depression.

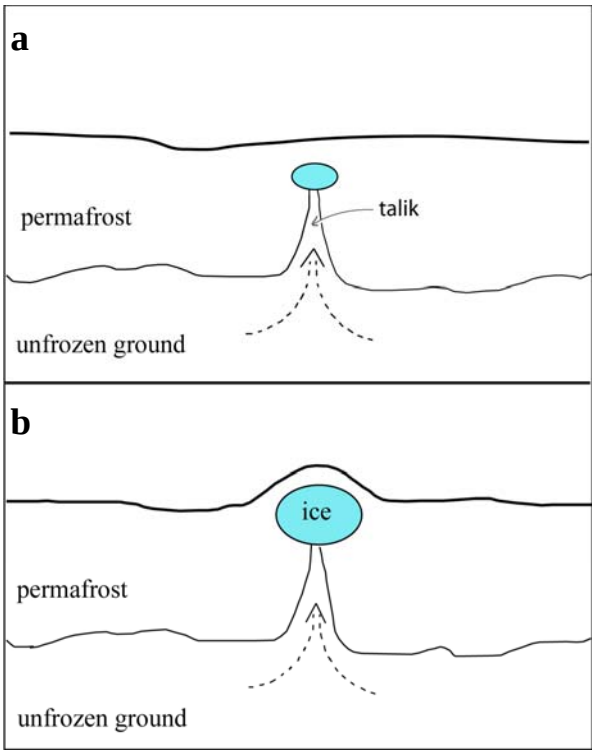

Fig.2 Schematic diagram showing the formation of an open-system pingo a) groundwater is injected through a talik in the permafrost. When water rises it encounters colder ground temperatures and begins to freeze b) groundwater continues to feed the ice core causing the ground up and the formation of the pingo.

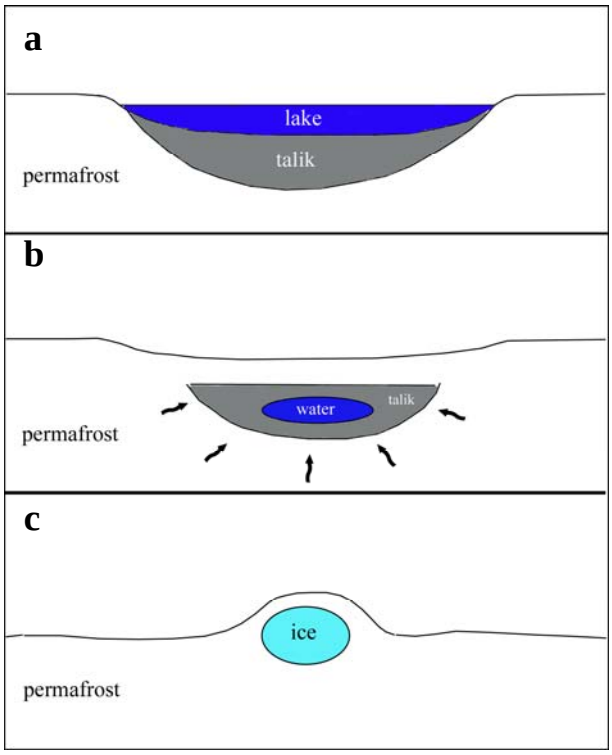

Fig. 3 Schematic diagram showing the formation of a closed-system pingo a) a lake within a continuous permafrost layer with a talik beneath b) lake drains and the talik shrinks progressively. The advancing of permafrost causes the concentration of the water at the centre c) the water freezes forming the ice core of the pingo.

3. Geological setting of Daedalia Planum and Elysium Planitia

Daedalia Planum is a plain in the Tharsis region located south west of the Arsia Mons. The volcanic nature of this region was revealed in images obtained by very early missions to Mars when a considerable number of lava flows were detected (e.g. Carr et al., 1977; Scott and Tanaka, 1986). Several different morphologies were detected on the Daedalia Planum lava field, like narrow lobated flows with central channels, pahoehoe flows and flows with brecciated surfaces. The detection of lava flows more than 1500 km long raises some questions about the factors that contribute to their emplacement. MRO/HiRISE (High-Resolution Imaging Science Experiment) and MGS/MOC (Mars Orbiter Camera) images analysis suggested the presence of some inflated flows inside the lava field as showed features like tumuli, lava rises and lava ridges on their surface. Calculation of effusion rate and lava rheological proprieties seems to further confirm this hypothesis (Giacomini et al., 2009).
Elysium Planitia is another important plain located south of Elysium Mons. Its origin however is more controversial since there is evidence that support both a volcanic and fluvial nature of the materials emplaced on its surface. Cerberus Fossae was indicated as the source of lava but also of water carving the outflow channels (Plescia 2003 and references therein). Various volcanic landforms were detected on the central Elysium Planitia, such as fissure vents, low shield volcanoes and cones (Plescia 2003). Moreover Keszthelyi et al. [2000] detected very young and extensive lava flows on the eastern Elysium Planitia with a typical platy-ridged surface morphology, indicative of large flood lavas.
However the morphology of some parts of Elysium Planitia suggests the occurring of a widespread fluvial event (Plescia, 2003). Athabasca Valles is an outflow channel system carved by flood water. The streamlined mesas detected in its channels are the most distinctive features attesting the aqueous flooding (Burr et al., 2002a).
Nevertheless these two environments do not exclude each other and can both occur in the same region at different times, as suggested by Plescia [2003] and Jaeger et al. [2007]. In particular, Fuller and Head [2002] suggest that both the outflow-channels and lava flows may have been generated by the same mechanism, i.e. a dike emplaced along Cerberus Fossae. This triggered water-flows that were followed by lavas emplaced in some of the valleys carved by out-flow channels.

4. Morphologic analysis of Daedalia Planum and Elysium Planitia flows

As described above, by studying HiRISE images many tumuli were detected on the surface of inflated Daedalia Planum lava flows, in particular associated with their front and edges. These features show both circular and elliptical map-shape with maximum length of about two hundred meters. Tumuli show different surface morphologies: some tumuli have clear radial or axial clefts on their top (Fig.4), but others lack extensional clefts and appear like mound with a rough surface covered by blocks (Fig.4) (Giacomini et al., 2009). However both these morphologies appear different to those detected on the southern Elysium Planitia and interpreted as tumuli by Keszthelyi et al. [2008]. Indeed, the latter are characterized by a circular shape, with a diameter range between 10-30 m, and show a smooth surface with medial and circumferential clefts (Fig.5). These features occurred on a particular uplifted terrain interpreted by Keszthelyi et al. [2008] as the result of the inflation (seeing Fig.6b). The great morphological difference between the Elysium and Daedalia

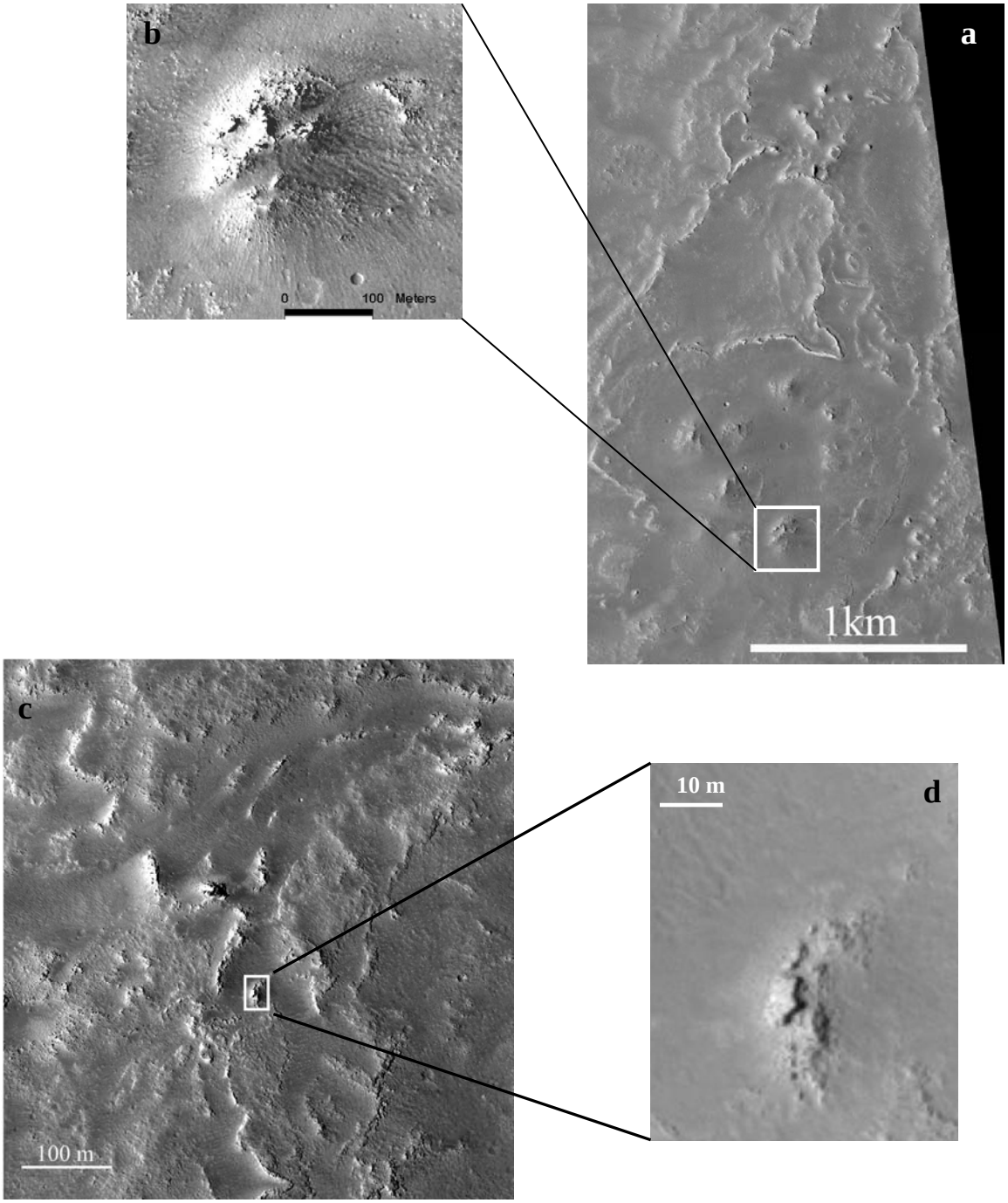

Fig. 4 Daedalia Planum areas where several mounds interpreted to be tumuli were detected by Giacomini et al. [2009] (PSPS_002711_1550). Some mounds show radial clefts (b) or axial crack (d), other mounds does not show any fractures on their top and show a rough, blocky surface (f, g, h).

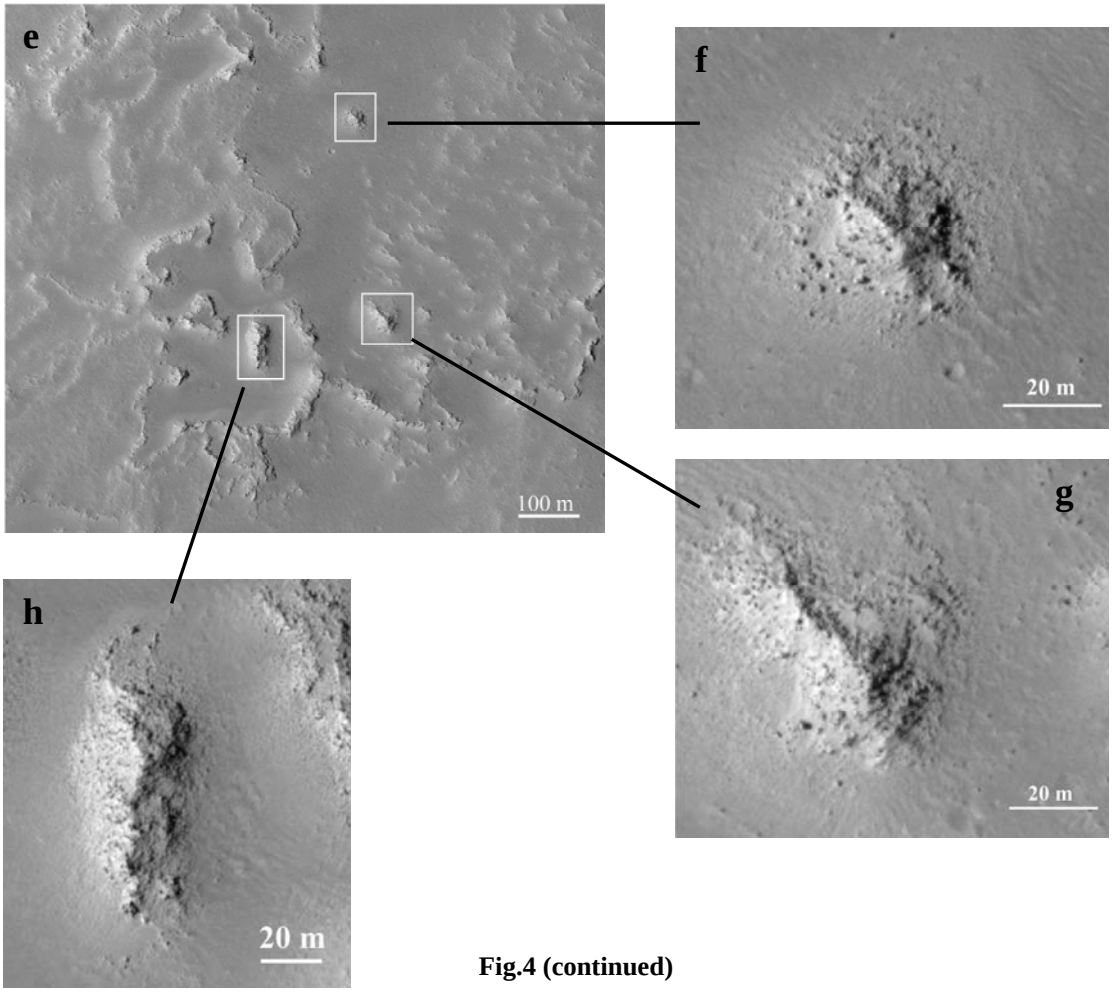

Fig.4 (continued)

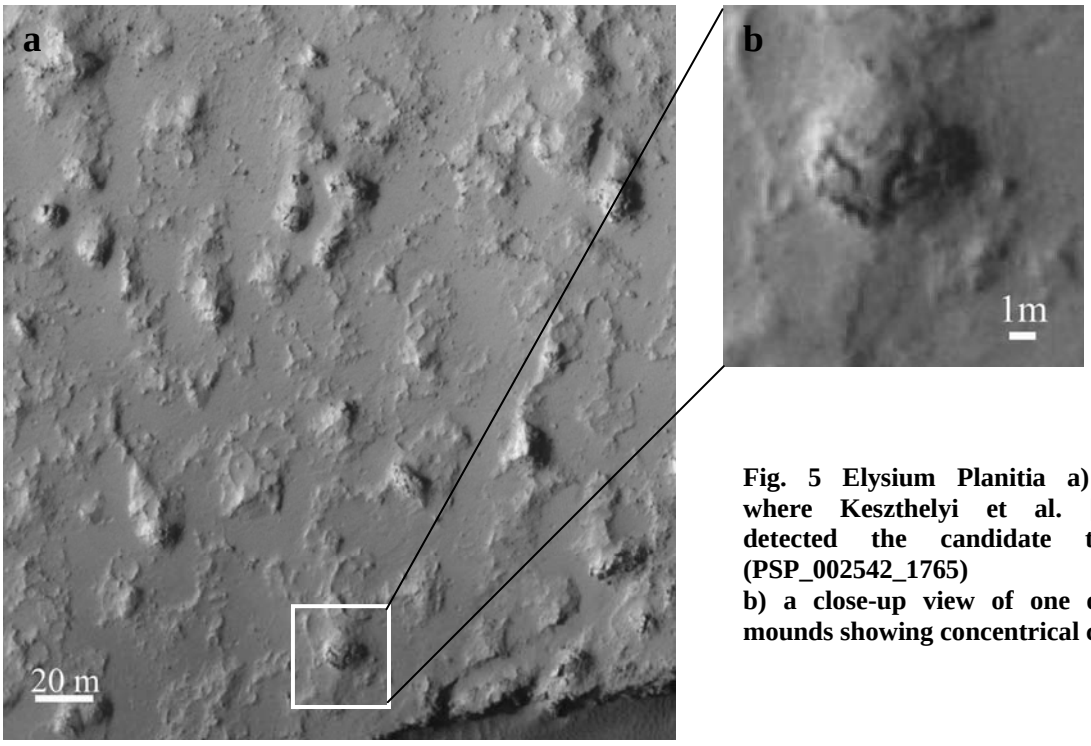

Fig. 5 Elysium Planitia a) area where Keszthelyi et al. [2008] detected the candidate tumuli (PSP_002542_1765)
b) a close-up view of one of the mounds showing concentrical clefts.

mounds raises some questions about the causes of such diversity. The possible explanations could be i) a different erosion time due to a different age of the two regions or ii) a different origin of the features that is reflected by diverse morphologies.

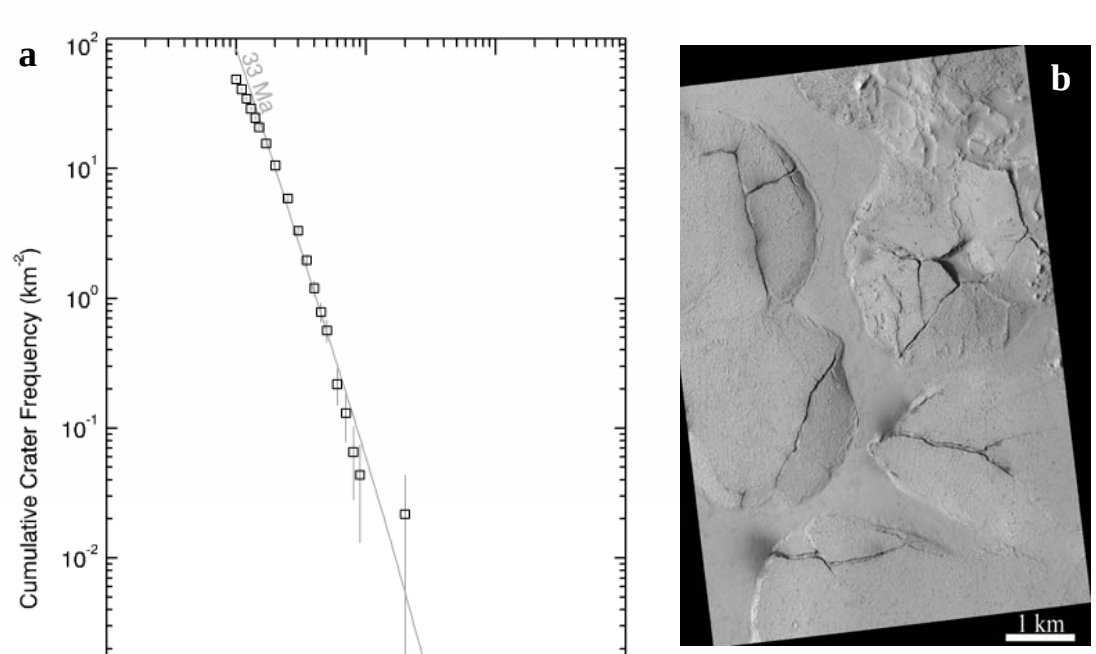

Fig. 6 Dating of Elysium Planitia terrain hosting the mounds considered in this work a) Cumulative plot of the Elysium Planitia area. The size frequency distribution has been plotted against NPF isochron of the derived model age. Error bars represent statistical errors. The cumulative plot was created with "Craterstats" DLR software (b) counting area of the investigated Elysium Planitia terrain (PSP_002542_1765 HiRISE image).

To verify the first hypothesis, the ages of the Daedalia Planum and Elysium Planitia surfaces have to be compared. This hypothesis is based on the assumption that the mounds located in the two regions are both tumuli. Since we can consider the tumuli as coeval to the inflated flow in which they occur, dating the surface permits to achieve also the age of the mounds. The dating of the Elysium surface was performed through crater counting (Fig.6) and fitting data by the Neukum crater production function (NPF) (e.g. Neukum et al., 2001). The result obtained is an age of 33±6 Myr, for 2720 craters in 45.87 km^2. Such an age is in agreement with the results of Hartmann and Berman [2000] that obtained an age range between 100 and 10 Myr for the southern Elysium Planitia flows. The dating of one of the youngest Daedalia Planum flows gave instead an age of 260±30Myr (Giacomini et al., 2009). Such great age difference between the two regions could be the reason for their different feature shapes, since the erosion time is longer for Daedalia Planum and this can justify the higher erosion degree of its features. This could explain also the different scale of the features observed in the two regions. The erosion may have caused the erasing of the smallest features on Daedalia Planum, leaving only the bigger mounds. On the contrary, the shorter time of erosion in Elysium Planitia allows the smaller mounds to endure. The hypothesis of a different time of erosion is supported also by the crater size-frequency distribution trend of the two regions. In the Daedalia Planum plot the craters with a diameter <40 m deviate from the isochron. In the Elysium Planitia plot, instead, the crater size-frequency distribution deviates slightly from the

isochron in correspondence of crater < 10 m in diameter. This could be due to the longer time of erosion affecting Daedalia Planum surface and causing the lack of the smallest craters.
All this kinds of evidence support the hypothesis that the Daedalia Planum and Elysium Planitia mounds are both tumuli affected by a different erosion degree.
However some recent works (Page and Murray, 2006; Page, 2007) documented the presence of some pingo fields on periglacial terrains in Elysium Planitia, suggesting the possibility that the mounds considered by Keszthelyi et al. [2008] could also be pingos, rather than tumuli. Such possibility was not completely excluded by Keszthelyi et al. [2008] too, as they considered the hypothesis that the uplifts were caused by freezing of groundwater. The heat of lava could have caused the melting of ground ice and the water can have flowed into nonlava materials in the considered region following the same mechanisms observed for the terrestrial hydraulic pingos (Keszthelyi et al., 2008).
The presence of periglacial environments at the low latitude of Elysium Planitia is confirmed by morphological fingerprints detected in the surrounding regions of Cerberus Plains and Athabasca Valles, like patterned ground and thermokarsts (Page and Murray, 2006;Page, 2007; Balme and Gallagher, 2009).
If we consider this as a probable scenario then it is possible that the Daedalia Planum and Elysium Planitia mounds are not comparable to each other since they have different genesis.

Table 1 Density of Daedalia Planum, Payen Matru and Elysium Planitia features

	Daedalia Planum mounds	Elysium Planitia mounds	Payen Matru (Argentina) tumuli
N° of features	269	471	460
Area considerate (km^2)	38.89	12.24	75.76
Density (per km^2)	6.9±0.4	38.5±1.8	6.1±0.3

The density of Daedalia Planum features and Payen Matru tumuli was taken from Giacomini et al. [2009]. The Martian flow considered belongs to D10 unit. The density of Elysium Planitia forms was calculated in the area visible on PSP_002542_1765 HiRISE image. The considerable different density values between Daedalia/Payun and Elysium validate the hypothesis of a different origin of the mounds of the two Martian regions. The errors of density are Poisson errors.

To verify this possibility we determined the density of the Elysium mounds to compare it with that of Daedalia Planum features. An area of 12.24 km^2 was considered obtaining a value of 38.5±1.8 per km^2 (Poisson error). Such result is about 5 times greater that the Daedalia one which is attested at 6.9±0.4 per km^2, a density comparable with that of the terrestrial inflated lava flows detected in Argentina (Giacomini et al., 2009).
The tumulus formation is influenced by some important factors like effusion rate, preexisting topography and slope (Glaze et al., 2005; Self et al., 1998). The tumulus formation model, proposed by Rossi and Gudmundsson [1996], is given by:

$$w_{\max} = \frac{\rho_m a^4}{64D} \frac{5+\upsilon}{1+\upsilon} \tag{4.1}$$

where $w_{\max}$ is the maximum deflection, ρ_m is the magmatic overpressure, which is directly related with the effusion rate (Hon et al., 1994), υ is the Poisson's ratio and D is the flexural rigidity.

The inflation mechanism requires very low and constant effusion rates to occur, generally in the range of few m^3/s (Walker, 1991; Hon et al., 1994). For this reason, although the effusion rates on Mars are generally higher than those on the Earth due to its lower gravity (Wilson and Head, 1994), we should expect comparable effusion rates for the Martian and terrestrial inflated lava flows, and then a comparable magmatic overpressure. In addition, all the plains considered (Dadalia Planum, Elysium Planitia and Payun-Matru plateau) are characterized by very low slope-angles (<1-2°) and lack of topographic confinements, hence they can be topographically analogues. On the basis of these assumptions the number of mounds per unit surface should directly reflect if the process of their formation is volcanic or not. Thus the similar density of mounds obtained for Daedalia Planum and Payen regions supports an inflation origin for the Daedalia Planum features and, consequently, very modest effusion rate of Arsia Mons at the time of their formation.
On the contrary the definitively higher density of Elysium Planitia features could reflect the different emplacement mechanism of the mounds and confirm their pingo-nature.
However the presence of pingos can not completely excluded in Daedalia Planum. Some of the lava flow morphologies observed in the lava field, like lobes and channels, can be easily confused with features detectable on mudflows. Therefore it is possible that some of the flows on Daedalia are in fact mudflows formed by fluidized volcanic sediments. The water could be created by melting of ground ice due to the magmatic heating, as proposed by Murray et al. [2009] for Ascraeus Mons flows. In this case the tumuli detected by Giacomini et al. [2009] could be pingos. However, as described above, pingo formation needs the presence of an unconsolidated sedimentary substrate and also of a periglacial environment (Burr et al., 2009). Even if Arsia Mons seems to have been affected by mountain glaciers on its north-western flank (Head and Marchant, 2003), on the south-west the typical glacier morphologies, like knobby terrain, ridged and arcuate lineations (Head and Marchant, 2003), are not observed. Nonetheless permafrost in unconsolidated terrain seems to affect some Daedalia areas as revealed by the presence of rampart craters. Several small rampart craters have been detected in the south-western Daedalia Planum region, suggesting that the permafrost layer is quite shallow in that area. However the flows where the analyzed mounds occur do not show this type of craters nor any signs of periglacial ice-rich terrain, like patterned terrain and thermokarst. This implies the absence of a permafrost involving unconsolidated terrains in that areas.
All this evidence suggests that the flows studied on Daedalia Planum by Giacomini et al. [2009] are effectively inflated lava flows that shown tumuli on their surface.

5. Conclusions

Tumuli and pingos are features that can be considered as fingerprints of inflated lava flows and periglacial terrain respectively. However they have similar morphological characteristics that make it difficult to distinguishing between them. Giacomini et al. [2009] detected some features interpreted being tumuli on Daedalia Planum lava flows. To confirm this hypothesis a comparative study with Elysium Planitia mounds, interpreted to be tumuli by Keszthelyi et al. [2008], was performed. This comparison reveal that the features appear however quite different one from the other. Such diversity can be explained in two ways: i) the features have different degree of erosion ii) the features have different origins.
The age difference between Daedalia, 260±30 Myr, and Elysium Planitia region, 33±6 Myr, suggests that the different morphologies may be due to different degree of erosion. However the environmental characteristics suggest an alternative interpretation. Several signs of periglacial conditions have been detected in the region surrounding Elysium Planitia whereas the Daedalia Planum flows investigated do not seem to affected by them. This coupled with a density of the Elysium mounds about 5 times higher that than of Daedalia ones, suggest that the feature emplaced

on Elysium are pingos, rather than tumuli. Therefore the different morphologies between the features present in the two regions can be explained has having different origin, in which case then they are not be comparable. However the morphological approach could be fruitfully integrated with a spectral study of these regions. As the area affected by these mounds are quite limited, MRO/CRISM (Compact Reconnaissance Imaging Spectrometer for Mars) would be the most appropriate instrument to find spectral features indicative of water or hydrated minerals and then distinguish lava flows from mudflows or outflow channel deposits.

References

Balme, M. R., Gallagher, C., 2009. *An equatorial periglacial landscape on Mars*. Earth and Planet. Sci. Lett.,285(1-2),1-15.

Burr D. M., Grier J. A., McEwen A. S., Keszthelyi L. P., 2002a. *Repeated Aqueous Flooding from the Cerberus Fossae: Evidence for Very Recently Extant, Deep Groundwater on Mars*. Icarus, 159(1), 53-73.

Burr, D. M., McEwen, A. S., Sakimoto, S. E. H., 2002b. *Recent aqueous floods from the Cerberus Fossae, Mars*. Geophys. Res. Lett., Volume 29, Issue (1), 13-1, DOI 10.1029/2001GL013345.

Burr, D. M., Soare, R.J., Wan Bun Tseung, J., Emery, J. P., 2005. *Young (late Amazonian), near-surface, ground ice features near the equator, Athabasca Valles, Mars*. Icarus,178(1), 56-73.

Burr, D. M., Tanaka, K. L., Yoshikawa, K., 2009. *Pingos on Earth and Mars*. Planetary and Space Science,57(5-6), 541-555.

Carr M. H., Greeley R., Blasius K. R., Guest J. E. and Murray J. B., 1977. *Some Martian volcanic features as viewed from the Viking orbiters*. J. Geophys. Res., 82, 3985-4015.

de Pablo, M. Ángel, Komatsu, G., 2009. *Possible pingo fields in the Utopia basin, Mars: Geological and climatical implications.* Icarus, 199(1), 49-74.

Fuller E.R., Head J.W., 2002. *Amazonis Planitia: The role of geologically recent volcanism and sedimentation in the formation of the smoothest plains on Mars*. JGR, 107 (E10), pp. 11-1, CiteID 5081, DOI 10.1029/2002JE001842.

Giacomini, L., Massironi, M., Martellato, E., Pasquarè, G., Frigeri, A., Cremonese, G., 2009. Inflated flows on Daedalia Planum (Mars)? *Clues from a comparative analysis with the Payen volcanic complex (Argentina).* Planetary and Space Science, Volume 57 (5-6), 556-570.

Glaze L. S., Anderson S. W., Stofan E. R., Baloga S., Smrekar S. E., 2005. *Statistical distribution of tumuli on pahoehoe flow surfaces: Analysis of examples in Hawaii and Iceland and potential applications to lava flows on Mars*. JGR, 110(B8), CiteID B08202.

Hartmann, W.K., Berman, D.C., 2000. *Elysium Planitia lava flows: Crater count chronology and geological implications*. J. Geophys Res., 105(E6), 15011-15026.

Head J.W. and Marchant D.R., 2003. *Cold-based mountain glaciers on Mars: Western Arsia Mons.* Geology**,** 31, 641-644.

Hon K., Kauahikaua J., Denlinger R. and Mackay K., 1994. *Emplacement and inflation of pahoehoe sheet flows; observations and measurements of active lava flows on Kilauea Volcano, Hawaii*. GSA Bulletin, 106, 351-370.

Keszthelyi L., Jaeger W., McEwen A., Tornabene L., Beyer R. A., Dundas C. and Milazzo M., 2008. *High Resolution Imaging Science Experiment (HiRISE) images of volcanic terrains from the first 6 months of the Mars Reconnaissance Orbiter Primary Science Phase*. J. Geophys. Res., 113, CiteID E04005.

Murray, J.B., van Wyk de Vries B., Marquez A., Williams D. A., Byrne P., Muller J., Kim J., 2009. *Late-stage water eruptions from Ascraeus Mons volcano, Mars: Implications for its structure and history*. Earth and Placet. Sci. Lett., In Press.

Page, D. P., Murray, J. B., 2006. *Stratigraphical and morphological evidence for pingo genesis in the Cerberus plains*. Icarus, 183(1), 46-54.

Page, D.P., 2007. *Recent low-latitude freeze thaw on Mars*. Icarus, 189(1), 83-117.

Plescia, J. B., 2003. Cerberus Fossae, Elysium, Mars: a source for lava and water. Icarus,164(1), 79-95.

Rossi M. J. and Gudmundsson A., 1996. *The morphology and formation of flow-lobe tumuli on Icelandic shield volcanoes*. J. Volc. Geotherm. Res., 72, 291-308.

Scott D. H. and Tanaka K. L., 1986. *Geologic map of the western equatorial region of Mars, scale 1:15,000,000*. U.S. Geol. Surv. Misc. Invest. Ser., Map I-1802-A.

Self S., Keszthelyi L., Thordarson Th., 1998. *The Importance of Pahoehoe*. Annual Review of Earth and Planetary Sciences, 26, 81-110.

Walker G.P.L., 1991. *Structure and origin by injection of lava under surface crust, of tumuli, "lava rises", "lava-rise pits", and "lava-inflation clefts" in Hawaii*. Bull. Volcanol., 53,546-558.

Wilson L. and Head J.W., 1994. *Mars: Review and analysis of volcanic eruption theory and relationships to observed landforms*. Rev. Geophys., 32, 221– 263.

CHAPTER 5 - Spectral analysis and mapping of Daedalia Planum lava field with OMEGA data

Abstract

The great variety of morphologies distinguished among the Daedalia Planum lava flows encouraged a more detailed study of their spectral characteristics, both to achieve some information about the lava composition and to detect possible differences in the flows spectra that help us to distinguish the flows inside the lava field. In this work we employed OMEGA data from the Mars Express mission. The spectra collected on the entire lava field appear rather similar to each other with absorptions between 0.8 and 1.4 μm and 1.8 and 2.5 μm, suggesting the presence of mafic minerals, like pyroxene and olivine. The continuum removal permits us to appreciate the presence of two classes of spectra related to the different content of Ca in the pyroxene. Both these classes are compatible with tholeiitic basalts. Despite these analogies, Daedalia spectra show some differences in reflectance and spectral slope. The SAM classification allows a spectral map to be created revealing that the differences among the spectra are generally in agreement with the lava flows mapped by Giacomini et al. [2009].This suggests that such variability is related to different surface textures of the lava flow. In some cases the spectral map highlights the presence of spectral subunits inside single units on the geological map of Giacomini et al. [2009] due likely to differences in mineralogy or rock texture. Therefore spectral analysis shows itself useful for improving the geological mapping of the Daedalia Planum region.

1. Introduction

Lava flows located on Daedalia Planum lava field show great morphological variability. The morphology of a flow depends on several factors such as effusion and cooling rate and rheology of lavas. To establish if flow variability could be related to a different composition of the lavas, a spectral analysis needed.
Up to date spectral analysis of volcanic regions have been performed using the Thermal Emission Spectrometer (TES) of Mars Global Surveyor, in the range of infrared wavelength from 6 to 50 μm, and OMEGA (Observatoire pour la Minéralogie, l'Eau, les Glaces et l'Activité), the Mars Express spectrometer in visible and near infrared range (0.4-2.5 μm). In particular such analyses have been used to assess the general rock composition of a region (e.g. Bandfield et al., 2000; Christesen et al., 2000; Wyatt et al., 2001), or to find evidence of volcanic rock-forming minerals as olivine and pyroxene (e.g. Mustard et al., 2005; Poulet et al., 2007, 2009a, 2009b).
In this work OMEGA data has been studied to partly infer the compositions of Daedalia Planum lavas and highlight the differences of their spectral behaviors. This allows us to realize a spectral map of the volcanic field to be compared with the stratigraphic analysis of Giacomini et al. [2009].

2. Composition of Mars volcanic rocks

Several instruments on past and current spacecraft, coupled with the geochemical analysis of Martian meteorites, have revealed that most of the surface of the planet is composed of basalt with a very small proportion of highly evolved siliceous rocks (e.g. quartz-bearing granitoid rocks; Christiansen et al., 2005).
By employing TES data, Bandfield et al. [2000] studied the composition of Martian low albedo regions, representing almost 50% of the Martian surface. Such regions were selected to minimize the influence of fine grained bright dust. The average spectra for each region show similar spectral shapes characterized by broad absorptions in the 8 to 12 μm and in the 20 to 50 μm wavelengths. Despite this overall similarity, some differences actually exist, allowing a separation in two groups. The first one (type 1) shows a square-shaped absorption at 8-12 μm whereas the 20-50 μm

absorptions are superimposed by minor ones and show an overall negative slope increasing the wavelengths. The second group (type 2) is characterized by a V-shaped absorption at 8-12 μm and shows a uniform absorption at the higher wavelength. The type 1 terrain is localized on the southern highlands and on Syrtis Major whereas type 2 is concentrated on the northern lowlands. Bandfield et al. [2000] compared these spectra with spectra of terrestrial rocks, concluding that they are similar to various volcanic compositions. In particular the type 1 spectral shape can be associated with terrestrial basalts composed mainly of plagioclase and clinopyroxene. The type 2 spectral shape, instead, is comparable to basaltic andesite and andesite composed primarily of plagioclase, potassium-rich glass and pyroxene.
Basalts are the expression of low differentiation of a mantle source and on Earth are common in hot-spot, flood volcanism and rifting environments. On the contrary andesites are more differentiated rocks and on the Earth are common along convergent margins, which however have not been observed yet on Mars. Wyatt and McSween [2002] suggest a different mechanism for the formation of "type 2 regions". In particular their modeled mineral abundances reveal that the type 2 spectral shape can be compatible also with the presence of plagioclase, pyroxene and alteration minerals, like clays, characteristic of altered basalt. For this reason they proposed that also the northern lowlands can be constituted by basalt, but weathered in a submarine environment.
On the basis of this evidence it seems plausible that the most part of Martian volcanism is basaltic. This interpretation is supported also by in-situ investigations performed by a panoramic camera (Pancam) and a thermal emission spectrometer (Mini-TES) installed on the Spirit Rover.
Spirit landed in Gusev crater and the spectra obtained by Pancam and Mini-TES discovered that the crater terrain is composed of volcanic material of basaltic composition (Squyres, 2004).
Recently, McSween et al. [2009] reviewed all the different geochemical data available on composition of the Mars surface, concluding that the basaltic rocks on the planet are principally represented by tholeiitic basalts. The presence of widespread sub-alkaline basalts, formed by extensive partial melting, supports the hypothesis of a very limited magmatic differentiation.

3. Regional setting of the Daedalia Planum lava field

Located south-west from Arsia Mons, Daedalia Planum is a lava plain where a huge number of lava flows have been emplaced (Carr et al., 1977; Moore et al., 1978; Schaber et al., 1978; Scott and Tanaka, 1981) over an almost flat terrain (<0.5° and commonly <0.1°) (Smith et al., 1999) (Fig.1). The youngest lava flows originated from the caldera rim of Arsia Mons, therefore they are associated with the magma chamber of the volcano. The source of oldest flows is instead more uncertain, as they could originate from flank pits buried by subsequent flows. One of the main characteristics of these old flows is their great length that typically reaches over 1500 km from the Arsia Mons caldera rim. Several factors could have contributed to the emplacement of these long flows but the detection of features like tumuli, lava rises and lava ridges on their surface suggests that inflation process are one of the most important factors in their development (Giacomini et al., 2009). Scott and Tanaka [1986] employing Viking images distinguished eight different geological units inside the volcanic plains. Recently, the higher resolution of THEMIS, MOC and HiRISE images has enabled the identification of thirteen geological units, on the basis of their stratigraphic relationships (Giacomini et al., 2009). Some units are constituted by flows characterized by distinguishing surface morphologies: for example the oldest ones include the most widespread flows of the area showing the typical pahoehoe and platy-ridged surface textures whereas the youngest units are represented by numerous narrow lava flows with central channels or with brecciated surfaces. Other units however are constituted by flows located on the same stratigraphical position but which do not show common characteristics, such as D12 or D6 units (see Fig.1).Scott and Tanaka [1986] collocated the Daedalia Planum lava flows between Hesperian and Amazonian; the dating by crater counting of one of the youngest lava flows of the area

(belonging to the unit At_5 of Scott and Tanaka map) confirms this estimate, as it gave an age of about 260 Myr, employing the Neukum Production Function method (NPF) (Giacomini et al., 2009).

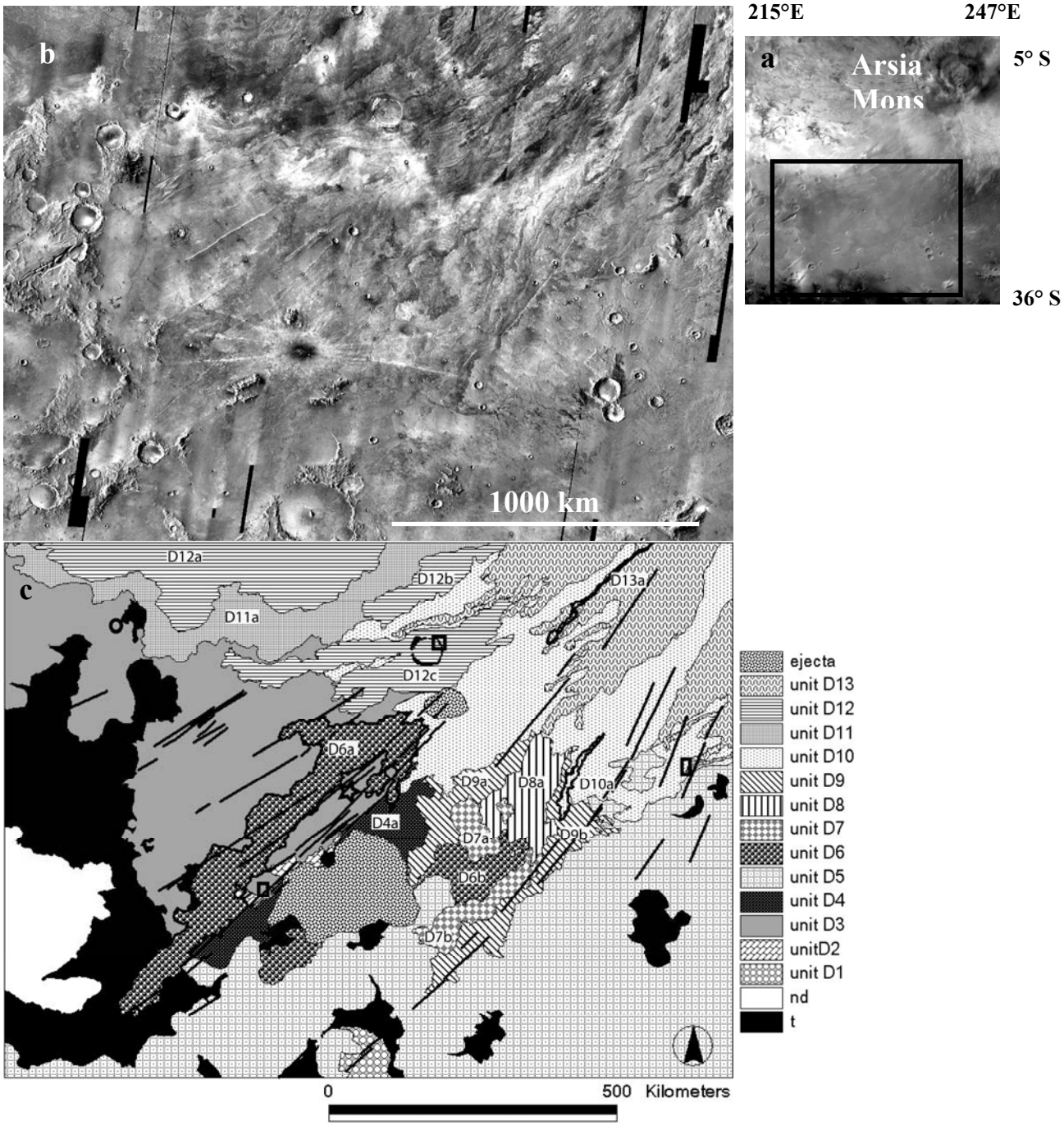

Fig.1 Daedalia Planum volcanic field a) MOC mosaic of red-filter (575-625 nm) Wide Angle Camera images. Black rectangle outlines the area of Daedalia Planum considered in this work b) THEMIS Day-IR (12.57 μm) mosaic c) geological map of Daedalia Planum (from Giacomini et al. [2009]).

The presence of dust cover is of paramount importance for any spectral investigation since dust may completely alter the spectral behavior of the underlying rocks. In Daedalia Planum dust cover is pervasive, but markedly inhomogeneous since it is confined along depressions between outcropping relieves. Hence on rugged terrain as pahoehoe and brecciated lava flow surfaces the bedrock is frequently exposed, whereas in plain terrain the dust cover is more widespread. However in almost all the analyzed localities the bedrock frequently outcrops from the cover (Fig.2) and consequently, should substantially contribute to the spectral behavior of the region.

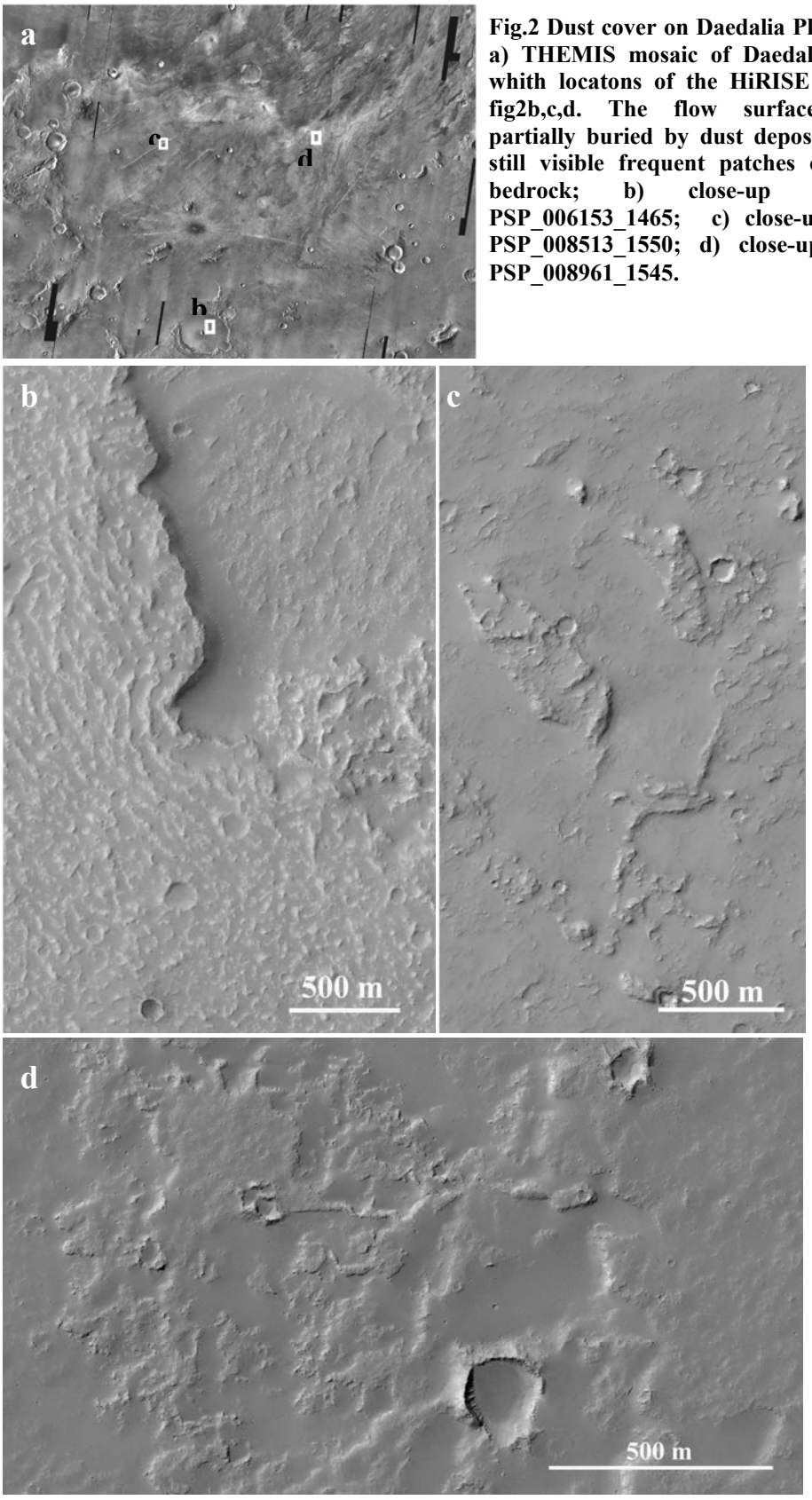

Fig.2 Dust cover on Daedalia Planum field a) THEMIS mosaic of Daedalia Planum whith locatons of the HiRISE images of fig2b,c,d. The flow surfaces appear partially buried by dust deposits but are still visible frequent patches of exposed bedrock; b) close-up view of PSP_006153_1465; c) close-up view of PSP_008513_1550; d) close-up view of PSP_008961_1545.

4. Data sets and methods

The OMEGA images (see Table 1) have been used to cover almost the whole area of Daedalia Planum geologically mapped by Giacomini et al. [2009].
OMEGA imaging spectrometer acquires 352 spectral channels, from the visible (0.36 μm) to the thermal infrared (5.2 μm, Birbring et al., 2005). A VNIR (Visible and Near Infra Red) spectrometer acquires spectra from 0.36 to 1.07 μm (VIS channel), whereas two SWIR (Short Wavelength IR) spectrometers, IRC and IRL channels, observe from 0.93 to 2.7 mm and from 2.6 to 5.2, respectively. The spectral sampling is 7 nm for the VNIR, 14 nm and 20 nm for the two SWIR spectrometer respectively. The OMEGA spatial resolution varies between 300 m to 4 km (Bibring et al., 2004).
We performed a radiometric calibration running the IDL routine SOFT04, downloaded from ESA's Planetary Science Archive (PSA). The atmospheric correction was applied assuming that the contributions of the surface and atmosphere were multiplicative and that the atmospheric contribution follows a power law variation with altitude (Bibring et al., 1989). Assuming a constant surface contribution, the spectra ratio between a spectrum from the base of Olympus Mons to one over the summit provides the atmospheric spectrum at a power function of the altitude. The atmospheric contribution was removed dividing the observation by the atmospheric spectrum. Such spectrum is scaled by the strength of the CO_2 atmospheric absorption measured in the observation (Mustard et al., 2005).
Both VIS and IRC data were used to describe the spectral absorptions and understand the composition of the surface material. In addition the IRC of all the orbits listed in Table 1 were used to produce a spectral map of the area.
We evaluated the composition of the Daedalia surface material for different orbits with different pixel resolution. The continuum was removed by subtracting a straight-line continuum tangent to the reflectance spectra on either side of an absorption feature.
Subsequently we derived a compositional map to represent the spectral differences seen within the OMEGA data. Following the morphological units described by Giacomini et al. (2009), we collected several spectra for each unit from every singular image. This operation was repeated for all the images (orbits). Subsequently the mean of all the spectra collected for each unit was calculated as well as the standard deviation.
Some units were represented by a homogenous distribution of spectra with a standard deviation less than 0.5%. In contrast, D3, D5, D6, D10 and D12c units are characterized by a larger standard deviation mainly due to a greater variability of the spectra data in terms of albedo and spectral slope. Hence these units were further subdivided using the spectral difference. The mean of the resulting new sub-spectral-units' standard deviation were then calculated, giving a standard deviation less than 0.5%.
The spectral map was finally obtained applying SAM (Spectral Angle Mapper) supervised classification for each orbit (Kruse et al., 1993).
The SAM classification is an automated method for directly comparing image spectra to a known spectra or an endmember. SAM is a physically-based spectral classification that uses a n-dimensional angle to match pixels to reference spectra. The algorithm determines the spectral similarity between two spectra (the questioned and known) by calculating the angle between the spectra and treating them as vectors in a space dimensionality equal to the number of bands. When used on calibrated reflectance data, this technique is relatively insensitive to illumination and albedo effect, therefore the spectral classification shouldn't take into account the albedo variations (Kruse et al., 1993).
In this case the endmembers are the mean spectra of the geological units calculated for each orbit. However the endmembers were further reduced by considering as a single endmember those spectra

completely superimposable after normalization at 1.3 μm (Fig.3). The result of our map shown in Fig. 4 is discussed in section 6.

Table1

List of OMEGA data employed for the Daedalia Planum spectral analysis

OMEGA ORBIT	Spatial resolution (pixel/degree)	Time of acquisition
ORB0457_1	55.19982	30/05/2004
ORB0479_2	54.99642	05/06/2004
ORB1316_3	34.37252	26/01/2005
ORB1404_4	23.53273	19/02/2005
ORB1448_4	23.53107	04/03/2005
ORB1448_5	16.00691	04/03/2005
ORB2014_5	87.50437	09/08/2005
ORB2025_5	86.94896	12/08/2005
ORB2505_2	59.22416	25/12/2005
ORB3192_6	56.77302	05/07/2006
ORB4582_2	55.56481	29/07/2007
ORB4593_3	55.68238	01/08/2007

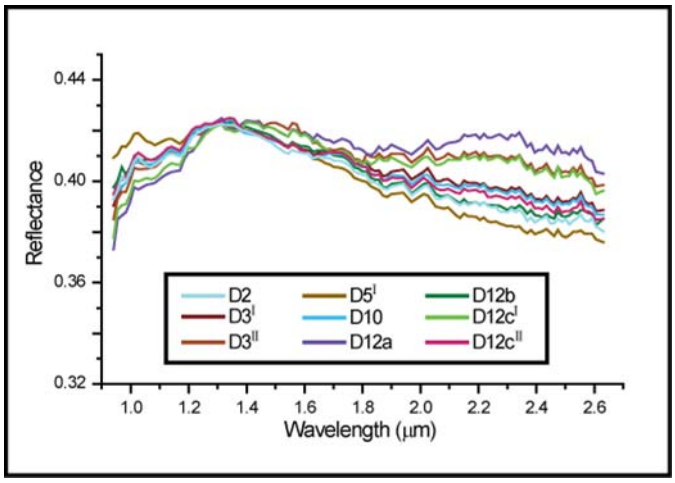

Fig.3 Example of IR spectra normalized at 1.3 μm used to highlight the superimposition of different spectra to reduce the endmember of the SAM initially obtained following unit from the map of Giacomini et al. [2009]. Roman number used to distinguish different spectra collected in the same unit.

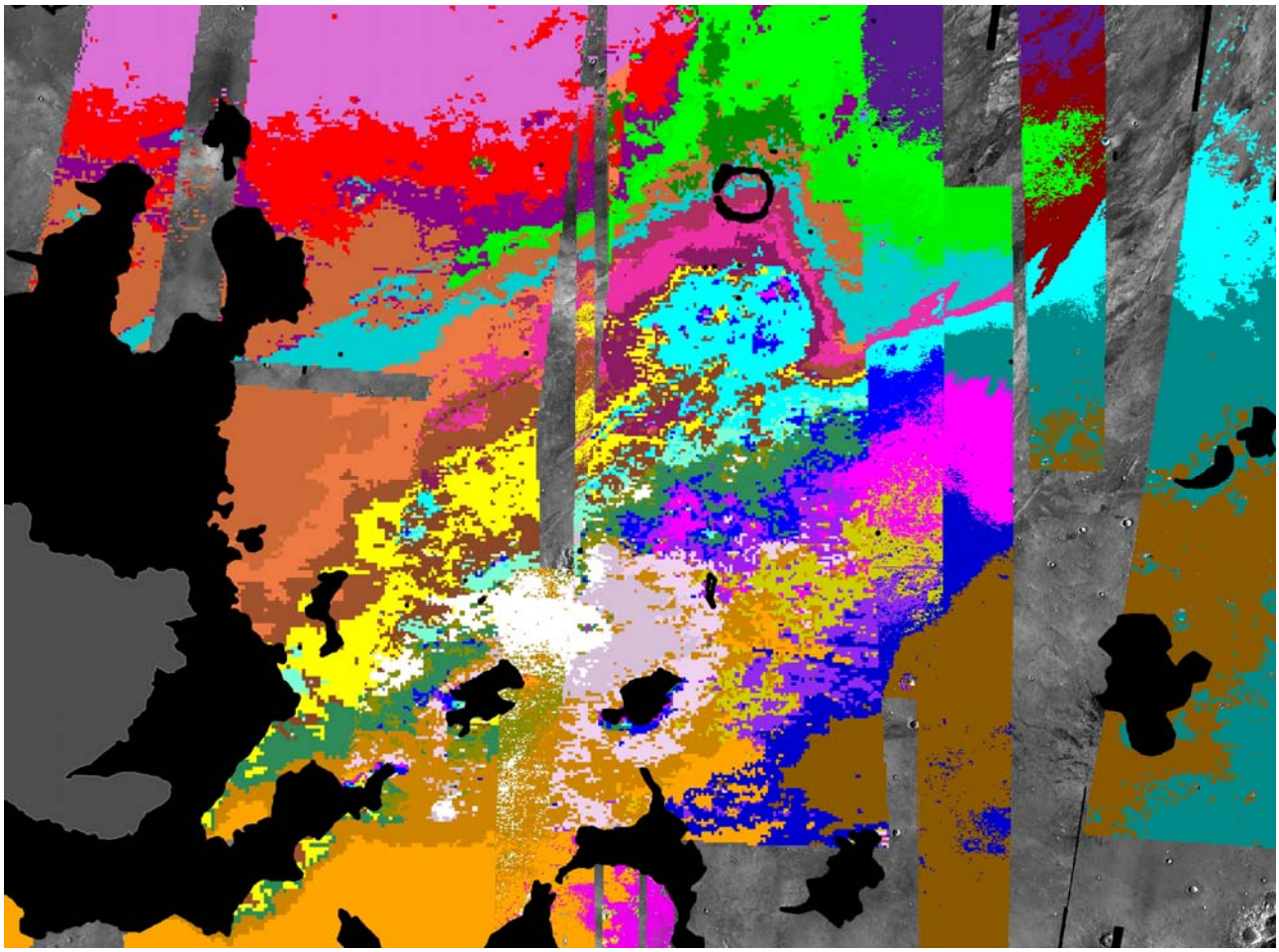

Fig.4 Spectral map of Daedalia Planum created by SAM classification employing the OMEGA data listed in Table 1. Several spectral differences inside the lava field are shown due to different flows surface morphologic characteristics, mineralogy or rock textures (see text). Crater rims and related terrain were not considered in the analysis and appear in black. Grey indicates lava flows not belonging to the Daedalia Planum field. On the background is THEMIS day IR mosaic.

5. Composition of Daedalia Planum lavas

All the OMEGA spectra collected show an absorption between 0.8 and 1.4 μm and a shallow absorption band in the 1.8 to 2.5 μm wavelength range. The maximum absorption depth is 2% and 1% of reflectance respectively. The spectra show no other resolvable minor absorptions features due, for example, to hydrate minerals alterations, and most spectra generally display a flat to blue slope at wavelengths longer than 1.5 μm (see Fig.5).

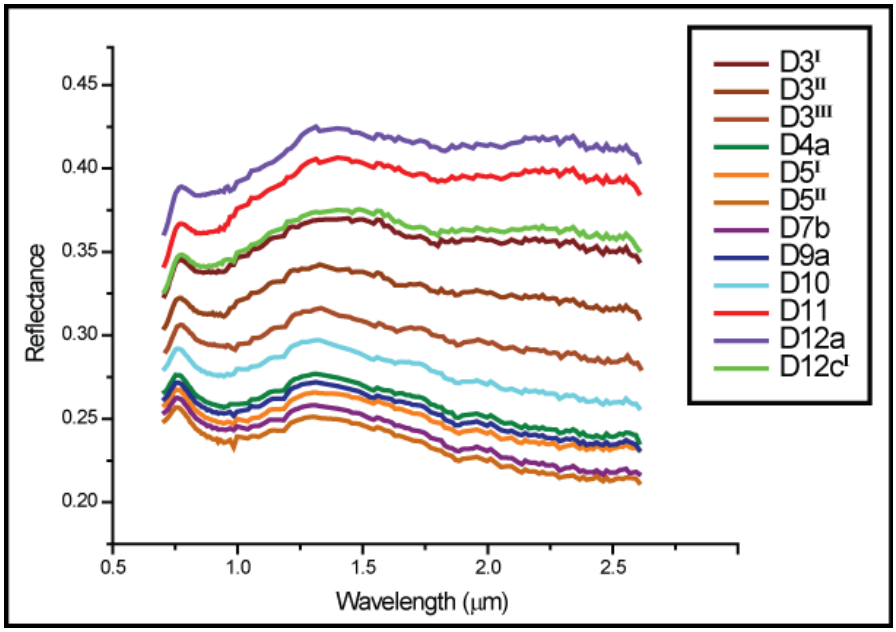

Fig.5 Example of some spectra of different unit from ORB1404_4. Roman number used to distinguish different spectra from the same unit.

Such spectral signatures indicate the presence of two main minerals: olivine and pyroxene. The olivine spectrum is characterized by a wide absorption at ~1.0 μm, due to the presence of Fe^{2+} in both M1 and M2 sites [Burns, 1993; Sunshine and Pieters 1990; 1998]. The pyroxene spectra generally show two absorption bands at ~ 1.00 and 2.00 μm. However the minimum position can shift and the band intensity can differ due to the presence of different cations (Fe^{2+}, Mg^{2+}, Ca^{2+}) in the M1 and/or M2 octahedral sites [Burns, 1993; Cloutis and Gaffey, 1991]. Low-Ca pyroxene (wollastonite <11%) spectra shows two well defined absorptions: i) a minimum between 0.91 at 0.93 μm (band I), having a linear relationship with the content of Fe^{2+} in M2 site, and ii) a less prominent absorption band between 1.80 and 2.00 μm (band II). The spectra of high Ca-pyroxene (wo <45%) show two different absorption bands indicative of the Fe^{2+} in the M2 site. In particular the high Ca pyroxene spectra show absorption bands at slightly longer wavelength than low-Ca pyroxene, between 0.95-1.05 μm (band I) and between 1.95-2.40 μm (band II). When wo~50%, the Ca-pyroxene shows only one complex absorption band with two minima close to 1.00 μm indicative of the presence of Fe^{2+} in M1(Cloutis and Gaffey, 1991).
In order to highlight the absorption features and better evaluate the composition of the studied material we remove the continuum from the original spectra. The resulting spectral shapes show some differences allowing us to group the spectra into two classes (Fig. 6). The spectra of the class A (Fig.6a) are characterized by a narrow band I with a minimum at 0.95 μm indicating the presence of a low calcium clinopyroxene, like pigeonite. This band shows an asymmetry at the longer wavelengths implying the presence of other absorptions in that region (Sunshine et al. 1990; Cloutis and Gaffey, 1991; Pompilio et al. 2008), probably due to a pyroxene richer in calcium, like augite,

olivine and/or Ca-plagioclase relatively rich in Fe^{2+}(Crown and Pieters, 1987) The band II shows a minimum at ~1.85 μm, consistent with the presence of pigeonite, and a slightly asymmetry at longer wavelengths consistent with the presence of augite, that usually has a minimum between 2.0 at 2.2 μm. The class B (Fig.6b) is characterized by spectra showing a more intense and wider band I with a minimum close to 1.00 μm. This wide band on OMEGA data is generally due to the presence of both pigeonite and augite (i.e.:Mustard et al., 2005). However, the band II is weaker than the class A band II, and has a minimum located at circa 2.0 μm, thus possibly supporting a higher abundance of augite, with less pigeonite. Class A spectra are more concentrated in the northern units, excluding D12a flow whereas the southern units and D12a flow show spectra that can be assigned to class B.

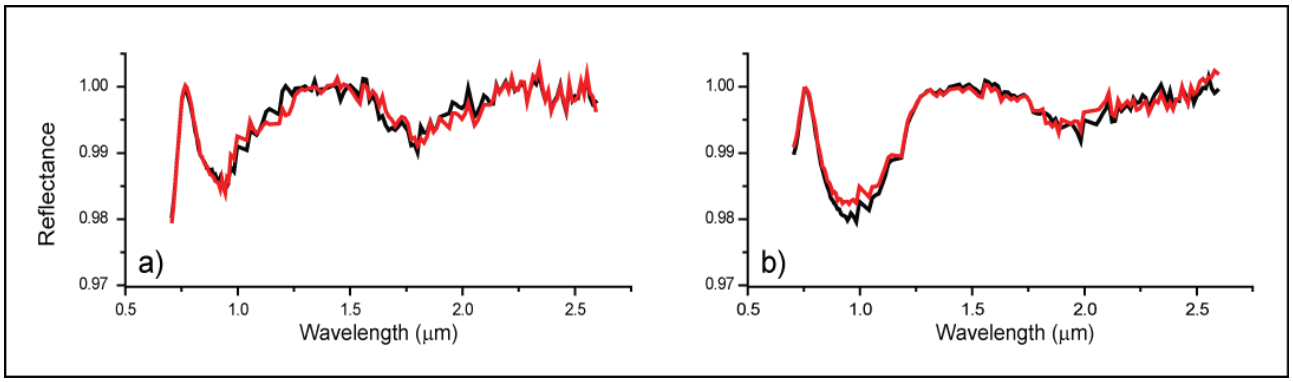

Fig.6 Example of continuum removed spectra: a) two spectra like class A with more asymmetric band I with minimum at 0.95μm; b) two spectra like class B with a band I minimum at 1.00μm (see text for more explanation).

Augite and pigeonite are both components of tholeiitic and alkali series basalts. They can be present either as phenocrysts or groundmass crystals, according to the Hawaiian basalts described in the Basaltic Volcanism Study Project (BVSP) [1981]. The variation of the augite composition can be used to distinguish alkali series basalt from tholeiitic ones, since augite of the alkali series basalts has higher calcium and iron contents (from high Ca-augite to diopsidic-augite) than tholeiitic ones (BVSP, 1981). Considering the minima of the Daedalia Planum, for both class A and class B spectra, we see that the positions of these absorptions are consistent with the presence of augite with a relatively low calcium content typical of tholeiitic series basalts.

Comparing the Daedalia spectra with spectra measured on terrestrial rock samples it was observed that the absorption shapes and wavelength positions are comparable with those characterizing laboratory spectra of powders of terrestrial basalts at different grain size (Fig.7).

The rock samples considered for the comparison originate from Iceland and Payen Matru (Argentina) (Fig.7). The Icelandic basalt is a tholeiitic basalt characterized by a low alkali content. The phenocrysts are constituted by plagioclase (2.25 vol %), clinopyroxene (0.60 vol %) and olivine (0.15 vol %), whereas the groundmass minerals are mainly represented by plagioclase, clinopyroxene, olivine and opaque minerals (Carli, 2009). The Payen Matru basalt is instead a hawaiite, with a rich Na-alkaline content ($Na_2O+K_2O \approx 5\%$). The rocks are holocrystalline with a small amount of olivine (5 vol %) and plagioclase (<5 vol %) phenocrysts. The groundmass shows intergranular textures with crystals of plagioclase, olivine, clinopyroxene and opaque minerals (Pasquarè et al., 2008).

However the Daedalia Planum spectra generally show a minimum at lower wavelength than Iceland and Payen Matru spectra, which would be compatible with the presence of a low Ca-pyroxene (pigeonite) as described above. The different overall reflectance and slope among the units of the Daedalia lava flows could be attributed to a variation in the grain size of the surface material Craig et al. [2008] showed that the albedo decreases and spectra change from flat or red to blue slope with increasing grainsize of the particulate samples of basalt. However other factors could also explain

the spectral variations, like different flow surface textures, the presence of glass or crystal isoorientations. Also the presence of dust cover may influence the spectra albedo and slope as the variation observed for the Daedalia Planum spectra is consistent with the influence of dust cover in the region. Ruff and Christiansen [2002] employed TES emissivity values to create a map of the dust cover index (DCI) that relates the emissivity, observed in a spectral range between 1350 and 1400 cm^{-1}, and the presence or absence of silicate dust whose particle size is <100 μm. Nevertheless on Daedalia Planum region the DCI variations have an E-W trend whereas our flow units show a general NE-SW trend. This proves that, despite the dust cover, OMEGA can distinguish the different spectra of the lava flows.

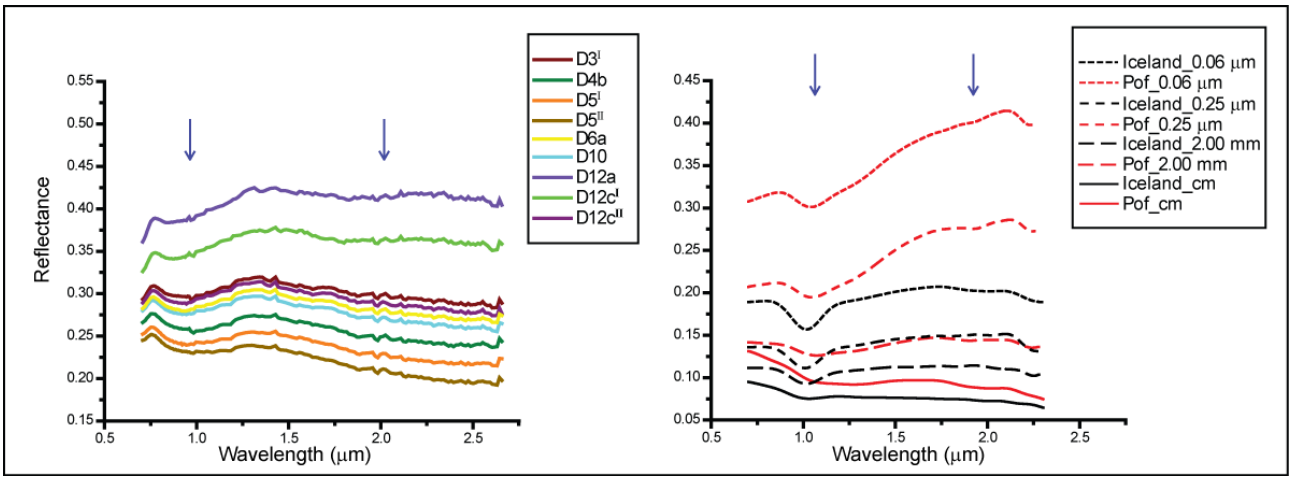

Fig.7 Comparison between spectra from Daedalia Planum (sx) and spectra of terrestrial basalts powders (dx, from Carli et al. 2009) from different geological context at different grain size. In both of case spectra show weak band I and II (blue arrows). Variation of spectra slope could be explained also with different grain size of the surface material as evident for the terrestrial basalts (Carli et al. 2009) and from Craig et al. [2008] (see text for more explanation).

6. Spectral versus morphological mapping of Daedalia lava field

Giacomini et al. [2009] grouped the Daedalia Planum lava flows into 13 different geological units on the basis of their stratigraphic relationships. The units were subsequently classified into subclasses to distinguish the single lava flows, except for D13, D10, D3 and D5 where the flow boundaries are not clearly detectable. To perform a geological mapping taking into account also the spectral characteristics we compared the geological map of Daedalia Planum with the new spectral map created with the OMEGA data. These two maps show several striking similarities and, although the boundaries in the spectral map are rougher due to the lower spatial resolution of OMEGA data, it is evident that the spectral units follow the NE-SW trend of the flows (Fig.8).
D6a flow is a significant example of such correspondence as well as the flows filling Pickering crater (Fig.9). Actually this 130 km-crater is filled by lava flows v belonging to two different units that in our case correspond to D1 and D5 (Caprarelli et al., 2009). These two units are clearly recognizable also on the spectral map and thanks to the good resolution of the OMEGA orbits used (ORB2025_5; ORB2014_5) the spectral unit follows the morphological boundaries with good precision.

The spectral map allowed the detection of boundaries between some flows not well defined from their morphologies. For instance the distal part of some lava flows, like D4a, D6a, D9b, are difficult to distinguish probably cause of the unsuitable sun angle illumination on THEMIS images, but the spectrally corresponding units enabled us to outline their fronts with more confidence.
In addition the spectral map reveals that the flows of Daedalia Planum show different spectral characteristics, even within the same stratigraphical unit (Fig.8b). By using THEMIS VIS, MOC and HiRISE we observed that sometimes the spectral behavior of the flows may be in agreement with surface morphological differences among them. Therefore these spectral differences can be interpreted as the surface textures influence on the spectral shapes, in particular albedo and slope. This occurrence can be observed for D12 and D13 units. D12a and D12b flows show different spectral behaviors in agreement with their morphological characteristics: D12a is characterized by lobes and tongues with irregular surface textures whereas D12b shows a smoother surface with lava channels. D12c is instead a more particular flow whose spectral behavior will be discussed subsequently. Finally D13 flows were not subdivided because they are spatially too close to each other, however flows with brecciated surface and flows with central channel were distinguished inside the same unit. This is reflected also on the spectral map that highlights two different spectral regions.
On the other hand some units that appear morphologically uniform can be divided into some

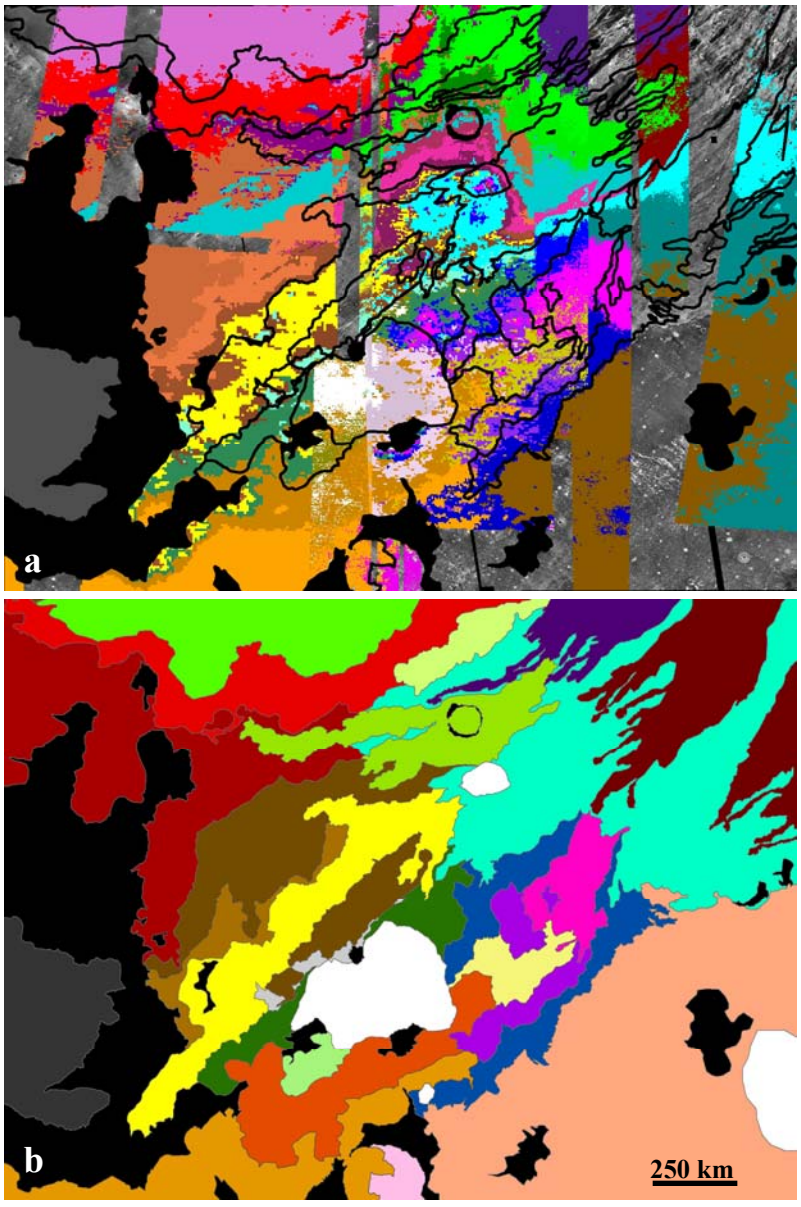

Fig.8 Spectral characteristics of Daedalia Planum lava field a) comparison between the geological map of Daedalia Planum after Giacomini et al., 2009 (black lines)), and the SAM classification results. The spectral units, showing a characteristic NE-SW trend are in general agreement with the geological ones; b) map of Daedalia Planum where all the spectral units distinguished on the base of spectral characteristics of flows are shown (see text for details).

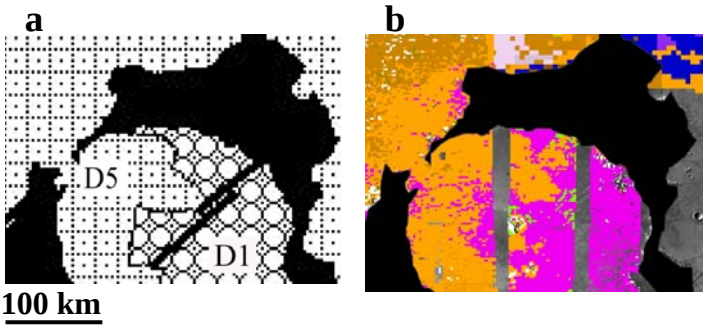

Fig. 9 Pickering crater a) A close-up view of the Giacomini et al. map [2009] b) a close-up view of the spectral map. The comparison between these two maps reveals that the boundaries of D5 and D1 units are clearly detectable also on spectral map.

spectral subunits in the spectral map. The presence of such subdivision may have different explanations: i) in some regions the high resolution images are not available and the THEMIS IR images don't permit the different surface textures of the flows to be appreciated; ii) it is possible that OMEGA data had detected slight variations in grain size of surface material or in mineralogy or in rock texture, such as the presence of glass or crystal isoorientations. D3 and D6 units are an example of such behavior. In THEMIS VIS, MOC and HiRISE images D3 old flow unit shows a ropy surface texture. However on the spectral map three different subunits were distinguished on the basis of their different albedo and spectrum slope.

D6a and D6b flows are in the same stratigraphic position and show the same surface textures, but they display clearly different spectral behaviors. In addition, D6b cannot be followed for its entire length because masked in the middle part by ejecta deposits of a 4 km diameter crater (Fig.10); hence the distal part of D6b could also represent another independent unit. This is further proved by its characteristics spectral signature with respect to all the other D6 flows (Fig.10).

For these reasons we proposed to map the units taking into account also their spectral subunits. The classification was performed adding another letter, such as α, β, γ, after the unit code of Giacomini et al. [2009] (Fig.13). Since OMEGA orbits were acquired in different time, the atmospheric conditions can differ and the dust cover can be differently distributed on the region; moreover the spatial resolution of OMEGA varies considerably for each orbit. Consequently the value of albedo and slope could be different among the orbits, even for the same flow. Nevertheless the mutual relationships among the spectra remain unchanged and then a classification is possible.

D5 unit underwent heavy changes since it results separated into two parts by the extension of the D9b flow. The D5 unit to the west of D9b shows two different spectral subunits that are bluer than the eastern counterpart (Fig.11a).

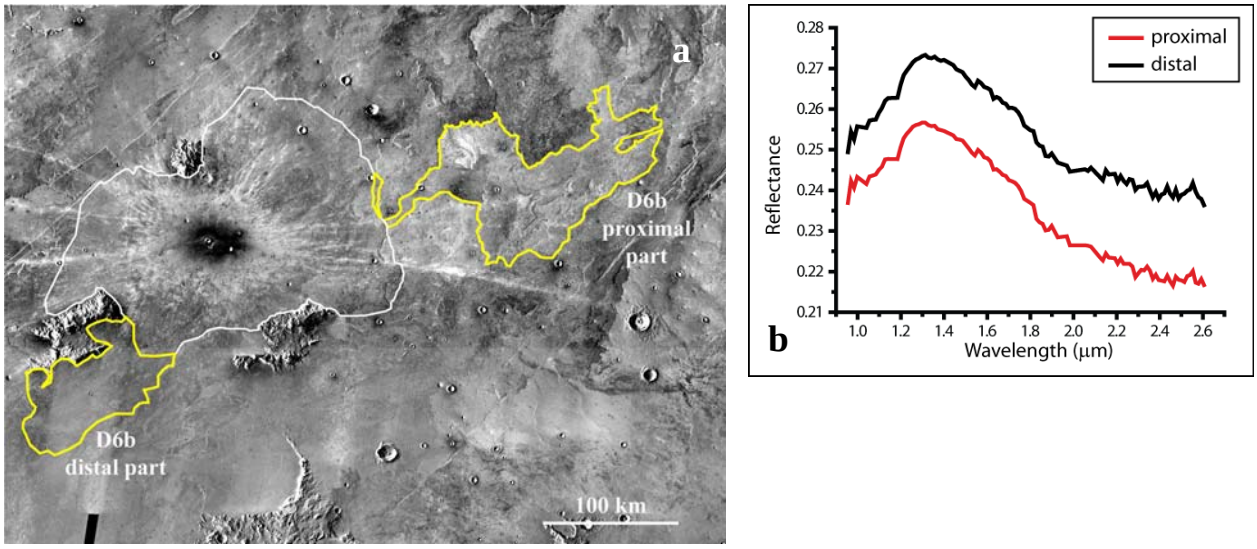

Fig.10 D6b flow a) THEMIS image mosaic shows the ejecta blanket (outlined in white) of a 4 km diameter crater covering the middle part of D6b flow (outlined in yellow) b) spectra of the proximal and distal part of D6b. The different shape of the two spectra suggests that they could represent different spectral units.

In addition THEMIS night IR images (12.57 μm) show a clear boundary between D9b flow and the "D5 east" (Fig.11b). Usually these images do not show particular differences among the flows inside the lava field, therefore the marked contact between these two units suggests that "D5 east" unit is different from the others and maybe does not belong to the lava field itself. This seems further proved from clusters of numerous rampart craters with different dimensions that are not visible in the other units and suggests the presence of an extended and tick deposits of fine sediments rather than lavas.
For these reasons we finally decided to exclude "D5 east" from the units belonging to Daedalia Planum volcanic field.

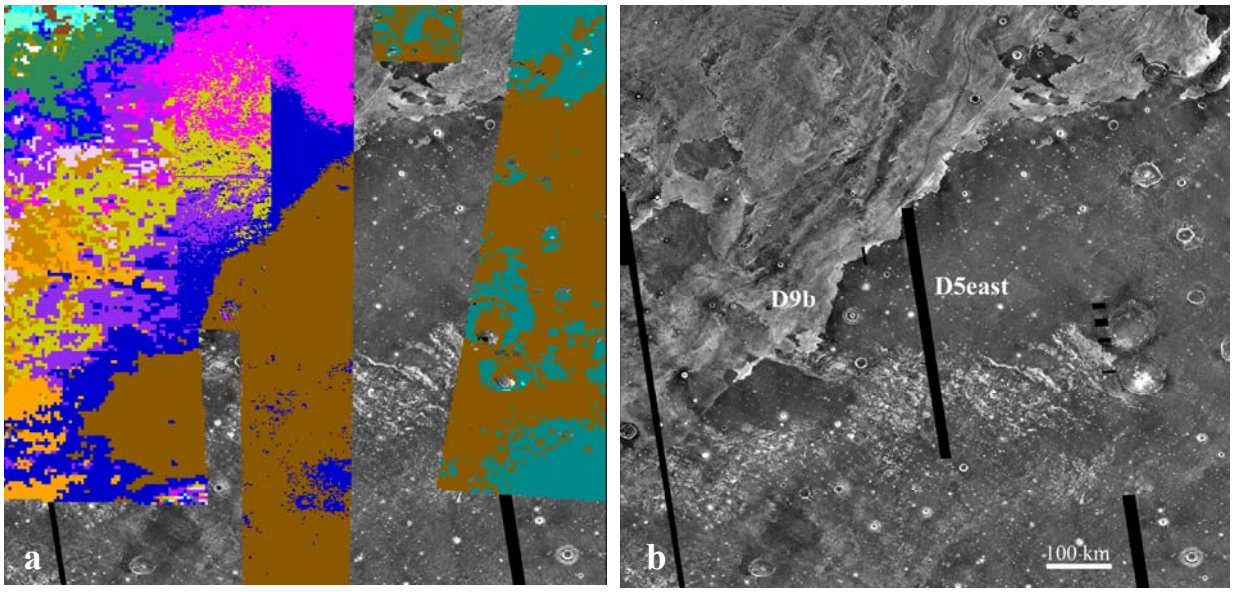

Fig. 11 Contact between D9b flow and D5east. a) THEMIS night IR mosaic (12.57 μm) shows a clear boundary between the two units. This contact is outlines also in the spectral map (b) where D9b is indicated with blue and D5est with brown.

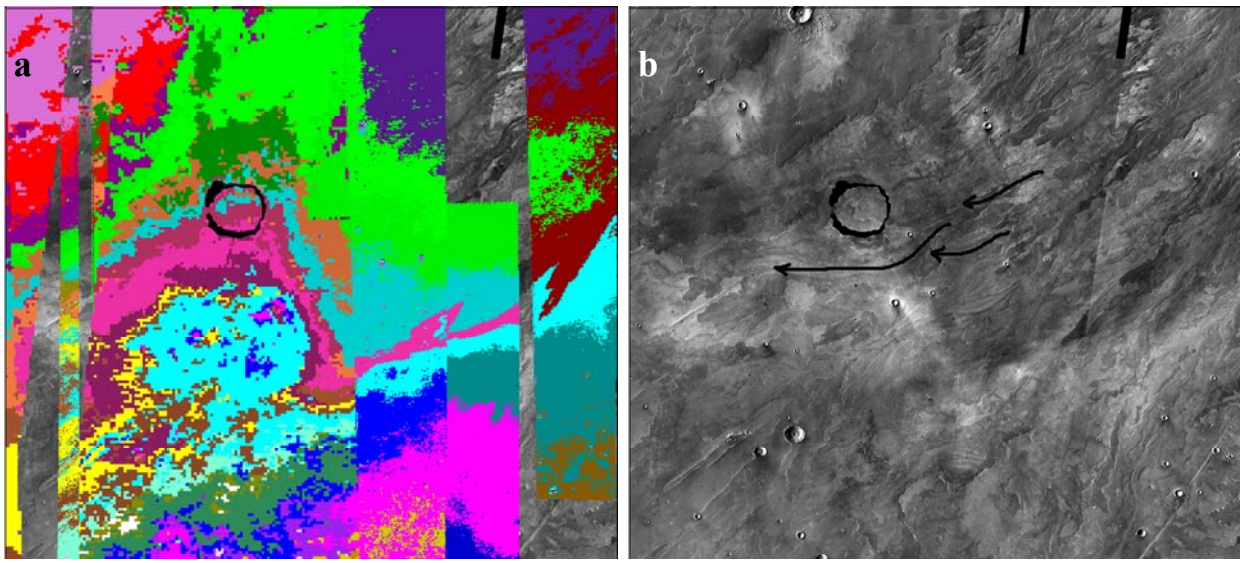

Fig. 12 The spectral anomaly individuated on Daedalia Planum a) a close-up view of the spectral map. Units form a rough circular shape b) THEMIS day IR images show as the flows deviate its trend toward west, as shown by the arrows.

The most evident discrepancy between spectral and morphological maps is located in correspondence of the central sector, involving D10 and D12c flows. In particular ORB1404_4 OMEGA orbit shows several spectral units that have no correspondences with any morphological units. By contrast a rough circular shape is visible, with the spectral units that deviate abruptly their path and continue towards north-west (Fig.12a).
The causes of this feature are uncertain. By observing the OMEGA image the region is darker than the surrounding, therefore it is characterized by a lower albedo. On the contrary, the THEMIS Day IR (12.57 μm) images show a high emissivity for the same region.
Comparing this map with the THEMIS mosaic it was observed that there is a correspondence between the bright area in THEMIS Day IR images and the region with an intermediate DCI in the Ruff and Christiansen [2002] dust cover map, characterized by a value between 0.94 and 0.95. Ruff and Christiansen [2002] related this intermediate value to surfaces partially covered by dust or composed by cemented fine particles. This correspondence between THEMIS IR mosaic and Ruff and Christiansen [2002] dust cover map suggests that the two elements can be linked to each other and that the presence of dust can influence the spectral signatures and hence the SAMs.
However observing the flows' trend it has been noted that D12c and some other flows of D10 unit approaching the anomalous region deviate slightly in trend from initially west-south-west to west (Fig.12b). This observation, coupled with the circular trend of spectral units, suggests the presence of a partly buried depression that could be a ghost crater or an ancient caldera.
Unfortunately the MOLA grid resolution (463m/pixel) may fail to detect both very abrupt slope gradients and low altimetric variation spanned along wide spatial ranges. If this is the case, the possible depression could have not been solved by MOLA data and an higher resolution DEM is required. Unfortunately there are no Mars Express/HRSC available up to date for the sector of interest in Daedalia Planum and consequently it is not possible to acquire other proofs of such a depression.
Terrain irregularities cause variations on local illumination angles and consequently on the materal spectra response which may differ from a Lambertian behavior. In this case the reflectance may vary as a function of the wavelength and the spectral slope can heavily modified. This phenomenon however can be negligible for the spectra acquired with small phase angle (Brivio et al., 2006), as in the case of OMEGA acquisition on more or less planar surfaces, so it should not influence our SAM map.
Nevertheless the presence of dust and of a depression are not mutually exclusive since the latter could have acted as a trap for the dust and together may have caused the spectral anomaly. Since this anomaly does not seem related to flow characteristics we did not consider it in the units' classification (Fig.13).

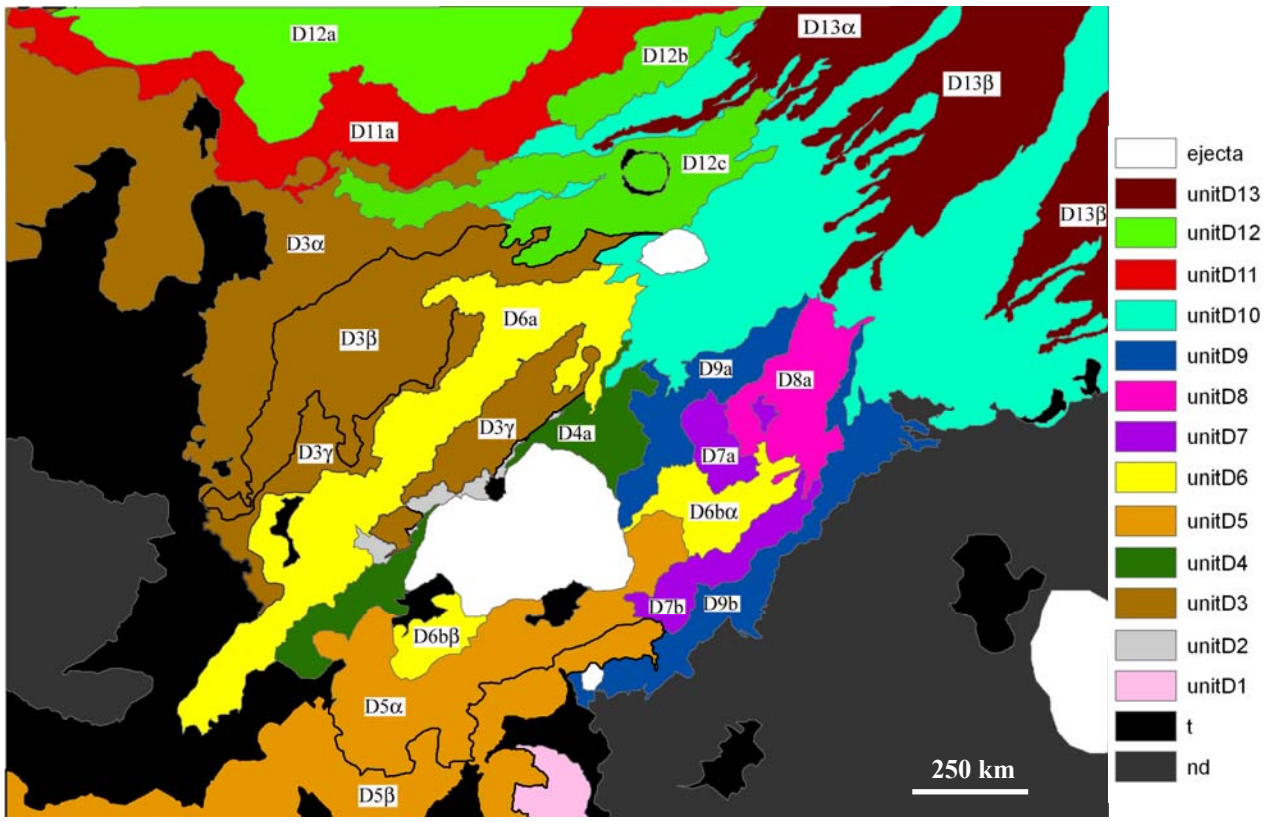

Fig.13 Geological map of Daedalia Planum after Giacomini et al [2009]. New subunits, found through spectral differences, were classified with α, β and γ after the code created by Giacomini et al. The spectral anomaly has not been taken into account (see text for details). Ejecta blankets are indicated in white. "t" indicates the crater related terrains whereas "nd" the area not belonging to Daedalia Planum lava field.

7. Discussion and Conclusions

Daedalia Planum lava field is characterized by a considerable number of lava flows showing a wide variety of morphologies. To assess if such variation is due to different composition of lavas we analyzed the OMEGA data. After the atmospheric corrections the spectra appear similar to each other and show absorptions between 0.8 and 1.4 μm and between 1.8 and 2.5 μm, suggesting the presence of mafic minerals (like olivine and pyroxene). Continuum removal permits us also to distinguish two different types of spectra, class A and class B, which are related to the presence of low-Ca clinopyroxene (pigeonite) and high-Ca clinopyroxene (augite) respectively. Both these types of spectra are compatible with a basaltic composition and the content of Ca in the augite indicates that Daedalia Planum flows are most likely composed by tholeiitic basalt.
However, despite the similarities, Daedalia spectra show some differences in albedo and spectral slope. These spectral variations could be due to several factors, like different surface textures of flows but also different mineralogy or rock texture, such as the presence of glass, crystal size or crystal isoorientation. This implies that the wide range of morphologies observed among the flows is due to their different mode of emplacement rather than to different compositions. The spectral map created with SAM classification reveals that these differences can be related to the different lava flows present in the lava field. The spectral map allowed us to improve the geological map of Daedalia Planum lava field as it allowed the boundaries between some flows not well morphologically defined to be detected and enabled spectral subdivisions inside some stratigraphic units.

Although SAM classification generally seems not biased by the presence of dust cover, it probably masked the spectral characteristics of lava flows in offside a particular circular shape observed in the central part of the spectral map. The presence of a shallow depression, not appreciable on MOLA data, is suggested to justify such spectral anomaly. This terrain irregularity could have entrapped dust particles consequently influencing the spectra signatures of surface and then the SAM classification.
All these lines of evidence demonstrate the great potential for improving Martian geological maps by integrating morphological analysis with the spectral characteristics of a region.

REFERENCES:

Bandfield, J.L., Hamilton, V.E., Christensen, P.R., 2000. *A Global View of Martian Surface Compositions from MGS-TES*. Science, 287, 1626-1629. DOI: 10.1126/science.287.5458.1626

Basaltic Volcanism Study Project, 1981. *Basaltic Volcanism on the Terrestrial Planets*. Pergamon Press, New York, 1286 p.

Bibring, J.-P., Combes, M., Langevin, Y., Soufflot, A., Cara, C., Drossart, P., Encrenaz, Th., Erard, S., Forni, O., Gondet, B., Ksanfomalfty, L., Lellouch, E., Masson, Ph., Moroz, V., Rocard, F., Rosenqvist, J., Sotin, C., 1989. *Results from the ISM experiment*. Nature 341, 591-593doi:10.1038/341591a0.

Bibring, J.-P., Soufflot, A., Berthé, M., Langevin, Y., Gondet, B., Drossart, P., Bouyé, M., Combes, M., Puget, P., Semery, A. et al., 2004. *OMEGA: Observatoire pour la Mineralogie, l'Eau, les Glaces et l'Activite.* European Space Agency Special Publication ESA SP-1240, 37–49.

Bibring, J.-P., Bibring, J-P, Langevin, Y., Gendrin, A., Gondet, B., Poulet, F., Berthé, M., Soufflot, A., Arvidson, R., Mangold, N, Mustard, J., Drossart, P., 2005. *Mars Surface Diversity as Revealed by the OMEGA/Mars Express Observations*. Science, 307, 1576; DOI: 10.1126/science.1108806.

Brivio P.A., Lechi G., Zilioli E., 2006. Principi e metodi di telerilevamento. CittàStudi, DeAgostini editore, pp. 525.

Burns, R.G., 1993. *Mineralogical applications of crystal field theory*. Cambridge University Press, Cambridge, pp. 551.

Carli C., 2009. *Analisi spettroscopica nel VNIR di rocce ignee. Caratterizzazione composizionale della superficie dei pianeti terrestri*. PhD Thesis, Univ. of Parma, Italy.

Caprarelli, G., Leitch, E.C., 2009. *Volcanic and structural history of the rocks exposed at Pickering Crater (Daedalia Planum, Mars)*. Icarus, 202, 453–461.

Carr, M.H., Greeley, R., Blasius, K.R., Guest, J.E., Murray, J.B., 1977. *Some Martian volcanic features as viewed from the Viking orbiters*. J. Geophys. Res., 82, 3985–4015.

Christensen, P.R., Bandfield, J.L., Smith, M.D., Hamilton, V.E., Clark R.N., 2000. *Identification of a basaltic component on the Martian surface from Thermal Emission Spectrometer data*. J. Geophys. Res., 105, E4, 9609-9621.

Christensen, P. R., McSween, H. Y., Bandfield, J. L., Ruff, S. W., Rogers, A. D., Hamilton, V. E., Gorelick, N., Wyatt, M. B., Jakosky, B. M., Kieffer, H. H. et al., 2005. *Evidence for magmatic evolution and diversity on Mars from infrared observations*. Nature, 436 (7052), 882.

Cloutis, E.A., Gaffey, M.J., 1991. *Pyroxene spectroscopy revisited: spectral-compositional combinations and relationships to geothermometry*. J. Geophys. Res., 96, 22809-22826.

Craig, M.A., Cloutis, E.A., Reddy, V., Bailey, D.T., Gaffey, M.J., 2008. *The effects of grain size, <10 μm - 4.75 mm, on the reflectance spectrum of planetary analogs from 0.35-2.5 μm*. Lun. Planet. Sci. XXXVIII, #1356.

Crown, D.A., Pieters, C.M., 1987. *Spectral properties of plagioclase and pyroxene mixtures and the interpretation of Lunar soil spectra*. Icarus, 72, 492-506.

Giacomini, L., Massironi, M., Martellato, E., Pasquarè, G., Frigeri, A., Cremonese, G., 2009. *Inflated flows on Daedalia Planum (Mars)? Clues from a comparative analysis with the Payen volcanic complex (Argentina).* Placet. Space Sci., 57(5-6), 556-570.

Griffes J. L., Arvidson R. E., Poulet F., Gendrin A., 2007. *Geologic and spectral mapping of etched terrain deposits in northern Meridiani Planum.* J. Geophys. Res., 112, E08S09, doi:10.1029/2006JE002811.

Kruse, F.A., Lefkoff, A.B., Boardman, J.B., Heidebrecht, K.B., Shapiro, A.T., Barloon, P.J., Goetz, A.F.H., 1993. *The Spectral Image Processing System (SIPS) - Interactive Visualization and Analysis of Imaging spectrometer Data*. Remote Sensing of the Environment, 44,. 145-163.

Mangold, N., Gendrin, A., Gondet, B., LeMouelic, S., Quantin, C., Ansan, V., Bibring, J.-P., Langevin, Y., Masson, Ph., Neukum, G., 2008. *Spectral and geological study of the sulfate-rich region of West Candor Chasma, Mars.* Icarus 194, 519–543.

McSween Jr., H.Y., Taylor, G.J., Wyatt, M.B., 2009. *Elemental Composition of the Martian Crust.* Science 324, 736-739. DOI: 10.1126/science.1165871

Moore, H.J., Arthur, D.W.G., Schaber, G.G., 1978. *Yield Strengths of Flows on the Earth, Moon, and Mars*. In: Proceedings of the Lunar Planetary Science Conference, 19th, 3351–3378.

Mustard, J.F., Poulet, F., Gendrin, A., Birbring, J.B., Langevin, Y., Gondet, B., Mangold, N., Bellucci, G., Altieri, F., 2005. *Olivine and Pyroxene diversity in the crust of Mars*. Science, 307, 1594- 1597.

Mustard, J.F., Murchie, S.L., Pelkey, S.M., Ehlmann, B.L., Milliken, R.E., Grant, J.A., Bibring, J.P., Poulet, F., Bishop, J., Dobrea, E.N., Roach, L., Seelos, F., Arvidson, R.E., Wiseman, S., Green, R., Hash, C., Humm, D., Malaret, E., McGovern, J.A., Seelos, K., Clancy, T., Clark, R., Des Marais, D., Izenberg, N., Knudson, A., Langevin, Y., Martin, T., McGuire, P., Morris, R., Robinson, M., Roush, T., Smith, M., Swayze, G., Taylor, H., Wolff, T.T.M., 2008. *Hydrated silicate minerals on Mars observed by the Mars Reconnaissance Orbiter CRISM instrument*. Letters Nature, ,305-309. doi:10.1038/nature07097.

Pasquarè, G., Bistacchi, A., Francalanci, L., Bertotto, G.W., Boari, E., Massironi, M., Rossetti, A., 2008. *Very long Pahoehoe inflated basaltic lava flows in the payenia volcanic province (Mendoza and La Pampa, Argentina).* Revista de la Asociaciòn geològica Argentina, 63, 131-149.

Pompilio, L., Pedrazzi, G., Craig, M.A., Sgavetti, M., Cloutis, E.A., 2008. *Spectral Modeling of Planetary Analogues, Preliminary Results*. Lun. Planet. Sci. *XXXIX*, #1550.

Poulet, F., Gomez, C., Bibring J.P., Langevin, Y., Gondet, B., Pinet, P., Belluci, G., Mustard, J.F., 2007. *Martian surface mineralogy from Observatoire pour la Mine´ralogie, l'Eau, les Glaces et l'Activite´ on board the Mars Express spacecraft (OMEGA/MEx): Global mineral maps*. J. Geophys. Res., 112, E08S02, doi:10.1029/2006JE002840

Poulet, F.,. Bibring, J.P, Langevin, Y., Mustard, J.F., Mangold, N., Vincendon, M., Gondet, B., Pinet, P.,. Bardintzeff, J.M, Platevoet, B., 2009a. *Quantitative compositional analysis of martian mafic regions using the MEX/OMEGA reflectance data 1. Methodology, uncertainties and examples of application.* Icarus, 201, 1, 69-83.

Poulet F.,, Mangold, N., Platevoet, B., Bardintzeff, J.M., Sautter, V., Mustard, J.F., Bibring J.P., Pinet, P., Langevin, Y., Gondet, B., Aléon-Toppani, A., 2009b. *Quantitative compositional analysis of martian mafic regions using the MEx/OMEGA reflectance data: 2. Petrological implications*. Icarus, 201, 1, 84-101.

Ruff, S.W., Christensen, P.R., 2002. *Bright and dark regions on Mars: Particle size and mineralogical characteristics based on Thermal Emission Spectrometer data*. J. Geophys. Res., 107, E12, 5127. doi: 10.1029/2001JE001580

Schaber, G.G., Horstman, K.C., Dial, A.L., 1978. *Lava flow materials in the Tharsis region of Mars.* Lunar Planetary Science Conference, 19th, 3433–3458.

Scott, D.H., Tanaka, K.L., 1981. *Mars: Paleostratigraphic restoration of buried surfaces in the Tharsis Montes area, Mars*. Icarus 45, 304–319.

Scott, D.H., Tanaka, K.L. 1986. *Geologic map of the western equatorial region of Mars, scale 1:15,000,000*. US Geol. Surv. Misc. Invest. Ser. (Map I-1802-A).

Smith, D.E., et al., 1999. *The global topography of Mars and implications for surface evolution*. Science, 284, 1495–1503.

Squyres, S.W., Arvidson, R.E., Bell III, J.F., et al., 2004. *The Spirit Rover's Athena Science Investigation at Gusev Crater, Mars*. Science, 305(5685), 794-800.

Farrand, W., Folkner, W., Golombek, M., Gorevan, S., Grant, J.A., Greeley, R., Grotzinger, J., Haskin, L., Herkenhoff, K.E., Hviid, S., Johnson, J., Klingelho¨ fer, G., Knoll, A., Landis, G., Lemmon, M., Li, R., Madsen, M.B., Malin, M.C., McLennan, S.M., McSween, H.Y., Ming, D.W., Moersch, J., Morris, R.V., Parker, T., Rice Jr., J.W., Richter, L., Rieder, R., Sims, M., Smith, M., Smith, P., Soderblom, L.A., Sullivan, R., Wa¨nke, H., Wdowiak, T., Wolff, M., Yen A., 2004. *The Spirit Rover's Athena Science Investigation at Gusev Crater, Mars*. Science, 305, 794-799. DOI: 10.1126/science.3050794

Sunshine, J.M., Pieters, C.M., Pratt, S.F., 1990. *Deconvolution of mineral absorption bands: an improved approach*. J. Geophys. Res., 95, 6955-6966.

Sunshine, J.M., Pieters, C.M., 1990. *Extraction of compositional information from olivine reflectance spectra: a New Capability for Lunar Exploration*. Lun. Planet. Sci., XXI, #1223.

Sunshine, J.M., Pieters, C.M., 1998. *Determining the composition of olivine from reflectance spectroscopy*. J. Geophys. Res., 103, 13675-13688.

Wyatt, M.B., Hamilton V.E., McSween Jr. H.Y., Christensen P.R., Taylor L.A, 2001. *Analysis of terrestrial and Martian volcanic compositions using thermal emission spectroscopy: 1. Determination of mineralogy, chemistry, and classification strategies*. J. Geophys Res., 106, 14,711–14,732.

Wyatt, M.B., McSween Jr., H.Y., 2002. *Spectral evidence for weathered basalt as an alternative to andesite in the northern lowlands of Mars*. Nature, 417, 263–266

Conclusions

This thesis has had the purpose of studying the Daedalia Planum lava plains located south-west of Arsia Mons and in particular understanding the emplacement history of its lava flows. To reach this aim two main approaches have been used: the analysis of their morphologies studying the images of the area and spectral characteristics employing OMEGA data. The main results obtained can be summarized as follows:

- Daedalia Planum flows show a great variety of morphologies: the longest and oldest flows show the typical pahoehoe and platy-ridged surface, the youngest and shortest flows are instead represented by narrow and generally lobated flows with brecciated surface or central channels. These differences, coupled with their stratigraphic relationships, were employed to create a geological map of Daedalia Planum (see cap.3);
- On some Daedalia Planum lava flows several inflation fingerprints like tumuli, lava rises and lava ridges were detected. This suggests that the inflation mechanism is one of the most important factors that contribute to the emplacement of the Daedalia long lava flows. Moreover this implies that on Mars this process could be more frequent than previously supposed and has important implication on the estimation of effusion rates and lavas' rheological proprieties, as up to date they are calculated assuming non inflated flows (see cap.3);
- The comparative analysis between the dome-like features identified on the Daedalia Planum flows and those observed on Elysium Planitia highlighted important morphological differences between them. These could be explained with a different origin of the mounds in the two regions. In particular the study of the contest where these features occurred and the estimation of their spatial distribution suggest that the Elysium Planitia mounds are more likely pingos formed on unconsolidated water-rich periglacial terrain, whereas the features detected on Daedalia Planum are more suitable with tumuli emplaced on inflated lava flows. This would confirm the hypothesis of the presence of the inflation process among the Daedalia Planum flows (see cap.4);
- The spectral analysis with OMEGA data revealed a uniform composition of the lavas on the volcanic field since all the spectra collected around the field show 2 main absorption bands at about 1.00 and 2.00 μm. Such bands indicate the presence of pyroxene which, together with plagioclase, is the main component of basalts. Moreover the content of Ca in the pyroxene asserts that Daedalia Planum flows are most likely composed by tholeiitic basalt (see cap.5);
- Despite the overall compositional similarities, OMEGA spectra show also differences in reflectance and spectral slope possibly related to different flows surface texture and to different grain size or rock textures (crystals isorientation, presence of glass). Frequently such differences can be related to the mapped flows, however in some cases do not fit any flow boundary. Therefore new spectral sub-units were distinguished on the geological map (see cap.5);
- The morphological and spectral analysis seems to be the most suitable method for geological mapping since the spectral characteristics permit to appreciate differences otherwise not detectable with the morphological analysis alone (see cap.5).

Acknowledgments

First of all I would like to thank my tutor Dr. Matteo Massironi for his precious help and patience during the writing of this thesis and mainly to his support and encouragements during my PhD research activity.

C. Carli, E. Martellato, G. Pasquarè, G. Cremonese, L. Pompilio, M. Sgavetti, D. Rothery, S. Smrekar, J. Murray and M. Balme are thanked for the scientific support and the helpful discussions.

D. Rothery, H. Hiesinger and J. Raitala are acknowledged for their revisions and useful suggestions.

Unending gratitude goes to my parents who have always supported me, especially during these last years, although my research field is not exactly their idea of a “real job”.
Thanks to all my office-mates, in particular Lidia, for the chats and to have listened to my outbursts on the bad days, Matteo, for his help when my laptop did not want to work, and Francesca who helped me with the documents for the request of the Doctor Europaeus qualification.
A special thanks also to my aunt Yvette who helped me many times with the English and Elena and Lisa for their support.
Thanks also to Laura and Elisa for their friendships although in these last three years I didn’t spend enough time with them.
Last but not least a great thanks to Cristian for his love, support and patience even if this thesis did not allow me to spend much time with him in these last months.